Università degli Studi di Ferrara

ADENOSINE RECEPTORS IN RESPIRATORY DISORDERS AS CHRONIC OBSTRUCTIVE PULMONARY DISEASE AND MALIGNANT PLEURAL MESOTHELIOMA

Settore Scientifico Disciplinare BIO/14

Dottorando
Dott. Targa Martina

Tutore
Prof. Varani Katia

Anni 2009/2011

TABLE OF CONTENTS

INTRODUCTION

Adenosine

The endogenous nucleoside adenosine is composed of a molecule of adenine attached to a ribose sugar molecule (ribofuranose) via a β-N9-glycosidic bond (Figure 1).
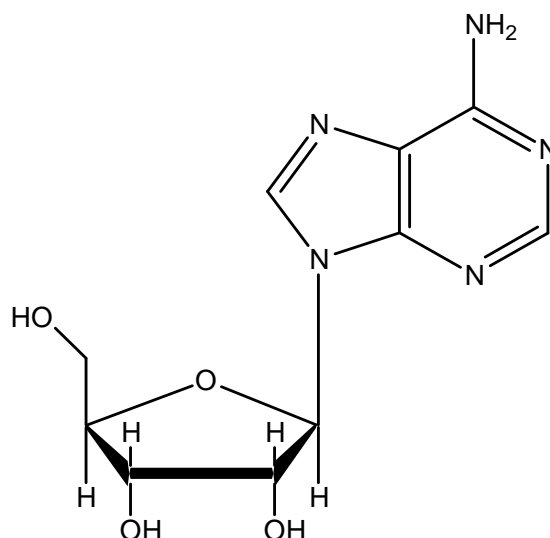

Figure 1 – Chemical structure of adenosine

Adenosine plays a central role as a structural element of nucleic acids and in the energy metabolism of all living organism. The physiological effects of adenosine were first described in the cardiovascular system and gastrointestinal tract [1]. Adenosine, acting on specific membrane receptors, produces a number of physiological and pathophysiological effects in the central nervous system (CNS) [2, 3], in the cardiovascular system [4], as an endogenous pain modular [5], in the immune system [6, 7], cell growth and apoptosis [8]. Under normal conditions, adenosine is continuously formed intracellularly as well as extracellularly. The intracellular production is mediated either by an intracellular 5'-nucleotidase, which dephosphorylates or by hydrolysis of S-adenosyl-homocysteine [9]. Adenosine generated intracellularly is transported into the extracellular space mainly via specific bi-directional transporters through facilitated diffusion that efficiently evens out the intra- and extracellular levels of adenosine. The dephosphorylation of extracellular AMP to adenosine, mediated by ecto-5'-nucleotidase, is the last step in the enzymatic chain that catalyzes the breakdown of extracellular adenine nucleotides, such as ATP, to adenosine. Ectonucleotidases include ectonucleoside triphosphate diphosphohydrolase which can

hydrolyze ATP or ADP, ectonucleotide pyrophosphatase/phosphodiesterases, alkaline phosphatases and 5'-nucleotidases [10]. When adenosine levels in the extracellular space are high, adenosine is transported into cells by means of transporters. It is then phosphorylated to AMP by adenosine kinase or degraded to inosine by adenosine deaminase. Adenosine deaminase, but not adenosine kinase, is also present in the extracellular space [9]. Another potential source of extracellular adenosine is cAMP, which can be released from neurons and converted by extracellular phosphodiesterases into AMP and thereafter by an ecto-5'-nucleotidase to adenosine. The transport of adenosine by facilitated diffusion is equilibrative and bidirectional, meaning that the net transport of adenosine either into or out of the cell depends upon the adenosine concentration gradient in both sides of the membrane. Inhibition of adenosine transport can, therefore, inhibit either adenosine release or adenosine uptake, depending upon the intra- and extracellular levels of adenosine [11]. However, since the extracellular formation of adenosine from released adenine nucleotides constitutes a second source of adenosine, which is not affected by transport inhibition, the transport inhibitors usually cause an increase in the extracellular adenosine levels. Under hypoxic and ischemic conditions there is a marked increase in cytoplasmatic adenosine leading to an intense release of adenosine, which is inhibited by adenosine uptake inhibitors [12].

Excitatory aminoacid-mediated release of adenosine is certainly involved; however, of greater importance is probably the fact that whenever intracellular levels of adenine nucleotides fall as a result of excessive energy use, the intracellular levels of adenosine will rise dramatically [9]. For example, following hypoxia there is a decrease of intracellular ATP, accompanied by an accumulation of 5'-AMP and subsequently adenosine. The nucleoside is thereafter transported into the extracellular space via the transporters. Furthermore, when the intracellular level of adenosine is very high, adenosine simply diffuses out of cells. Direct release of intracellular adenine nucleotides, such as ATP, that is thereafter converted extracellularly by ecto-ATPase and ecto-ATP-diphosphohydrolase (ecto-apyrase) to AMP and dephosphorylated by ecto-5'-nucleotidase to adenosine, should also be considered [12]. Adenosine is neither stored nor released as a classical neurotransmitter since it does not accumulate in synaptic vesicles, being released from the cytoplasm into the extracellular space through a nucleoside transporter. The adenosine transporters also mediate adenosine reuptake, the direction of the transport being dependent upon the concentration gradient at both sides of the membrane [9].

G protein-coupled receptors

Considering the overall protein structure, adenosine receptors (ARs) display the topology typical of an important class of transmembrane proteins is the superfamily of G protein-coupled receptors (GPCRs) which are known as seven transmembrane (7TM) or heptahelical receptors. Sequence comparison between the different GPCRs revealed the existence of different receptor families sharing no sequence similarity even if specific fingerprints exist in all GPCR classes. They constitute a prominent superfamily targeted by many drugs. Up to 50% of all modern-day medicines act on GPCRs [13]. This makes GPCRs of great interest to both pharmaceutical and academic research, which is focused on drug discovery and the function and malfunction of various human systems. GPCRs play a vital role in signal transduction and may be activated by a wide variety of ligands, including photons, amines, hormones, neurotransmitters and proteins. GPCRs are single polypeptide chains having seven hydrophobic transmembrane-spanning segments that couple in the presence of an activator to an intracellular effectors molecule through a trimeric G protein complex [14]. The latter protein name originates from its interaction with guanine nucleotides. The class of guanine nucleotide binding proteins (G proteins) initiate some of the important signalling pathways in the cell. The members of the GPCR superfamily share two major structural and functional similarities. The first principal feature are the setup by seven membrane-spanning α-helices (TM1-7) connected by alternating intracellular (IL1, IL2, and IL3) and extracellular loop domains (EL1, EL2, and EL3). The orientation of the N and C terminus is also conserved across all GPCRs. The N-terminal tail is exposed to the extracellular environment and the C-terminal tail is located in the cytosol of the cell and thought to maintain an interaction with cytosolic G proteins. The family A of receptors, which comprises the well characterized rhodopsin/β2-adrenergic receptors, contains 90% of all GPCRs and is by far the largest and the most studied [15]. The high degree of conservation among these key residues suggests that they have an essential role for either the structural or functional integrity of the receptors. Only for class A, crystal structures of four GPCRs are known providing detailed molecular information on these receptors. G proteins transmit extracellular signals from GPCRs to downstream effectors proteins, which then cause further rapid changes in intracellular responses through signalling molecules such as cAMP, cGMP, inositol phosphates, diacylglycerol, arachidonic acid and cytosolic ions [16].

Adenosine receptors

The ARs are members of the superfamily of GPCRs belonging to the subfamily of rhodopsin-like receptors and thus, show the typical heptahelical structure. The adenosine receptor subtypes in a tissue or isolated cells are characterized by their G protein coupling preference. Biological functions of extracellular adenosine are mediated by four different adenosine receptor subtypes; including the A_1 and A_3AR subtypes, which couple to a Gi protein that inhibit the intracellular adenylate cyclase (AC) and thus leading to a decrease of cAMP, and the A_{2A} and $A_{2B}AR$, which couple to a Gs protein that stimulate cAMP production in brain slices at low (0.1-1 μM) and high (≥ 10 μM) adenosine concentration, respectively [17]. The four ARs have been cloned from several mammalian species, including human. There is extensive sequence similarity between species for the A_1, A_{2A} and $A_{2B}ARs$, whereas A_3ARs are more variable. Each ARs has different but overlapping functions. Each of them is unique in pharmacological profile, tissue distribution, binding partners and on coupling to other second messenger systems, activation of K^+ channels (A_1), or phospholipase C (all subtypes) has been described [9]. Generally, the $A_{2B}ARs$ requires higher concentration of adenosine than other subtypes to be significantly activated. In particular, all of the ARs subtypes can also be characterized according to the potency of the natural agonist adenosine: the A_1 and A_{2A} subtypes are high-affinity receptors activated by adenosine in nanomolar concentrations, while the A_{2B} and A_3ARs are low-affinity subtypes that require high micromolar concentrations for activation. Based on the extensive roles of the ARs in both physiologic and pathophysiologic events, these subtypes are becoming important drug targets in the treatment of several diseases because they have a role in controlling physiological processes [18].

A_1 adenosine receptors

The adenosine A_1ARs are widely expressed throughout the body, having its highest expression in the brain, spinal cord, atria and adipose tissue [19]. Adenosine, via A_1ARs, reduces heart rate, glomerular filtration rate, and renin release in the kidney, induces bronchoconstriction and inhibits lipolysis [20]. A_1ARs can be coupled to different pertussis toxin-sensitive G proteins, which mediate inhibition of adenylate cyclase and regulate calcium and potassium channels, as well as inositol phosphate metabolism [9]. A_1ARs and

A_{2A}ARs are primarily responsible for the central effects of adenosine [21]. In addition to their postsynaptic locations in different brain regions, A_1ARs can be found pre-synaptically and modulate neurotransmitter release. Pre-synaptic A_1ARs are the prototype of GPCRs, the stimulation of which decreases the probability of neurotransmitter release. The main mechanism of A_1AR-mediated inhibition of exocytosis is a direct inhibitory effect on voltage-dependent Ca^{2+} channels [22]. A_1AR displays two different affinities for agonist, which have classically been attributed to a different coupling to heterotrimeric G proteins. According to this two independent site model, coupled receptor–G protein complexes display high affinity for agonists and uncoupled receptors display low affinity. The reported cluster-arranged cooperative model predicts that the high- and low-affinity sites are a consequence of the negative cooperativity of agonist binding and do not seem to be related to the content of G protein-coupled or –uncoupled receptors [9]. Like other GPCR members, A_1AR expression is regulated in response to agonist or antagonist stimulation. Desensitization of A_1ARs has been described in intact animals and in cell cultures. Prolonged administration of A_1AR agonists to animals leads to functional desensitization of A_1ARs in guinea pig heart, rat adipocytes, rat atrial muscle, and rat brain [23]. The reduced functional response is attributable to a net loss of A_1ARs or down-regulation, a decrease in the proportion of A_1ARs displaying the high-affinity state for agonists, and a decrease in the content of Gi proteins. The loss of binding sites on the cell membrane owing to internalization of A_1ARs is a slower event. Ser/Thr phosphorylation seems to be related to short-term clustering and desensitization, as well as long-term internalization of A_1ARs [24].

A_{2A} adenosine receptors

The A_{2A}ARs exists in a wide variety of organs including major peripheral tissues (liver, heart, lung, and the immune system) and the CNS [25]. In the developing rat brain, the expression of A_{2A}AR is transiently regulated in various areas (e.g., the striatum, cortex, and hippocampus), perhaps implying a role of adenosine in neuronal development. Soon after neurogenesis, the A_{2A}AR is highly expressed by striatal neurons and co-localizes with the D2 dopamine receptor in GABAergic striatopallidal neurons [26]. In addition to the intense expression in the striatum, low levels of A_{2A}ARs are found in many brain regions (e.g., cortex and hippocampus) and it has been suggested that adenosine via A_{2A}AR regulates important neuronal functions including neuronal protection and synaptic transmission [26].

The regulation of $A_{2A}AR$ gene expression is therefore likely to play an important role in neuronal development, basal ganglia activity, and many other peripheral functions. In the CNS, l-DOPA enhanced the gene expression of the striatal $A_{2A}AR$ in 6-OHDA-lesioned rats [27]. Treatment with an antagonist of the NMDA receptor (memantine) was also reported to elevate the transcript level of striatal $A_{2A}ARs$ [28]. Like other GPCRs it can also interact with other G proteins if the receptor is very over-expressed, but the evidence for such coupling in vivo is not compelling. In striatum the $A_{2A}ARs$ interacts with Golf proteins [29]. Most effects are probably due to activation of adenylyl cyclase and production of cAMP. The $A_{2A}AR$ can recruit β-arrestin via a GRK-2 dependent mechanism, influenced by activation of cytokine receptors, which cause reduced desensitization of the $A_{2A}AR$ [30]. The cAMP responsive element-binding protein (CREB) is critical for many forms of neuronal plasticity as well as other neuronal functions, phosphorylation of CREB at Ser133 by protein kinase A (PKA) activates CREB and turns on genes with cAMP responsive elements (CRE sites) in their promoters. One important feature of CREB is that it is a point of convergence for the cAMP/PKA and MAPK pathways [31]. The stimulation of $A_{2A}ARs$ counteracts the inhibition of neurite outgrowth due to MAPK blockade. The $A_{2A}AR$ activation alone also stimulates the Ras/Raf-1/MEK/ERK signalling through PKA-dependent and PKA-independent pathways via Src- and Sos- mediated mechanisms, respectively [32]. Interestingly, phosphorylation/activation of CREB has been shown to compete with nuclear factor-κB (NF-κB) p65 for an important co-factor, CBP. Phosphorylated CREB was therefore proposed to mediate the anti-inflammatory effect of $A_{2A}ARs$ and inhibition of NF-κB by $A_{2A}AR$ activation during in vivo acute inflammation [2]. An interesting observation is that $A_{2A}ARs$ activation facilitates adenosine transporters via a protein kinase C (PKC)-dependent pathway in the hippocampus, and reduces the level of extracellular adenosine available for A_1AR activation. In addition, PKC was shown to play a key role in mediating the enhancement of noradrenaline release by $A_{2A}ARs$ in rat tail artery [33]. Activation of multiple signalling pathways by $A_{2A}ARs$ appears to contribute to their complex functions in various tissues.

A_{2B} adenosine receptors

$A_{2B}AR$ mRNA was originally detected in a limited number of rat tissues by Northern blot analysis, with the highest levels found in cecum, bowel, and bladder, followed by brain, spinal cord, lung, epididymis, vas deferens, and pituitary. The use of more sensitive reverse

_____

transcriptase-polymerase chain reaction techniques revealed a ubiquitous distribution of $A_{2B}ARs$ [34]. mRNA encoding $A_{2B}AR$ was detected at various levels in different rat tissues studied, with the highest levels in the proximal colon and lowest in the liver. In situ hybridization of $A_{2B}ARs$ showed widespread and uniform distribution of $A_{2B}AR$ mRNA throughout the brain [35]. In brain, functional $A_{2B}ARs$ are found in neurons, glial cells, in astrocytes and in different glioma cell lines [36]. The expression of $A_{2B}ARs$ in glial cells, which represent a majority of the brain cell population, can explain the original observation that slices from all brain areas examined showed an adenosine-stimulated cAMP response. Functional $A_{2B}ARs$ have been found in fibroblasts and various vascular beds, hematopoietic cells, mast cells, myocardial cells, intestinal epithelial and muscle cells, retinal pigment epithelium, endothelium, and neurosecretory. The activation of $A_{2B}ARs$ can also increase phospholipase C in human mast cells and in mouse bone marrow-derived mast cells. In addition, $A_{2B}AR$ activation elevates inositol triphosphate levels, indicating this receptor can couple also to Gq-proteins. $A_{2B}ARs$ have been implicated in the regulation of mast cell secretion, gene expression, intestinal function, neurosecretion, vascular tone and in particular asthma [37].

A_3 adenosine receptors

The A_3AR is the only adenosine subtype which was cloned before its pharmacological identification. It was originally isolated as an orphan receptor from rat testis, having 40% sequence homology with canine A_1 and $A_{2A}ARs$ and was identical with the A_3AR later cloned from rat striatum [38]. Homologs of the rat striatal A_3ARs have been cloned from sheep and human, revealing large interspecies differences in A_3AR structure. For example, the rat A_3AR presents only 74% sequence homology with sheep and human A_3AR, while there is 85% homology between sheep and human A_3AR. The A_3AR has been mapped on human chromosome 1p21-p13 [39] and consists of 318 aminoacid residues. The A_3AR is a G-protein-coupled receptor characterized by its C-terminal portion facing the intracellular compartment and 7 TM spanning domains. In contrast to other adenosine receptors, the C-terminal region presents multiple serine and threonine residues, which may serve as potential sites of phosphorylation that are important for rapid receptor desensitization upon agonist application [40]. Phosphorylation leads to a decrease of the number of receptors in the high-affinity state and a decrease of agonist potency to inhibit adenylyl cyclase activity. At the same time, the receptor is reversibly internalized in an agonist-dependent fashion

_____

[41]. The A_3AR has widely distributed its mRNA being expressed in testis, lung, kidneys, placenta, heart, brain, spleen, liver, uterus, bladder, jejunum, proximal colon and eye of rat, sheep and humans. The classical pathways associated with A_3AR activation are the inhibition of adenylyl cyclase activity, through the coupling with Gi proteins, and the stimulation of phospholipase C, inositol triphosphate and intracellular Ca^{2+}, via Gq proteins [9].

Adenosine receptors in the respiratory system

Increased adenosine levels have been found in the lungs of individuals with asthma or COPD, and ARs are known to be expressed on most, if not all, inflammatory and stromal cell types involved in the pathogenesis of these diseases [42]. A_1ARs are responsible for many effects induced by adenosine. In particular, this signalling nucleoside has been implicated in the regulation of asthma and chronic obstructive pulmonary disease (COPD); adenosine levels are elevated in the asthmatic lungs to an extent that can be directly correlated with the degree of inflammatory insult [43]. A_1AR expression is also increased in the epithelium and airway smooth muscle of human asthmatics. The involvement of A_1ARs in asthma was provided by studies on allergic rabbit models, where the adenosine-induced acute bronchoconstrictor response was attenuated by pretreatment with A_1AR antagonists. In particular, activation of A_1ARs in human airway epithelial cells causes an increase in the expression of the MUC2 gene, which is responsible for mucus hyper secretion. Moreover, activation of A_1ARs is known to produce pro-inflammatory effects on various types of human cells. The non-selective AR antagonists theophylline and doxofylline have been launched as bronchodilators for the treatment of various respiratory disorders [44]. Likewise, it has been recently reported that A_1AR inhibits transendothelial and transepithelial polymorphonuclear cell migration in a murine model of lipopolysaccharide (LPS)-induced lung injury, presumably by reducing the release of chemotactic cytokines into the alveolar space. In addition, A_1AR is involved in decreasing microvascular permeability and leukocyte transmigration in endothelial cells, suggesting also a protective and anti-inflammatory role for A_1AR [45].

Pharmacological treatment of allergic rats with an A_{2A} agonist has been shown to result in diminished pulmonary inflammation. Moreover, a recent study in an ADA-deficient model has demonstrated that genetic removal of A_{2A} leads to enhanced pulmonary inflammation, mucus production and alveolar airway destruction [46]. Furthermore, $A_{2A}ARs$ induced on

_____

invariant natural killer T cells and natural killer cells can reduce pulmonary inflammation in mice with sickle-cell anemia, improving baseline pulmonary function and preventing hypoxia-reoxygenation-induced exacerbation of pulmonary injury [47]. These findings further confirm the involvement of A_{2A}ARs in the anti-inflammatory networks of the lung.

Recently, A_{2B}ARs have been implicated in the mediation of several pro-inflammatory effects of adenosine in inflammatory cells of the lung. A_{2B}ARs have been reported to mediate degranulation and activation of canine mastocytoma and human mast cells line, thereby potentially playing a role in allergic and inflammatory disorders [48]. Adenosine constricts the airways of asthmatic patients through the release of histamine and leukotrienes from sensitized mast cells; although the receptor involved seems to be the A_3ARs in rats and the A_{2B}ARs in humans. Accordingly, A_{2B}ARs antagonists potently inhibit the activation and degranulation of HMCs induced by adenosine. In addition to mast cells, functional A_{2B}ARs have been found in bronchial smooth muscle cells and lung fibroblasts. In these cells, adenosine, through stimulation of the A_{2B} subtype, increases the release of various inflammatory cytokines, lending weight to evidence that A_{2B}ARs play a key role in the inflammatory response associated with asthma [49]. Furthermore, it has been reported that, through A_{2B}ARs activation, adenosine-differentiated dendritic cells express high levels of angiogenic, pro-inflammatory, immune suppressor and tolerogenic factors, including vascular endothelium grow factor (VEGF), interleukin 8 (IL-8), interleukin 6 (IL-6), interleukin 10 (IL-10) and ciclooxigenase 2 [50]. Moreover, using ADA knockout animals, it has been shown that dendritic cells with a pro-angiogenic phenotype are highly abundant in vivo under conditions associated with elevated levels of extracellular adenosine. The first evidence for the involvement of A_{2B}ARs in asthma was provided by studies concerning the selectivity of enprofylline, a methylxanthine structurally related to theophylline [50], and further support came from research demonstrating the presence of A_{2B}ARs on various type of cells involved in cytokine release in asthmatic disease, such as smooth muscle cells, lung fibroblasts, endothelial cells, bronchial epithelium and mast cells. Expression of A_{2B}ARs has also been found in the mast cells and macrophages of patients affected by COPD. In another study, activation of A_{2B}ARs in the HMC-1 mast cell line provoked an increase in IL-8 release in vitro [51].

Particular relevance to the presence of A_3ARs in the respiratory system has been reported. A_3ARs are expressed in human neutrophils where, together with A_{2A}, they are involved in the reduction of superoxide anion generation; they have also been implicated in the suppression of tumor necrosis factor α (TNF-α) release induced by endotoxin from human

monocytes [52]. In neutrophils, however, A_3ARs also play a role in chemotaxis, in conjunction with P2Y receptors. Moreover, A_3ARs activation seems to inhibit degranulation and superoxide anion production in human eosinophils [53]. Indeed, transcript levels for the A_3 subtype are elevated in the lungs of asthma and COPD patients, where expression is localized to eosinophilic infiltrates. Similar evidence has also been observed in the lungs of ADA knockout mice exhibiting adenosine-mediated lung disease [54]. Treatment of ADA knockout mice with 3-propyl-6-ethyl-5-[(ethylthio)carbonyl]-2phenyl-4-propyl-3-pyridine carboxylate (MRS 1523), a selective A_3 antagonist, prevented airway eosinophilia and mucus production. Nevertheless, these findings contrast sharply with the results of experiments performed in human eosinophils ex vivo, where chemotaxis was reduced by A_3AR activation, suggesting that significant differences exist between the impact of A_3ARs signalling on eosinophil migration ex vivo and in the whole animal. More recently, the involvement of the A_3AR in a bleomycin model of pulmonary inflammation and fibrosis has been explored. Results demonstrated that A_3AR knockout mice exhibit enhanced pulmonary inflammation that involves an increase in eosinophils. Accordingly, a selective upregulation of eosinophil-related chemokines and cytokines was found in the lungs of A_3AR knockout mice exposed to bleomycin, thereby suggesting that the A_3AR performs anti-inflammatory functions in the bleomycin model [53].

Nonetheless, the role of the A_3ARs in the human lung, and indeed in asthma, still remains to be clarified. In general, receptor knockouts have provided significant new insights into adenosine's control of complex physiological (i.e., cognition) and pathological (i.e., neuroinflammation) phenomena, suggesting that further studies in these animal models would help to clarify the role of A_3ARs in inflammatory lung disease [55].

Adenosine receptors in cancer

Adenosine, which is released to the microenvironment by metabolically active tumor cells, fulfils a multitude of functions in regulating tumor cell proliferation [56]. At micromolar (μM) concentrations it directly induces an anti-proliferative effect toward various tumor cell types. Indirectly, it affects tumor development via its capability to affect cytokine release, cell migration, angiogenesis, and chemotaxis [57]. Moreover, adenosine induces activation or suppression of T killer or natural killer cells that affect tumor cell development [58]. It is quite impossible to assess the effect of adenosine in vivo due to the rapid metabolization by ADA. The effect of adenosine and of the agonists/antagonists on tumor cells depends on

_____

their extracellular concentrations and on the expression of different adenosine receptor subtypes. Upon receptor activation, various signal transduction pathways are generated, resulting in a direct inhibitory effect on tumor growth [59]. Other cell types, such as immunocytes or endothelial cells, may respond to receptor activation by the release of cytokines and mediators that indirectly affect tumor growth [60]. Interestingly, among the four receptor subtypes, the A_3AR was found to mediate a potent antitumor effect [61]. The specificity of this target results from the finding that this receptor is highly expressed in tumor cells, whereas low receptor expression is reported in normal cells [59]. A_3ARs are involved in the tumor growth, in the regulation of cell cycle and mediate both pro and anti-apoptotic effects closely associated with the level of receptor activation [62, 63]. A_3ARs involve the inhibition of telomerase activity and arrest the G0/Gi phase of the cell cycle leading to a cytostatic effect in Nb2-11C lymphoma cells [64]. The A_3ARs reduce the ability of prostate cancer cells to migrate in vitro and metastasize in vivo. In particular it has been reported that activation of the A_3ARs in prostate cancer cells reduced PKA-mediated stimulation of ERK1/2 leading to lower NADPH oxidase activity and cancer cell invasiveness [65]. A_3AR density was upregulated in colon carcinoma tissues closely correlated to the disease severity. In addition the alteration of A_3ARs reflected a similar behavior shown in lymphocytes or neutrophils derived from colon cancer patients suggesting that these receptors may represent an interesting biological marker [66]. Recently, it has been reported that A_3AR selective agonists induce anti-inflammatory and anti-cancer effect in xenograft animal model utilizing Hep-3B hepatocellular carcinoma cells [61]. In this model, the A_3AR upregulation was present in inflammatory liver tissues similarly to those previously found in other inflammatory conditions [68].

The A_3AR agonist 2-chloro-N^6-(3-iodobenzyl)adenosine-5′-N-methyl-uronamide (CF102) inhibited tumor growth via de-regulation of the NF-kB signal transduction pathways, resulting in apoptosis of tumor cells [69]. Pharmacological studies demonstrated that A_3AR agonists inhibited the growth of melanoma cells while promoting the proliferation of bone marrow cells, reduced cell viability in human breast cancer cells and induced arrest of cell cycle progression in human lung cancer cells [70-72]. 2-chloro-N^6-(3-iodobenzyl)adenosine-5′-N-methyl-carboxamide (Cl-IB-MECA) enhanced apoptosis via the modulation of NF-kB signalling pathway in thyroid cancer cells and reduced the ability of prostate cancer cells to migrate in vitro and metastasize in vivo [67]. Moreover, preclinical and Phase I studies showed that A_3AR agonists are safe and well tolerated in humans and thus may be considered possible therapeutic agents for certain cancer diseases [73].

AIM OF THE THESIS

The environmental risk factor such noxious particles exposure, in combination with a genetic predisposition, results in two causes of morbidity and mortality worldwide namely chronic obstructive pulmonary disease (COPD) and malignant pleural mesothelioma (MPM). Oxidative stress provided by inhalation of exogenous particles, smokes of sigarette for COPD and asbestos for MPM, may lead to the activation of many intracellular pathways including kinases, transcription factors and epigenetic events that modulate the inflammatory response and cell cycling/proliferation [74]. COPD is the fourth leading cause of mortality worldwide [75]. COPD is a disease state characterized by airflow limitation that is not fully reversible. The airflow limitation is usually both progressive and associated with an abnormal inflammatory response of the lung to noxious particles or gases. The main cause of COPD is cigarette smoking [76]. Adenosine has been suggested to play a role in the pathogenesis of COPD [77]. The exact role of adenosine in the pathogenesis of COPD is unknown and probably complex because adenosine receptors in the lungs, in vitro and in animal models, have both pro- and anti-inflammatory effects and may also cause bronchoconstriction [78].

On this background, the aim of this study is to describe a detailed analysis, of A_1, A_{2A}, A_{2B} and A_3ARs expression in peripheral lung parenchyma, the major site of airflow obstruction in COPD using immunohistochemistry, radioligand binding and real time quantitative polymerase chain reaction (RT-QPCR). ARs were analyzed in age-matched smokers with normal lung function (control group) and COPD patients. Moreover, we have investigated whether changes in affinity and density of these receptors are correlated with clinical parameters such as forced expiratory volume in one second (FEV_1)/forced vital capacity (FVC) ratio. We have also investigated, using the in vitro model of human lung type 2 alveolar-like cells (A549 cells), the effect of pro-inflammatory cytokines on adenosine receptor subsets. COPD is characterized by an increased oxidative and nitrosative stress correlates with decreases in lung function and disease severity [79]. In addition, there is clear evidence for persistent inflammation in the lungs and airways of COPD patients which increases with disease severity. In COPD patients the inflammation and oxidative stress persist many years after smoking cessation [80]. Alveolar macrophages are considered to have a central role in the pathogenesis of COPD whereas the pathogenetic role of mast cells in COPD peripheral lung is more controversial [81]. For this reason the A_{2B}AR expression in bronchoalveolar lavage (BAL) macrophages from COPD smokers and age-matched with normal lung function was investigated. The effect of oxidative and nitrosative stress and of pro-inflammatory cytokines (TNF-α and IL-1β) on A_1, A_{2A}, A_{2B}

and A$_3$ARs expression and on their functionality in human leukaemic monocyte lymphoma cell line (U937), before and after phorbol 12-myristate 13-acetate (PMA)-treatment, and in the human mast cell line (HMC-1) was evaluated.

Considerable evidence have highlighted that adenosine through the interaction with its receptors plays an important role in controlling tumorigenesis via its receptors. MPM is a highly aggressive neoplasm whose incidence is increasing due to asbestos exposure [82]. The capacity of asbestos to induce MPM has been linked to the release of TNF-α that promotes mesothelial cell survival via NF-kB pathway [82]. To date, there is no standard curative therapy for MPM that is largely unresponsive to conventional chemotherapy or radiotherapy [83]. As a consequence, more effective therapeutic strategies are needed for this fatal disease with the aim to identify new candidates for targeted therapies. A$_3$ARs have been involved in the regulation of the cell cycle and both pro- and anti-apoptotic effects was closely associated with the level of receptor activation [84]. A$_3$ARs play a role in the modulation of mitogen-activated protein kinase (MAPK) activity and in the regulation of extracellular signal-regulated kinases (ERK1/2). It has been accepted that A$_3$ARs are highly expressed in tumor cells showing an important role in the development of cancer [85]. The serine/threonine kinase Akt/PKB has a central role in cell signalling downstream of growth factors, cytokines, and other cellular stimuli. Aberrant loss or gain of Akt/PKB activation underlies the pathophysiological properties of a variety of complex diseases, including cancer [86, 87]. Therefore, the purpose of this thesis, is to describe the alteration of A$_3$ARs in human MPM in comparison with healthy mesothelial pleura (HMP). We also studied the alteration of A$_3$ARs in healthy mesothelial cells (HMC) treated with crocidolite asbestos and in malignant mesothelioma cells (MMC) respect to untreated HMC. We investigated the reduction of Akt phosphorylation and NF-kB activation in tumor cells, mediating by A$_3$ARs. Furthermore, A$_3$AR stimulation on proliferation and apoptosis in MMC and in HMC exposed to asbestos and TNF-α was analyzed.

ADENOSINE RECEPTORS IN CHRONIC OBSTRUCTIVE PULMONARY DISEASE PATIENTS

Chronic obstructive pulmonary disease

COPD is a common inflammatory lung disease and a major cause of illness and death throughout the world. The Global Initiative for Chronic Obstructive Lung Disease defines COPD as "a pulmonary disease characterized by airflow limitation that is not fully reversible. The airflow limitation is usually progressive and associated with an abnormal inflammatory response of the lung to noxious particles or gases" [88]. The abnormal inflammatory response is a pathology of COPD which it shares with asthma. In COPD this inflammatory process leads to a co-presence of small airway diseases (obstructive bronchiolitis) with fibrosis and obstruction, parenchymal lung tissue destruction (emphysema), loss of lung elasticity and closure of small airways and chronic bronchitis, characterized by cough and mucous hypersecretion. As a consequence, the airways undergo structural changes with further loss of lung elasticity and airflow limitation. These pathological mechanisms manifest at different degrees in COPD patients [89]. Despite its high global prevalence, there is still a fundamental lack of knowledge about the cellular, molecular and genetic causes of COPD and no available therapy which may reduce the disease progression or mortality [90].

COPD affects > 10% of the world population over the age of 40 years and every year almost 3 million people die of this disease [91]. According the World Health Organization WHO, in 2007 COPD was the 4th cause of death worldwide and it is predicted to become the 3rd leading cause of death by 2030 [91]. COPD is the 13th cause of morbidity today and will become the 5th cause of morbidity by 2020 [92]. Therefore, the economic and social burden of the disease is immense today and will dramatically increase in the future, also considering that at present the disease is under-estimated, it is insufficiently recognized and is poorly diagnosed [92]. For an individual, of course, the disease may dramatically lower the quality of life. Paradoxically, despite its global impact and compared to asthma, research in COPD is less progressing and highly under-funded.

COPD is a complex, multi-factorial pathology and both environmental and host-depended factors are needed for the clinical manifestation of the disease. However, cigarette smoking is undoubtedly the major causative environmental risk factor for COPD. It accounts for approximately 90% of all cases and a dose-dependent relationship between tobacco consumption and the development and severity of COPD has been observed [93].

Important is the age at which a person started smoking, the numbers of packages of cigarettes smoked per year, and the current smoking status. Passive exposure to cigarette smoke is another risk factor that is increasing the total amount of inhaled particles into the lung. However, only 10-20% of the smokers develop clinical symptoms of COPD and susceptibility and other environmental factors are therefore crucial for the pathology of COPD [94]. Additional environmental risk factors are occupational dust and chemical exposure, indoor and outdoor air pollution, bacterial and viral infections, the socioeconomic status, and asthma [95]. Although there is no conclusive evidence, adults with asthma are found to have a twelvefold higher risk of acquiring COPD than subjects without asthma [96]. Like many other diseases, COPD is a polygenic disease and gene-environment interactions are critical for the development of this disorder. So far, the best investigated genetic cause for the development of COPD is the hereditary deficiency of the alpha-1 antitrypsin, an inhibitor of serine proteases. The lack of this protein is leading to the development of emphysema and decline in lung function due to digestion of the lung forming extracellular matrix and cell-cell interactions [97].

Pathological changes in COPD include chronic inflammatory processes and airway remodeling, both localized in the proximal and peripheral airways, in the lung parenchyma and in pulmonary vasculature [98]. The chronic inflammation of COPD is characterized by an accumulation of neutrophils, macrophages, B cells, lymphoid aggregates and CD4+ and CD8+ T cells particularly in the small airways [99] and the degree of inflammation increases with the disease severity as classified by the Global Initiative for Chronic Obstructive Lung Disease (GOLD) [100]. Neutrophils and activated macrophages release oxygen radicals, elastase, and cytokines that are essential to the pathogenesis of COPD, with effects on goblet cells and submucosal glands, and on the induction of emphysema and inflammation. Monocytes/ macrophages are important effector cells in COPD due to the release of reactive oxygen species, extracellular matrix proteins, lipid mediators, cytokines, chemokines and matrix metalloproteinases and their numbers increase with increasing severity [101-103].

Cigarette smoking is by far the most prominent cause for COPD. The inflammatory processes and the airway remodeling increase with disease severity and persist after cessation of smoking. Therefore, it is assumed that after a certain threshold of disease severity is passed, simply quitting smoking may not be sufficient to prevent disease progression. In recent years, investigations on COPD led to a major expansion of paradigms explaining the pathobiology of the disease and many different models are proposed today.

For example, COPD can be seen as a disease of accelerated lung aging, since many cellular pathological processes are due to the accumulation of reactive oxygen species [104, 105]. There is also a group of scientist that define COPD as an auto-immune disease which response to antigens released after smoke induced tissue or cell injuries [106]. Although other mechanisms that may be involved in COPD have been investigated and potential targets for a therapeutic approach proposed, an efficient cure for this disease is still not available today.

In COPD the predominant inflammatory cells are neutrophils, macrophages, and CD8 positive T-cells. Especially, macrophages seem to play a pivotal role in COPD [103]. COPD patients with emphysema show a 25-fold increase in the numbers of macrophages in the tissue and in the alveolar space when compared to normal smokers and there is a correlation between macrophage numbers in the airways and the severity of COPD. The key inflammatory mediators in COPD are IL-8, LTB4 and TNF-α [107] and the inflammation is localized in the peripheral airways, the lung parenchyma and in addition the pulmonary vessels are affected, the bronchioles are obstructed and present with fibrosis. In COPD, the typical inflammatory cascade is triggered by noxious air-borne particles, mainly by oxidants derived from cigarette smoke, that activate macrophages to release IL-8, TNF-α and matrix metalloproteinase. The release of these factors is promoted by the inactivation of histone deacetylase (HDAC) leading to the transcription of NF-κB inducible cytokines [108]. Oxidative stress is defined as an excess of reactive oxygen species (ROS) that cannot be neutralized by the antioxidant defense mechanisms and thus leading to cell damage. There is evidence that oxidative stress plays a major role in the pathogenesis of COPD [109]. On one side, inflammatory cells are able to generate ROS, but also cigarette smoke itself contains ROS at high concentrations. ROS activate NF-κB, which induces the transcription of multiple inflammatory genes leading to an inflammatory response in the lung [104, 110]. Interestingly, oxidative stress in COPD may be also linked to the poor response to corticosteroids in COPD patients. Oxidative stress impairs the translocation of the glucocorticoid receptors to the nucleus and the binding to its corresponding target DNA sequence [111, 112].

Adenosine receptors in COPD

Adenosine has been suggested to play a role in COPD [113]. Patients with COPD are significantly more responsive to AMP than healthy smoking volunteers and smokers have

significantly increased concentrations of adenosine in the airway lining fluid [114]. Adenosine is released during tissue hypoxia and inflammation, and all inflammatory cells express ARs [115]. Indeed, adenosine-based approaches are currently being developed for the treatment of various disorders where inflammatory modulation is a key component [116]. It has both pro- and anti-inflammatory features, which are mediated by ARs [117]. Activation of ARs can have different effects, with respect to the cell types involved, activation of A_1AR on neutrophils promotes adherence to endothelial cells and chemotaxis, indicating a pro-inflammatory response [117], whereas activation of A_1AR on cells from the monocytes/macrophage lineage inhibits the production of several pro-inflammatory cytokines (TNF-α, IL-8, and IL-6) and enhances the release of the anti-inflammatory cytokine IL-10, displaying an anti-inflammatory response [118]. Therefore, each receptor can be either beneficially and/or detrimentally implicated in the inflammatory process of COPD [119]. Since activation of ARs can influence the secretion of mediators from inflammatory cells, we related changes in adenosine and its receptors with changes in growth factors such as VEGF and chemokines (monocyte chemoattractant protein 1) related to remodeling and inflammation that may underlie lung function loss in COPD. The effect of adenosine on cytokine production by macrophages has attracted considerable attention, because macrophage-derived cytokines are crucial initiators and orchestrators of immune responses [113]. As TNF-α was one of the first cytokines to be discovered, a substantial body of information has accumulated regarding the ability of ARs activation to limit TNF-α production following macrophage activation [120, 121].

Until recently, the limited specificity of available selective agonists and antagonists has made it difficult to identify the expression of the different ARs. However, in the last few years significant advances in A_1 and A_{2A}ARs pharmacology have been made through the use of highly potent and selective agonist and/or antagonist radioligands such as [^{3}H]-1,3-dipropyl-8-cyclopentyl-xanthine ([^{3}H]-DPCPX) and [^{3}H]-4-(2-[7-amino-2-(2-furyl)[1,2,4]triazolo[2,3-a][1,3,5]triazin-5-yl-amino]ethyl)phenol ([^{3}H]-ZM 241385), respectively [122, 123]. More recently, the pharmacological characterization of a new, high-affinity, potent and selective radioligand ([^{3}H]-N-benzo[1,3[dioxol-5-yl-2-[5-(2,6-dioxo-1,3-dipropyl-2,3,6,7-tetrahydro-1H-purin-8-yl)-1-methyl-1H-pyrazol-3-yl-oxy]-acetamide, [^{3}H]-MRE 2029F20) that is able to bind human A_{2B}ARs has allowed a better characterization of this receptor subtypes in different human tissues [124]. In addition, the discovery of the new, high-affinity, and selective radioligand, [^{3}H]-5N-(4-methoxyphenylcarbamoyl) amino-8-propyl-2-(2-furyl) pyrazolo [4,3-e]-1,2,4-triazolo[1,5-

c]pyrimidine ([^{3}H]-MRE 3008F20) that is able to bind the human A_3AR with high affinity has allowed its pharmacological characterization [66, 125].

Combined immunohistochemical and radioligand binding studies could be very useful to clarify the specific effects determined by differential expression of A_1, A_{2A}, A_{2B} and A_3ARs.

Materials and methods

Subjects

We recruited thirty-four subjects undergoing lung resection for a solitary peripheral carcinoma, all subjects were recruited from the Section of Respiratory Diseases of the University Hospital of Ferrara, Italy. For the immunohistochemistry study six subjects were smokers with COPD and twelve were smokers with normal lung function (Table 1A). In addition, eight smokers with COPD and eight smokers with normal lung function were selected for the binding and RT-QPCR experiments (Table 1B). Seven smokers with COPD and six smokers with normal lung function were recruited for the western blot assays and immunocytochemistry experiments on the BAL from the Section of Respiratory Diseases of the University Hospital of Ferrara and the Section of Respiratory Diseases of the University Hospital of Katowicach, Poland (Table 1C). All former smokers had stopped smoking for more than one year. COPD and chronic bronchitis were respectively defined, according to international guidelines, as the presence of post-bronchodilator FEV_1/FVC ratio <70% or the presence of cough and sputum production for at least three months in each of two consecutive years. None of the study subjects had suffered a recent exacerbation, defined as increased dyspnea associated with a change in quality and quantity of sputum that would have led them to seek medical attention during the month previous the study. All subjects were free of acute upper respiratory tract infections and none had received glucocorticoids, theophylline, anti-oxidants or antibiotics within the preceding month. They were also nonatopic (i.e. they had negative skin tests for common allergen extracts) and had no past history of asthma or allergic rhinitis. All subjects were free from preoperative chemotherapy and/or radiotherapy. BAL was performed according to the local Ethics Committee Guidelines. Pulmonary function tests were performed as previously described [126] according to published guidelines. Predicted values for the different measures were calculated from the regression equations published by Quanjer [127]. The study was approved by the local Ethic Committee of the University Hospital of Ferrara and informed consent was obtained from each participant in accordance with the principles outlined in the Declaration of Helsinki.

Lung tissue processing

Two to four randomly selected tissue blocks were taken from the subpleural parenchyma of the lobe obtained at surgery, avoiding areas invaded by tumor. Tissue specimens were cut for immunohistochemical analysis and were placed on charged slides as previously reported [128]. Another piece of lung parenchyma was also taken and used in radioligand binding and RT-QPCR experiments.

Fiberoptic bronchoscopy, collection and processing of BAL

All subjects attended the bronchoscopy suite at 8.30 am after having fasted from midnight and were pre-treated with atropine (0.6 mg IV) and midazolam (5-10 mg IV). Oxygen (3 l/min) was administered via nasal prongs throughout the procedure and oxygen saturation was monitored with a digital oximeter. Using local anesthesia with lidocaine (4%) to the upper airways and larynx, a fiberoptic bronchoscope (Olympus BF10 Key-Med, UK) was passed through the nasal passages or mouth into the trachea. Further lidocaine (2%) was sprayed into the lower airways. BAL was performed from the right middle lobe using four successive aliquots of 60 ml of 0.9% NaCl. BAL cells were spin (500 g, 10 min) and washed twice with Hanks' buffered salt solution (HBSS). Cell Cytospin (Cytospin II; Shandon, UK) slides were prepared with native pellet, and one of them stained with May-Grunwald Giemsa to determine the leukocyte differential cell count. A total of at least 500 cells (excluding epithelial cells) per slide was examined at x1000 magnification. Cell viability was assessed using the trypan blue exclusion method. The remaining cell pellet was frozen at -80°C until its analysis [127].

Immunostaining for A_1, A_{2A}, A_{2B} and A_3ARs in lung sections

After deparaffinization and rehydration to expose the immunoreactive epitopes of ARs, the sections to be stained, immersed in citrate buffer 5 mM at pH 6.0, were incubated in a microwave oven (model NN S200W; Panasonic, Italy) on high power for 40 min or treated with trypsin. Endogenous peroxidase activity was blocked by incubating slides in 3% hydrogen peroxide (H_2O_2) in phosphate-buffered saline (PBS) followed by washing in PBS. Non-specific labeling was blocked by coating with blocking serum (5% normal rabbit or goat serum) for 20 min at room temperature. After washing in PBS the sections were

incubated for 1 h at room temperature with goat or rabbit anti-human A_1, A_{2A}, A_{2B} and A_3ARs at dilution of 1:100 of a 200 µg/ml solution. The primary antibodies were purchased from Alpha Diagnostics (rabbit polyclonal anti-human A_{2B}R code A2BR23-A) and Santa Cruz Biotechnology (goat polyclonal anti-human A_1R code sc-7500; goat polyclonal anti-human A_{2A}R code sc7502; rabbit polyclonal anti-human A_3R code sc-13938). For the negative control slides normal goat or rabbit non-specific immunoglobulins (Santa Cruz Biotechnology, CA) were used at the same protein concentration as the primary antibody. After repeated washing steps with PBS, the sections were subsequently incubated with anti-goat or anti-rabbit biotinylated antibody (Vector ABC Kit, Vector Laboratories, UK) for 30 min at room temperature. After further washing the sections were subsequently incubated with ABC reagent (Vector ABC Kit, Vector Laboratories, UK) for 30 min at room temperature. Slides were then incubated with chromogen-fast diaminobenzidine (DAB), with or without cobalt enhancement, for 1-5 min or 3-amino-9 ethylcarbazole (AEC) as chromogenic substances. After which they were counterstained in haematoxylin and mounted on permanent mounting medium [128].

Immunoperoxidase double staining in lung sections

Some sections were stained for A_{2A} or A_{2B}ARs as described above except that sections were stained for either CD68, tryptase or actin (smooth muscle specific) prior to counterstaining with haematoxylin. Non-specific labeling was again blocked by coating with blocking serum (5% normal horse serum) for 20 min at room temperature. After washing in PBS the sections were incubated for 1 h at room temperature with mouse anti-human CD68 (Dako, UK, 1:50 dilution of a 160 µg/ml solution) or with mouse anti-human tryptase (Dako, UK, 1:150 dilution of a 105 µg/ml solution) or with mouse anti-human actin (smooth muscle specific) (Dako, UK, 1:50 dilution of a 70 µg/ml solution). For the negative control slides, normal mouse non-specific immunoglobulins (Santa Cruz Biotechnology, CA) were used at the same protein concentration as the primary antibody. After repeated washing steps with PBS, the sections were subsequently incubated with anti-mouse biotinylated antibody (Vector Alkaline Phosphatase Kit, Vector Laboratories, UK) for 30 min at room temperature. After further washing the sections were subsequently incubated with ABC reagent (Vector Alkaline Phosphatase Kit, Vector Laboratories, UK) for 30 min at room temperature. Slides were then incubated with chromogen fast red for 10-

20 min, after which they were counterstained in haematoxylin and mounted on permanent mounting medium [128].

Immunocytochemical staining for A$_{2B}$AR in BAL cytospins

BAL macrophage cytospins were allowed to warm at room temperature, were fixed in cold acetone at -20°C for 5 min, and air-dried for 10 min. Endogenous peroxidase activity was blocked by incubating sections with methanol containing 3% hydrogen peroxide (H$_2$O$_2$) for 1 h followed by washing in PBS. Immunostaining procedures were performed using the Vector ABC Kit (Vector Laboratories, UK)**.** Non-specific labeling was blocked by coating with blocking serum (5% normal goat serum) for 20 min at room temperature. After washing in PBS the cytospins were incubated for 1 h at room temperature with rabbit anti-human A$_{2B}$AR at a dilution of 1:100 of a 200 µg/ml solution (Alpha Diagnostics, TX, code A2BR23-A). For the negative control slides normal rabbit non-specific immunoglobulins (Santa Cruz Biotechnology, CA) were used at the same protein concentration as the primary antibody. After repeated washing steps with PBS, the slides were subsequently incubated with anti-rabbit biotinylated antibody (Vector ABC Kit, Vector Laboratories, UK) for 30 min at room temperature. After further washing the sections were subsequently incubated with ABC reagent for 30 min at room temperature. Slides were then incubated with chromogen-fast diaminobenzidine (DAB) as chromogenic substance after which they were counterstained in haematoxylin and mounted on permanent mounting medium [128].

Saturation binding experiments for A$_1$, A$_{2A}$, A$_{2B}$ and A$_3$ARs in peripheral lung parenchyma

Peripheral lung parenchyma, was homogenized and filtered through two layers of gauze using a tris HCl 50 mM buffer pH 7.4. The homogenate was centrifuged at 40000 g for 10 min and the pellet was suspended in the same buffer described above containing 2 UI/ml ADA and incubated for 30 min at 37°C. After the incubation the suspension was centrifuged again at 40000 g for 10 min. The final pellet was suspended and used for radioligand binding assays [122-124]. Saturation binding experiments to A$_1$ARs were performed according by the method described previously using [3H]-1,3-dipropyl-8-cyclopentyl-xanthine ([3H]-DPCPX, specific activity 120 Ci/mmol; NEN-Perkin Elmer Life and Analytical Sciences, USA) as radioligand [122]. The lung parenchyma membranes

(100 μg of protein/assay) with 8 to 10 concentrations of the radioligand [3H]-DPCPX (0.01-30 nM) were incubated for 90 min at 25°C. Non specific binding was determined in the presence of DPCPX 1 μM. Saturation binding experiments to A_{2A}ARs were performed according by the method described previously using [3H]-4-(2-[7-amino-2-(2-furyl)[1,2,4]triazolo[2,3-a] [1,3,5]triazin-5-ylamino] ethyl ([3H]-ZM 241385, specific activity 17 Ci/mmol; Tocris Cookson Ltd, UK) as radioligand [123]. The lung membranes (100 μg of protein/assay) were incubated for 60 min at 4°C with 8 to 10 concentrations of the radioligand [3H]-ZM 241385 (0.01-50 nM). Non specific binding was determined in the presence of ZM 241385 1 μM. Saturation binding experiments to A_{2B}ARs were performed using [3H]-N-benzo[1,3[dioxol-5-yl-2-[5-(2,6-dioxo-1,3-dipropyl-2,3,6,7-tetrahydro-1H-purin-8-yl)-1-methyl-1H-pyrazol-3-yl-oxy]-acetamide ([3H]-MRE 2029F20, specific activity 123 Ci/mmol; Amersham International Chemical Laboratories, UK) as radioligand E5. The membranes (100 μg of protein/assay) with 8 to 10 concentrations of [3H]-MRE 2029F20 in the range 0.01-20 nM were incubated for 4°C at 60 min. Non specific binding was determined in the presence of MRE 2029F20 1 μM. Saturation binding experiments to A_3ARs were performed using [3H]-5N-(4-methoxyphenylcarbamoyl)amino-8-propyl-2-(2-furyl)pyrazolo[4,3-e]-1,2,4-triazolo [1,5-c]pyrimidine ([3H]-MRE 3008F20, specific activity 67 Ci/mmol; Amersham International Chemical Laboratories, UK) as radioligand [122]. The membranes (100 μg of protein/assay) with 8 to 10 concentrations in the range 0.01-50 nM of [3H]-MRE 3008F20 were incubated for 4°C at 150 min. Non specific binding was determined in the presence of MRE 3008F20 1 μM. In saturation binding experiments at the end of the incubation time, bound and free radioactivity were separated by filtering the assay mixture through Whatman GF/B glass fiber filters by use of a Brandel cell harvester. The filter bound radioactivity was counted using a 2500 TR liquid scintillation counter Packard with an efficiency of 58%.

Real time quantitative polymerase chain reaction on peripheral lung parenchyma

Total messenger RNA was extracted by the acid guanidinium thiocyanate phenol method. RT-QPCR was carried out using gene-specific double fluorescent labeled TaqMan MGB probe (minor groove binder) in a ABI Prism 7700 Sequence Detection System (Applied Biosystems, UK) [129]. For the RT-QPCR of mRNA of A_1, A_{2A}, A_{2B} and A_3AR-the assays-on demand ™ Gene expression Products NM 000674, NM 000675, NM 000676 and NM 000677 were used respectively. As an internal control for loading the human

glyceraldehyde-3-phosphate dehydrogenase (GAPDH) kit was used, and the fluorescent-labeled probe was VICTM (Applied Biosystems, UK). The mRNA content of each adenosine receptor was expressed as adenosine receptor mRNA/GAPDH mRNA. Similar results were obtained by using β-actin mRNA as internal control and the probe was fluorescent labeled with VICTM (Applied Biosystems, UK) [130].

Western blotting analysis of ARs expression in BAL macrophages

Whole cell proteins were extracted from human bronchoalveolar cell pellet (more of 95% cells were macrophages). Cells were suspended with mechanical disruption in RIPA lysis buffer with a protease inhibitors cocktail immediately frozen to –70° C and thawed after at least 60 min. Particulate matter was removed by centrifugation at 12000 g for 10 min at 4°C. Protein concentration was measured in the supernatant by the Bradford method according to the manufacturer's instructions (Bio-Rad Laboratories, UK). An equal volume of Laemmli sample buffer 2X concentrate was added to the final volume of the sample. At least 50 µg/lane of whole-cell proteins were subjected to 10% SDS-polyacrylamide gel electrophoresis, and transferred to nitrocellulose filters (Hybond-ECL, GE Healthcare, UK) by blotting. Filters were blocked for 45 min at room temperature in Tris-buffered saline (TBS), 0.05% Tween 20, 5% non-fat dry milk. The filters were then incubated with rabbit anti-human $A_{2B}AR$ (Alpha Diagnostic, TX, code $A_{2B}AR23$-A; dilution 1:1000) antibodies for 1 h at room temperature in TBS, 0.05% Tween 20, 5% non-fat dry milk at dilution of 1:1000. Filters were washed three times in TBS, 0.5% Tween 20 and then incubated for 45 min at room temperature with secondary antibody conjugated to horseradish peroxidase (Dako, UK) in TBS, 0.05% Tween 20, 5% non-fat dry milk, at a dilution of 1:4000. After further three washes in TBS, 0.05% Tween 20, visualization of the immunocomplexes was performed using the ECL as recommended by the manufacturer (GE Healthcare, Chalfont St. Giles, UK). As an internal control we reprobed each filter with an anti-human actin antibody (Santa Cruz Biotechnology, CA). The 43kDa (actin) and 55kDa ($A_{2B}AR$) bands intensities were quantified using densitometry with Grab-It and VisionWorks LS software (UVP, Cambridge, UK) and expressed as the ratio with the corresponding β-actin optical density value of the same lane [129].

Cell culture and treatment conditions

A549 (American Type Culture Collection number CCL185), epithelial, human lung type 2 alveolar-like cells were grown in Dulbecco's modified Eagle's medium containing 10% fetal calf serum before incubation for 48 h in serum-free media [131]. At the onset of each experiment, cells were placed in fresh medium and then cultured in the presence of IL-1β (1 ng/ml) or TNF-α (10 ng/ml) (R&D Systems, UK). The IKK2 inhibitor (AS602868) was kindly provided by Dr Michel Dreano (Basle, Switzerland). Cells were treated with AS602868 for 0.5 h before stimulation with IL-1β or TNF-α for 6 h.

U937 cells were grown in RPMI 1640 medium containing 10% fetal calf serum, 100 IU/ml penicillin and 100 µg/mg streptomycin before incubation for 48 h in serum-free media. At the onset of each experiment, cells were placed in fresh medium and cultivated with or without the addition (in various combinations) of: a) IL-1β (1 ng/ml) or TNF-α (10 ng/ml) (R&D Systems, UK); b) hydrogen peroxide (H_2O_2) or SIN-1 at different concentrations from 1 to 100 µM; c) N-acetylcysteine (NAC) 100 µM prior to the beginning of the experiments. Cell viability was assessed after the addition of the solutions by trypan blue staining and viability was at least 90% at the beginning and at the end of each experiment. For the membrane preparation the cell suspension was centrifuged at 1000 g for 10 min and the cell pellet was suspended in hypotonic buffer. The suspension was then homogenized, centrifuged at 40000 g for 30 min and the membrane pellet was frozen at −80°C until the use in saturation binding experiments. Analogous experiments were also performed in the same experimental conditions on phorbol 12-myristate 13-acetate (PMA)-transformed U937 cells. In addition, in the same cell lines the capability of NAC to reduce H_2O_2 or SIN-1 effects was also investigated.

HMC-1 cells (Prof. Massimo Triggiani, University of Naples, Italy) were originally obtained from a patient with mast cell leukemia [132]. Cells were grown at 37°C with 5% CO_2 in MEM without phenol red supplemented with 10% dialyzed fetal calf serum (FCS) from Gibco BRL (Invitrogen, France). Experiments analogous to the U937 cells were also carried out in the same experimental conditions in HMC-1 cells. In addition the capability of NAC to reduce the H_2O_2 or SIN-1 effects was also investigated.

Saturation Binding Assays of ARs in A549, in untreated or PMA treated U937 and HMC-1 membranes

Saturation binding experiments to ARs were performed in U937 or HMC-1 membranes (60 µg of protein/assay) with 8 to 10 concentrations of the radioligands and were incubated. At the end of the incubation time, bound and free radioactivity were separated by filtering the assay mixture, and the filter bound radioactivity was counted using a 2500 TR liquid scintillation counter Packard. A detailed description of the methods utilized is as previously described (see: Saturation binding experiments for ARs in peripheral lung parenchyma). Analogous binding experiments were performed using A549 cells membranes to evaluate the presence and the effect of pro-inflammatory cytokines IL-1β (1 ng/ml) or TNF-α (10 ng/ml) with or without NF-κB inhibitor (AS602868) on A_1, A_{2A}, A_{2B} and A_3ARs density and affinity.

Real time quantitative polymerase chain reaction on A549 and U937 cell lines

RNA extraction from A549 cells and from U937 cells was performed using an RNeasy Mini Kit according to the manufacturer's instructions (Qiagen, UK). RT-QPCR assay was performed using specific primers for A_1, A_{2A}, A_{2B} and A_3 receptor mRNAs. Relative levels of cDNAs were established using the ΔCt methods against the housekeeping gene: β-actin for A549 (Ambion Ltd, UK), and GAPDH for U937 (Qiagen, UK). Thermal cycling conditions were 15 min at 95°C, followed by 45 cycles of 15 s at 94°C, 25 s at 60°C, 25 s at 72°C and 5 s at 86°C. After normalization the value of ΔCt was subtracted from 45 (total number of RT-PCR cycles), thus higher ΔCt levels indicate higher mRNA levels. Also relative levels of mRNAs were expressed as the ratio of the Ct value for the gene of interest Ct/housekeeping gene. A non-template control was run with every assay and all determinations were performed at least in duplicates to achieve reproducibility [131].

Western blotting for ARs in U937 cells and in A549 cells

Whole cell proteins were extracted from U937 and A549. A549 cells were suspended with mechanical disruption in RIPA lysis buffer with a protease inhibitors cocktail immediately frozen to –70° C and thawed after at least 60 min. Particulate matter was removed by

centrifugation at 12000 g for 10 min at 4°C. Protein concentration was measured in the supernatant by the Bradford method according to the manufacturer's instructions (Bio-Rad Laboratories, UK). An equal volume of Laemmli sample buffer 2X concentrate was added to the final volume of the sample. At least 50 µg/lane of whole-cell proteins were subjected to a 10% SDS-polyacrylamide gel electrophoresis, and transferred to nitrocellulose filters (Hybond-ECL, Amersham Pharmacia Biotech) by blotting. Filters were blocked for 45 min at room temperature in Tris-buffered saline (TBS), 0.05% Tween 20, 5% non-fat dry milk. The filters were then incubated with anti-human antibody: for detecting $A_{2A}ARs$ in whole cell protein from A549 we used goat anti-human $A_{2A}AR$ antibody (sc-7502; from Santa Cruz Biotechnology, USA) and for detecting $A_{2B}ARs$ in whole cell protein from U937 we used goat anti-human $A_{2B}AR$ antibody (Alpha Diagnostic, TX, code $A_{2B}AR23$-A; dilution 1:1000). The filters were then incubated for 1h at room temperature in TBS, 0.05% Tween 20, 5% non-fat dry milk at dilution of 1:500. These antibody are specifics does not cross-react with other adenosine receptors family proteins. Filters were washed three times in TBS, 0.5% Tween 20 and after incubated for 45 min at room temperature with rabbit anti-goat antibody conjugated to horseradish peroxidase (Dako, UK) in TBS, 0.05% Tween 20, 5% non-fat dry milk, at dilution of 1:4000. After further three washes in TBS, 0.05% Tween 20, visualization of the immunocomplexes was performed using the ECL as recommended by the manufacturer (Amersham Pharmacia Biotech). As an internal control we reprobed each filter with an anti-human actin antibody (Santa Cruz Biotechnology). The 43 kDa (actin), 55kDa ($A_{2B}AR$) or 45 kDa ($A_{2A}AR$) bands were quantified using densitometry with Grab-It and GelWorks software (UVP, UK) and expressed as the ratio with the corresponding β-actin optical density value of the same lane [129].

Cyclic AMP production of U937 cells

U937 cells (before and after PMA-treatment) were suspended in 0.5 ml incubation mixture containing NaCl 150 mM, KCl 2.7 mM, NaH_2PO_4 0.37 mM, $MgSO_4$ 1 mM, $CaCl_2$ 1 mM, glucose 5 mM, Hepes 5 mM, $MgCl_2$ 10 mM, pH 7.4 at 37°C. Then adenosine deaminase (2 units/ml) and Ro20-1724 (0.5 mM), a phosphodiesterase inhibitor, were added and pre-incubated for 10 min in a shaking bath at 37°C. A typical adenosine agonist 5'-N-ethylcarboxamidoadenosine (NECA, 1 nM-10 µM, Sigma Aldrich, St Louis, MO) was incubated for 10 min with the aim of evaluating its ability to stimulate adenylyl cyclase activity in the absence and in the presence of MRE 2029F20 (1 µM). The reaction was

terminated by the addition of cold 6% trichloroacetic acid (TCA). The final aqueous solution was tested for cAMP levels by competition protein binding assays [37]. At the end of the incubation time (150 min at 4° C) and after the addition of charcoal the samples were centrifuged at 2000 g for 10 min. The clear supernatant was mixed with 4 ml of liquid scintillant (Atomlight, Perkin-Elmer, MA) and counted in a TriCarb Packard 2500 TR scintillation counter.

Cell proliferation assay of U937 cells

U937 cells (before and after PMA-treatment) were seeded in fresh medium with 1 µCi/ml [³H]-Thymidine in Dulbecco's modified Eagle's medium containing 10% fetal calf serum, penicillin (100 units/ml), streptomycin (100 µg/ml), L-glutamine (2 mM) and simultaneously treated with NECA in the absence or in the presence of MRE 2029F20 (1 µM) [86]. After 24 h of labeling, cells were trypsinized, dispensed in four wells of a 96-well plate, and filtered through Whatman GF/C glass fiber filters using a Micro-Mate 196 cell harvester (Perkin Elmer, MA). The filter-bound radioactivity was counted on Top Count Microplate Scintillation Counter with Micro Scint 20.

A$_{2B}$AR siRNA transfection of U937 cells

U937 cells were plated in flasks and grown to 50-70% confluence before transfection. siRNA transfection was performed via Nucleofector technology by using 10^6 cells in 100 µl Cell Line Nucleofector Solution C (Amaxa Inc, MD) and nucleofected with 0.3 µM of siRNA directed against human A$_{2B}$AR (Santa Cruz Biotechnology, CA) by using the preloaded W001 program in the Nucleofector II device (Amaxa Inc, MD) [133]. Using the same conditions, U937 cells were nucleofected with 0.3 µM of siRNA scramble as negative control (Dharmacon, UK) and 0.3 µM of siRNA cyclophillin as positive control (Ambion, TX). To evaluate transfection efficiency U937 cells were also transfected with a siRNA control labeled with fluorescein and by flow cytometry a transfection efficiency of 90±10% was observed. Following nucleofection the cells were immediately mixed with 500 µl of pre-warmed RPMI 1640 medium and transferred into well plates containing 1.5 ml RPMI 1640 medium per well. Cells were incubated at 37° C for 0, 2, 4, 8, 16 and 24 h and total RNA was isolated for real time PCR analysis of A$_{2B}$AR mRNA. Aliquots of cells were also

incubated at 37° C for 0, 24 and 48 h for Western blot analysis to $A_{2B}AR$ protein. Cell proliferation and cAMP content of the cells were measured with the techniques described above.

Statistical analysis of the data

Protein concentrations were determined by Bio-Rad assay [134] with bovine albumin as reference standard (Bio-Rad, CA). Dissociation equilibrium constants for saturation binding, K_D, as well as the maximum densities of specific binding sites, Bmax, were calculated for a system of one or two-binding site populations by non-linear curve fitting using the program Ligand [135] (Kell Biosoft, MO). Functional experiments were calculated by non linear regression analysis using the equation for a sigmoid concentration-response curve (PRISM GraphPAD, CA). Analysis of data was performed by one-way analysis of variance (ANOVA). Differences between control group and COPD subjects were analyzed with Dunnett's test and were considered significant at a value of $p < 0.05$. All data are reported as mean $\pm$ SEM (n = 3-6).

Results

Clinical parameters and pulmonary function of the patients are summarized in Tables 1. The two groups of subjects were similar with regard to age and gender and there was no significant difference in the smoking history (pack/years) between COPD and smokers with normal lung function. Moreover, no difference was found in the prevalence of chronic bronchitis between groups. As expected from the selection criteria, smokers with COPD had a significantly lower forced expiratory volume in one second (FEV_1) and FEV_1/ FVC ratio as compared to control smokers.

Immunohistochemical localization of A_1, A_{2A}, A_{2B} and A_3ARs in peripheral lung parenchyma

Peripheral lung parenchyma is a mixture of many cell types including bronchiolar and alveolar epithelial cells, endothelial, smooth muscle cells (localized in bronchiolar and vessel walls), fibroblasts, mast cells, neutrophils, macrophages and lymphocytes. Immunohistochemical analysis with anti-$A_{2A}AR$ antibody demonstrated staining of the bronchiolar and alveolar epithelial cells, bronchiolar smooth muscle cells, endothelial cells and infiltrating cells with no significant difference seen between COPD patients and the control group (Figure 2). A_1AR was expressed only in few alveolar macrophages (Figure 3) whereas the staining seen for the A_3AR, show that this receptor was expressed in alveolar septa and bronchiole (Figure 4). In contrast, $A_{2B}AR$ was expressed only in mast cells and macrophages (Figure 5).

Density and affinity of A_1, A_{2A}, A_{2B} and A_3ARs in peripheral lung parenchyma

The affinity and density of A_1, A_{2A}, A_{2B} and A_3ARs in membranes of peripheral lung from control group and COPD subjects are shown in Figures 6.

The affinity of A_1AR was significantly decreased in COPD patients compared with control group (K_D 3.15±0.19* vs 1.70±0.14 nM; *, $p<0.01$; Figure 6A). However, A_1AR density was significantly increased in COPD patients compared with control group (Bmax 53 ± 4* vs 32 ± 3 fmol/mg protein; *, $p<0.01$; Figure 6A). Similarly, the affinity of A_{2A} and A_1ARs was significantly decreased in COPD patients compared with control group whereas their

density was increased (K_D 7.88±0.68* vs 1.87±0.09 nM for $A_{2A}AR$ (Figure 6B) and 9.34±0.27* vs 4.41±0.25 nM for A_3AR (Figure 6D); Bmax 852±50* vs 302±12 fmol/mg protein for $A_{2A}AR$ (Figure 6B) and 2078±108* vs 770±34 fmol/mg protein for A_3AR (Figure 6D), respectively; *, p<0.01). In comparison, the affinity of A_{2B} receptors was not significantly different between the control group and COPD patients (K_D 2.46±0.45 vs 2.10±0.26 nM, Figure 6C). However, the density of $A_{2B}AR$ was significantly decreased in COPD patients compared with the control group (Bmax 66±5* vs 189±16 fmol/mg protein; *, p<0.01; Figure 6C).

Expression of A_1, A_{2A}, A_{2B} and A_3ARs mRNA in peripheral lung parenchyma

Using RT-QPCR we examined the expression of mRNA for all four adenosine receptors in the peripheral lung from both groups of subjects (Figure 7). GAPDH mRNA was used as an internal control for loading. The fold increase in ratio between $A_{2A}AR$/GAPDH (2.46±0.25; *, p<0.01) and A_3AR/GAPDH mRNA (1.71±0.18; *, p<0.01) was significantly increased in COPD patients (Figure 7). In contrast, the $A_{2B}AR$/GAPDH mRNA ratio was significantly decreased (0.47±0.05* vs 1.03±0.12; *, p<0.01) in COPD patients (Figure 7). No differences in A_1AR mRNA expression was seen between groups (Figure 7).

$A_{2B}AR$ expression in human alveolar macrophages of control smokers and COPD patients

Immunocytochemical analysis of BAL macrophages demonstrated a similar level of $A_{2B}AR$ expression in COPD patients and control smokers with normal lung function. The number of BAL macrophages expressing $A_{2B}ARs$ was 59±5% in COPD patients and 63±9% of total macrophages in healthy smokers (Figure 8A-C). Western blotting and densitometric analysis in BAL macrophages indicates a significant 68% decrease in $A_{2B}AR$ expression in COPD patients compared to control smokers with normal lung function ($A_{2B}ARs$/β-actin ratio: 3.52±0.84[*] vs 1.08±0.13; *, p<0.01) (Figure 8D and E).

Correlation between binding and clinical parameters

A direct correlation was found between FEV_1/FVC ratio and $A_{2A}AR$ (Figure 9A) and A_3AR (Figure 9B) receptor affinity (K_D) and density (Bmax). Furthermore an inverse correlation was found between the affinity and density of $A_{2B}AR$ and FEV_1/FVC ratio (Figure 9C). No other significant correlation were found between the affinity and/or density of A_1AR and any clinical parameters.

Effect of inflammatory stimuli on adenosine receptor expression in A549 cells

Saturation binding experiments on A549 membranes revealed the presence of A_1, A_{2A} and A_3ARs. However, $A_{2B}AR$ were not detectable on A549 membranes. IL-1β (1 ng/ml) and TNF-α (10 ng/ml) both significantly induced $A_{2A}AR$ expression (Bmax) 1.5–fold without affecting binding affinity (Table 2). Upregulation of $A_{2A}AR$ expression was attenuated by pre-treatment of cells with the NF-κB inhibitor AS602868. Similar data was seen for the induction of $A_{2A}AR$ mRNA and protein as determined by RT-QPCR and western blotting analysis (Figure 10). In contrast, neither IL-1β not TNF-α were not able to modify the affinity and the density of the A_1 and A_3AR (Table 2).

Presence of ARs in untransformed or PMA-transformed U937 membranes

Saturation binding experiments in U937 membranes were used to investigate mechanisms that may underlie this reduction in $A_{2B}AR$ expression demonstrated in BAL of COPD by western blotting. Affinity values (K_D, nM) and receptor density (Bmax, fmol/mg protein) of A_1, A_{2A}, A_{2B} and A_3ARs in untransformed U937 cell (monocyte-like) or PMA-transformed cell (macrophage-like) membranes are shown (Figure 11A and B, Table 3). ARs are present in U937 membranes with affinity values in the nanomolar range and with a receptor density from 10 to 186 fmol/mg protein. The affinity (K_D, nM) of A_1, A_{2A}, A_{2B} and A_3ARs did not change in PMA-transformed U937 cells as compared to untreated cells. No differences were found after PMA treatment for A_1 or $A_{2B}AR$ density. After PMA transformation A_{2A} and A_3ARs were significantly increased by 1.98 and 1.74-fold as compared to untransformed U937 cells (Table 3). Saturation curves of A_{2A} and A_3ARs are shown and

the linearity of the Scatchard plots indicates the presence of one high affinity binding site (Figure 11C-F).

Time course and concentration-dependent effect of H_2O_2 on ARs in untransformed or PMA-transformed U937 membranes

No differences in A_1, A_{2A} and A_3AR binding parameters in either untransformed or PMA-transformed U937 cells were found following exposure of cells to H_2O_2 (Tables 3, 4). The treatment of H_2O_2 (100 µM) for 12, 24 and 48 h reduced $A_{2B}AR$ density without affecting the affinity values (Figure 12A). The maximum effect was obtained after 48 h of H_2O_2 (100 µM) in both untransformed or PMA-transformed U937 cells showing a reduction of 76% and 71%, respectively. The effect of H_2O_2 on $A_{2B}AR$ density (Bmax values) at various times (0, 12, 24 and 48 h) and at different concentrations (from 1 to 100 µM) in untransformed or PMA-transformed U937 cells has been reported in Figure 12A and B, respectively. The effect of H_2O_2 involved only $A_{2B}ARs$ mediating a reduction on their Bmax values which was strictly dependent to time and concentration of H_2O_2 used. Similar results were obtained in untransformed or PMA-transformed U937 cells (Tables 3, 4). [^{3}H] MRE 2029F20 saturation binding curves following exposure of cells to H_2O_2 for different incubation times and concentrations are reported in Figure 13A and C, respectively. The relative Scatchard plots are shown in Figure 13B and D, respectively. H_2O_2 (100 µM) also reduced $A_{2B}AR$ mRNA levels from 2 to 24 h (Figure 14A) in U937 cells which was matched by a similar reduction in $A_{2B}AR$ protein expression as measured by western blot analysis (Figure 14C and E).

Time course and dose-dependent effect of SIN-1 on ARs in U937 cell membranes

Treatment with 3-morpholinosydnonimine, a peroxynitrite generator (SIN-1), at the 100 µM concentration for 2, 4, 6 and 12 h, reduced $A_{2B}AR$ density without affecting the affinity values (Figure 12C, Table 5). No differences in binding parameters of A_1, A_{2A} and A_3ARs were found in untransformed U937 cells treated with SIN-1 when compared with controls (Table 5). [^{3}H] MRE 2029F20 saturation binding curves in the absence and in the presence of SIN-1 over a 12 h time-course indicate a loss of $A_{2B}AR$ binding (Figure 13E). Scatchard analysis of [^{3}H] MRE 2029F20 binding indicates that SIN-1 causes a significant time-dependent reduction in $A_{2B}AR$ density without affecting receptor affinity (Figure 13F,

Table 5). The effect of SIN-1 is concentration-dependent (Figure 12D, Table 6) resulting in a 70% reduction of Bmax from 81 ± 4 to $26\pm2*$ fmol/mg protein; *, $p<0.01$. Analogous results were also obtained in PMA-transformed U937 cells (Figure 13G and H, Table 6). The maximum effect was obtained after 12 h of 100 µM SIN-1 exposure in both untransformed and PMA-transformed U937 cells (Figure 12C). SIN-1 treatments (100 µM) for 0, 2, 4, 8, 16 and 24 h induced a decrease of $A_{2B}AR$ mRNA levels as shown in Figure 14B. Similarly 6 and 12 h treatment of SIN-1 mediated a significant reduction ($p<0.01$) of $A_{2B}AR$ protein expression as reported in Figure 14D and confirmed by the relative densitometric analysis (Figure 14F).

Effect of NAC on ARs in U937 cell membranes

The effect of both H_2O_2 (100 µM) and SIN-1 (100 µM) at 24 and 6 h respectively was blocked by the antioxidant NAC (100 µM) (Figure 12E). NAC was able to normalize $A_{2B}AR$ density reaching values similar to control conditions: H_2O_2, $A_{2B}AR$ Bmax=19 ± 2 fmol/mg protein; H_2O_2+NAC, $A_{2B}AR$ Bmax=79 ± 6 fmol/mg protein; SIN-1, $A_{2B}AR$ Bmax=22 ± 2 fmol/mg protein; SIN-1+NAC, $A_{2B}AR$ Bmax=81 ± 7 fmol/mg protein. No differences were found in affinity values of $A_{2B}ARs$ in the absence or in the presence of NAC. An equivalent effect was seen in both untransformed and PMA-transformed U937 cell membranes (Figure 12E).

Effect of pro-inflammatory cytokines on ARs expression in U937 cells

In contrast to the reduction in $A_{2B}AR$ expression seen with H_2O_2 and SIN-1, the effect of typical pro-inflammatory cytokines IL-1β (1 ng/ml) and/or TNF-α (10 ng/ml) on A_1 and $A_{2B}AR$ binding parameters in untransformed or PMA-transformed U937 cell membranes were shown (Figure 12F, Table 7). IL-1β and TNF-α alone induced an increase in A_{2A} and A_3AR Bmax without affecting the receptor affinity. Co-stimulation with IL-1β and TNF-α produced an additional increase in A_{2A} and A_3AR Bmax. Analogous results were also obtained in PMA-transformed U937 cells. Addition of 100 µM H_2O_2 to U937 cells incubated with IL-1β and TNF-α resulted in a decrease in $A_{2B}AR$ Bmax and an increase in A_{2A} and A_3AR Bmax (Figure 12F, Table 7).

ARs binding parameters in HMC-1 cell membranes

Saturation binding experiments of A_1, A_{2A}, A_{2B} and A_3ARs were also performed in HMC-1 membranes obtained by cells incubated in the absence or in the presence of oxidative/nitrosative stress. A_{2A}, A_{2B} and A_3ARs were present in these cells with K_D values in the nanomolar range (from 1.67 to 2.60 nM) and with a receptor Bmax of 75, 120 and 315 fmol/mg protein, respectively. In these cells, A_1ARs were undetectable and the treatment with H_2O_2 or SIN-1 did not modify binding parameters of A_{2A}, A_{2B} and A_3ARs (Table 8). These data suggest that the reduction in A_{2B}AR expression by oxidative/nitrosative stress is cell-type specific.

A_{2B}AR-silencing in U937 cells

To evaluate the direct involvement of the A_{2B}ARs, siRNA directed against A_{2B}AR was transfected in U937 cells. Transfection efficiency in these cells was $90\pm10\%$ as determined by transfection with a fluorescein-labeled siRNA and flow cytometry. After transfection, the cells were cultured in complete media and total RNA was isolated at 0, 2, 4, 8, 16 and 24 h and RT-PCR analysis for A_{2B}AR mRNA was performed. In untransformed U937 cells A_{2B}AR mRNA was almost completely suppressed by 4 h (Figure 15A). A time-course of A_{2B}AR expression using western blot analysis confirmed that A_{2B}AR protein expression was strongly attenuated in A_{2B}AR siRNA-treated but not in control cells (Figure 15B and C).

Effect of NECA on cAMP and proliferation assays in U937 cells

The functional effect of A_{2B}ARs in U937 cells was determined by examining the effect of NECA on cAMP production and cell proliferation assays. NECA stimulated cAMP levels in a concentration-dependent manner, with an EC_{50} in the nanomolar range (Figure 16A). In the presence of H_2O_2 100 µM, NECA demonstrated a marked decrease in potency ($EC_{50}=5.6\pm0.4*$ vs 0.52 ± 0.04 µM; *, p<0.01) probably due to the loss of A_{2B}AR expression. Similarly, nitrosative stress induced by SIN-1 (100 µM) mediated a reduction in NECA potency ($EC_{50}=5.3\pm0.4$ µM) (Figure 16A). The effect of H_2O_2 or SIN-1 was blocked by the antioxidant agent NAC (100 µM) in untransformed or PMA-transformed U937 cells

(Figure 16A). Interestingly, 100 nM MRE 2029F20, a potent and selective $A_{2B}AR$ antagonist, was also able to decrease the potency of NECA towards increasing intracellular cAMP levels (EC_{50}=6.7±0.5* µM, vs controls; *, p<0.01) (Figure 16C). siRNA-mediated knockdown of $A_{2B}AR$ expression resulted in a significant reduction in the ability of NECA to induce cAMP production in untransformed U937 cells (EC_{50}=7.4±0.6* µM, vs controls; *, p<0.01) (Figure 16C). Analogous results were obtained in PMA-transformed U937 cells although the potency of NECA appears to be slightly modified (Figure 16A and D).

Untransformed U937 cells were also stimulated for 24 h in the presence of increasing concentrations of NECA (1-10 µM) and [^{3}H]-Thymidine incorporation was evaluated as a measure of cell proliferation. NECA stimulated [^{3}H]-Thymidine incorporation in a concentration-dependent manner, with an EC_{50}=4.2±0.5 µM (Figure 16B). In the presence of 100 µM H_2O_2 the potency of NECA was increased (EC_{50}=185±14 nM) probably due to the $A_{2B}AR$ reduction. Interestingly, also SIN-1 (100 µM) mediated an increase in NECA potency (EC_{50}=226±19 nM). NAC was able to normalize $A_{2B}AR$ function showing EC_{50} values similar to control conditions (Figure 16B). In addition, 100 nM MRE 2029F20 was able to increase NECA potency (EC_{50}=125±11 nM) (Figure 16E). Furthermore, siRNA-mediated knockdown of $A_{2B}AR$ expression resulted in a significant reduction in the ability of NECA to induce cell proliferation in untransformed and PMA-transformed U937 cells (Figure 16E and F).

TABLE 1 – Characteristics of smokers with normal lung function and COPD patients

A Subjects for the immuno-histology study	n	Age	Sex	Smoking history	Pack-years	Chronic Bronchitis	FEV$_1$ %pred	FEV$_1$/FVC %
Smokers	12	68.7±2.0	11M/1F	9 ex-smokers 3 current smokers	46.2±12.1	2 with and 10 without chronic bronchitis	95.2±5.1	77.0±1.4
COPD	6	69.2±3.1	5M/F	6 ex-smokers	41.2±8.2	2 with and 4 without chronic bronchitis	78.2±6.7*	60.4±3.7*
B Subjects for binding and RT-QPCR	n	Age	Sex	Smoking history	Pack-years	Chronic Bronchitis	FEV$_1$ %pred	FEV$_1$/FVC %
Smokers	8	66.3±4.6	6M/2F	4 ex-smokers 4 current smokers	33.8 ± 6.6	2 with and 6 without chronic bronchitis	99.8±7.8	76.1±2.1
COPD	8	71.0±2.8	8M	7 ex-smokers 1 current smoker	40.5 ± 9.5	2 with and 6 without chronic bronchitis	73.2±8.0*	57.0±4.2*
C Subjects for Bal experiments	n	Age	Sex	Smoking history	Pack-years	Chronic Bronchitis	FEV$_1$ %pred	FEV$_1$/FVC %
Smokers	6	61.8±3.1	6M	3 ex-smokers 3 current smokers	38.3±8.4	2 with and 4 without chronic bronchitis	94.1±6.1	76.4±2.3
COPD	7	65.0±3.7	6M/1F	4 ex-smokers 3 current smokers	37.8±4.5	1 with and 6 without chronic bronchitis	62.2±7.5**	54.9±6.0**

Definition of abbreviations: COPD = chronic obstructive pulmonary disease; M: Male; F: Female; FEV$_1$ = forced expiratory volume in 1 second; FVC = forced vital capacity. For COPD and smokers with normal lung function subjects FEV$_1$ % predicted and FEV$_1$/FVC% are post-bronchodilator values. Data are expressed as mean ± SEM; *, $p<0.05$; **, $p<0.01$ versus smoking subjects.

TABLE 2 – Radioligand binding assay for adenosine receptors in A549 cell membranes

A549 membranes	[³H]-DPCPX A₁AR K_D (nM) Bmax (fmol/mg protein)	[³H]-ZM 241385 A₂ₐAR K_D (nM) Bmax (fmol/mg protein)	[³H]-MRE2029F20 A₂ᵦAR K_D (nM) Bmax (fmol/mg protein)	[³H]-MRE3008F20 A₃AR K_D (nM) Bmax (fmol/mg protein)
Controls	3.04±0.35 230 ± 25	2.99±0.31 110 ± 9	ND	3.65±0.38 220 ± 26
+ TNF-α (10 ng/ml)	2.88 ± 0.3 215 ± 27	3.03±0.32 167 ± 12*	ND	3.55±0.36 212 ± 24
+ IL-1β (1 ng/ml)	2.82±0.27 210 ± 23	2.89±0.27 173 ± 14*	ND	3.70±0.35 223 ± 22
+ TNFα (10 ng/ml) **AS 602868** (0.5 μM)	2.95±0.28 220 ± 29	3.01±0.29 104 ± 11	ND	3.44±0.35 217 ± 25
+ IL1β (1 ng/ml) **AS 602868** (0.5 μM)	2.93±0.25 227 ± 26	3.02±0.33 108 ± 10	ND	3.52±0.37 225 ± 20

Definition of abbreviations: ND not detectable; Data are expressed as mean ± SEM; *, $p < 0.01$ versus controls.

Column 1: [³H]-DPCPX A$_1$AR, K$_D$ (nM), Bmax (fmol/mg protein)

Column 2: [³H]-ZM 241385 A$_{2A}$AR, K$_D$ (nM), Bmax (fmol/mg protein)

Column 3: [³H]-MRE2029F20 A$_{2B}$AR, K$_D$ (nM), Bmax (fmol/mg protein)

Column 4: [³H]-MRE3008F20 A$_3$AR, K$_D$ (nM), Bmax (fmol/mg protein)

TABLE 3 - Time course of the effect of H_2O_2 on adenosine receptors in untransformed and PMA-transformed U937 cell membranes

Cell membranes	Time treatment H_2O_2 (100 μM)	[³H]-DPCPX A₁AR K_D (nM) Bmax (fmol/mg protein)	[³H]-ZM 241385 A₂ₐAR K_D (nM) Bmax (fmol/mg protein)	[³H]-MRE2029F20 A₂ᵦAR K_D (nM) Bmax (fmol/mg protein)	[³H]-MRE3008F20 A₃AR K_D (nM) Bmax (fmol/mg protein)
U937 PMA-untreated	0 h	2.34 ± 0.14 10.4 ± 0.8	1.69 ± 0.12 49 ± 2	3.28 ± 0.13 80 ± 4	3.86 ± 0.28 186 ± 12
	12 h	2.32 ± 0.11 9.5 ± 0.8	1.57 ± 0.11 46 ± 3	3.10 ± 0.12 50 ± 3*	3.52 ± 0.27 172 ± 13
	24 h	2.41 ± 0.18 9.7 ± 0.9	1.71 ± 0.09 47 ± 2	3.41 ± 0.10 22 ± 2*	3.60 ± 0.19 178 ± 13
	48 h	2.37 ± 0.10 9.2 ± 0.9	1.62 ± 0.14 48 ± 3	3.26 ± 0.19 19 ± 2*	3.67 ± 0.32 181 ± 15
U937 PMA-treated	0 h	2.21 ± 0.12 10.6 ± 0.8	1.74 ± 0.15 97 ± 8	3.11 ± 0.12 82 ± 3	3.65 ± 0.31 325 ± 32
	12 h	2.32 ± 0.13 10.1 ± 0.9	1.67 ± 0.12 93 ± 6	3.05 ± 0.13 57 ± 4*	3.57 ± 0.29 316 ± 32
	24 h	2.27 ± 0.11 10.5 ± 0.9	1.71 ± 0.13 95 ± 7	3.08 ± 0.12 28± 3*	3.55 ± 0.34 317 ± 28
	48 h	2.19 ± 0.12 10.5 ± 0.9	1.76 ± 0.14 95 ± 7	3.14 ± 0.14 24± 2*	3.61 ± 0.32 304 ± 30

Data are expressed as mean ± SEM ; n= 3-6 experiments; *, $p < 0.01$ vs untransformed or PMA-treated U937 cells in control conditions.

TABLE 4 - Concentration-dependent effect of H_2O_2 on adenosine receptors in untransformed and PMA-transformed U937 cell membranes

Cell membranes	Treatment H_2O_2 (24 h)	[³H]-DPCPX A_1AR K_D (nM) Bmax (fmol/mg protein)	[³H]-ZM 241385 $A_{2A}AR$ K_D (nM) Bmax (fmol/mg protein)	[³H]-MRE2029F20 $A_{2B}AR$ K_D (nM) Bmax (fmol/mg protein)	[³H]-MRE3008F20 A_3AR K_D (nM) Bmax (fmol/mg protein)
U937 PMA-untreated	-	2.34±0.14 10.4±0.8	1.69±0.12 49±2	3.28±0.13 80±4	3.86±0.28 186±12
	1 μM	2.31±0.10 9.7±0.6	1.59±0.11 47±3	3.38±0.15 62± 4**	3.55±0.23 170±10
	10 μM	2.37±0.15 9.9±0.9	1.65±0.12 48± 2	3.43±0.12 55± 4*	3.57±0.15 174±11
	50 μM	2.35±0.13 9.6±0.7	1.55±0.13 46±3	3.15±0.14 38± 3*	3.54±0.25 178±12
	100 μM	2.41±0.18 9.7±0.9	1.71±0.09 47± 2	3.41±0.10 19±2*	3.60±0.19 178±13
U937 PMA-treated	-	2.20 ± 0.12 10.6 ± 0.8	1.74 ± 0.15 97 ± 8	3.11 ± 0.12 82 ± 3	3.65 ± 0.31 325 ± 32
	1 μM	2.23 ± 0.11 10.1 ± 0.7	1.70 ± 0.11 95 ± 7	3.09 ± 0.13 68 ± 6**	3.72 ± 0.34 320 ± 28
	10 μM	2.21 ± 0.12 10.4 ± 0.5	1.73 ± 0.12 99 ± 6	3.13 ± 0.11 58 ± 4*	3.84 ± 0.27 319 ± 27
	50 μM	2.19 ± 0.13 10.2 ± 0.5	1.72 ± 0.12 98 ± 6	3.11 ± 0.12 45 ± 4*	3.82 ± 0.26 322 ± 30
	100 μM	2.27 ± 0.11 10.5 ± 0.9	1.71 ± 0.13 95 ± 7	3.08 ± 0.12 27± 3*	3.53 ± 0.28 317 ± 28

Data are expressed as mean ± SEM ; n= 3-6 experiments, **, $p<0.05$ and *, $p<0.01$, vs untransformed or PMA-transformed U937 cell membranes in control conditions.

TABLE 5 - Time course of the effect of SIN-1 on adenosine receptors in untransformed or PMA-transformed U937 cell membranes

Cell membranes	Time treatment SIN-1 (100 μM)	[³H]-DPCPX A₁AR K_D (nM) Bmax (fmol/mg protein)	[³H]-ZM 241385 A₂AAR K_D (nM) Bmax (fmol/mg protein)	[³H]-MRE2029F20 A₂BAR K_D (nM) Bmax (fmol/mg protein)	[³H]-MRE3008F20 A₃AR K_D (nM) Bmax (fmol/mg protein)
U937 PMA-untreated	0 h	2.34 ± 0.14 10.4 ± 0.8	1.69 ± 0.12 49 ± 2	3.28 ± 0.13 80 ± 4	3.86 ± 0.28 186 ± 12
	2 h	2.30 ± 0.09 9.6 ± 0.7	1.51 ± 0.13 48 ± 3	3.04 ± 0.11 76 ± 4	3.51 ± 0.25 171 ± 14
	4 h	2.28 ± 0.12 9.7 ± 0.8	1.55 ± 0.12 47 ± 3	3.10 ± 0.12 48 ± 3*	3.51 ± 0.25 171 ± 14
	6 h	2.39 ± 0.17 9.5 ± 0.9	1.69 ± 0.10 48 ± 2	3.28 ± 0.10 25 ± 3*	3.63 ± 0.18 173 ± 12
	12 h	2.33 ± 0.11 9.3 ± 0.8	1.63 ± 0.13 45 ± 3	3.26 ± 0.19 22 ± 2*	3.64 ± 0.26 175 ± 16
U937 PMA-treated	0 h	2.21 ± 0.12 10.6 ± 0.8	1.74 ± 0.15 97 ± 8	3.11 ± 0.12 82 ± 3	3.65 ± 0.31 325 ± 32
	2 h	2.31 ± 0.10 9.7 ± 0.8	1.51 ± 0.13 48 ± 3	3.04 ± 0.11 77 ± 4	3.51 ± 0.25 171 ± 14
	4 h	2.31 ± 0.11 10.2 ± 0.9	1.67 ± 0.12 95 ± 6	3.06 ± 0.11 52 ± 3*	3.57 ± 0.29 315 ± 28
	6 h	2.25 ± 0.10 10.4 ± 0.8	1.71 ± 0.13 96 ± 7	3.11 ± 0.10 23 ± 3*	3.55 ± 0.34 314 ± 26
	12 h	2.17 ± 0.11 10.3 ± 0.9	1.76 ± 0.14 98 ± 7	3.25 ± 0.12 21 ± 2*	3.61 ± 0.32 317 ± 29

Data are expressed as mean ± SEM; n= 3-6 experiments; *, $p<0.01$, vs untransformed or PMA-transformed cell membranes in control conditions.

TABLE 6 - Concentration-dependent effect of SIN-1 on adenosine receptors in untransformed or PMA-transformed U937 cell membranes

Cell membranes	Treatment SIN-1 (6 h)	[³H]-DPCPX A₁AR K_D (nM) Bmax (fmol/mg protein)	[³H]-ZM 241385 A_2AAR K_D (nM) Bmax (fmol/mg protein)	[³H]-MRE2029F20 A_2BAR K_D (nM) Bmax (fmol/mg protein)	[³H]-MRE3008F20 A₃AR K_D (nM) Bmax (fmol/mg protein)
U937 PMA-untreated	-	2.34±0.14 10.4±0.8	1.69±0.12 49±2	3.28±0.13 81±4	3.86±0.28 186±12
	1 µM	2.30±0.11 9.7±0.6	1.59±0.11 48±3	3.38±0.15 62± 4**	3.54±0.22 172±10
	5 µM	2.37±0.15 9.8±0.9	1.65±0.12 46± 2	3.43±0.12 45± 4*	3.56±0.14 175±10
	10 µM	2.36±0.13 9.6±0.7	1.55±0.13 47±3	3.15±0.14 26± 3*	3.53±0.24 177±13
	100 µM	2.29±0.18 10.1±0.9	1.71±0.09 48± 2	3.41±0.10 26±2*	3.60±0.19 178±13
U937 PMA-treated	-	2.21 ± 0.12 10.6 ± 0.8	1.74 ± 0.15 97 ± 8	3.11 ± 0.12 82 ± 3	3.65 ± 0.31 325 ± 32
	1 µM	2.23 ± 0.11 10.2 ± 0.7	1.66 ± 0.12 96 ± 7	3.08 ± 0.11 65 ± 4**	3.71 ± 0.33 325 ± 32
	5 µM	2.21 ± 0.12 10.5 ± 0.5	1.74 ± 0.13 97 ± 8	3.12 ± 0.12 46 ± 4*	3.83 ± 0.26 325 ± 32
	10 µM	2.19 ± 0.13 10.3 ± 0.5	1.63 ± 0.11 98 ± 7	3.10 ± 0.10 29 ± 3*	3.81 ± 0.27 322 ± 30
	100 µM	2.27 ± 0.11 10.4 ± 0.9	1.72 ± 0.12 96 ± 8	3.09 ± 0.11 27± 3*	3.52 ± 0.26 317 ± 28

Data are expressed as mean ± SEM; n=3-6 experiments; *, p<0.05; *, p<0.01 vs untransformed or PMA-transformed cell membranes in control conditions.

TABLE 7- Effect of various inflammatory stimuli on adenosine receptors in untransformed or PMA-transformed U937 cell membranes

Cell membranes	Treatment	[³H]-DPCPX A₁AR K_D (nM) Bmax (fmol/mg protein)	[³H]-ZM 241385 A₂ₐAR K_D (nM) Bmax (fmol/mg protein)	[³H]-MRE2029F20 A₂ᵦAR K_D (nM) Bmax (fmol/mg protein)	[³H]-MRE3008F20 A₃AR K_D (nM) Bmax (fmol/mg protein)
U937 PMA-untreated	-	2.34±0.14 10.4±0.8	1.69±0.12 49±2	3.28±0.13 80±4	3.86±0.28 186±12
	+ IL-1β	2.35±0.10 9.8±0.8	1.57±0.14 97±5*	3.38±0.22 74±6	3.77±0.35 285±17*
	+ TNF-α	2.37±0.13 10.2±0.9	1.61±0.15 102±5*	3.21±0.19 75±7	3.81±0.24 305±22*
	+IL-1β +TNF-α	2.36±0.11 10.5±0.7	1.71±0.16 116±8*°	3.16±0.25 78±9	3.92±0.29 906± 82*§
	+ H₂O₂ +IL-1β +TNF-α	2.38±0.15 10.7±0.8	1.75±0.13 120±10*°	3.27±0.17 18.7±1.5*	3.95±0.31 1050±95*§
U937 PMA-treated	-	2.21 ± 0.12 10.6 ± 0.8	1.74 ± 0.15 97 ± 8	3.11 ± 0.12 82 ± 3	3.65 ± 0.31 325 ± 32
	+ IL-1β	2.17 ± 0.10 10.4 ± 0.7	1.74 ± 0.15 146 ± 10*	3.15 ± 0.11 81 ± 4	3.46 ± 0.29 475 ± 28*
	+ TNF-α	2.19 ± 0.11 10.3 ± 0.6	1.74 ± 0.15 163 ± 11*	3.12 ± 0.10 84 ± 5	3.52 ± 0.34 512 ± 34*
	+IL-1β +TNF-α	2.35±0.13 10.6±0.7	1.67±0.14 193±11*°	3.27±0.15 80±5	3.63±0.32 1225± 105*§
	+ H₂O₂ +IL-1β +TNF-α	2.29±0.13 10.3±0.7	1.69±0.14 217±15*°	3.22±0.16 35±3*	3.75±0.31 1307± 112*§

Doses of different treatments: H_2O_2 (100 nM), IL-1β (1 ng/ml), TNF-α (10 ng/ml). Data are expressed as mean ± SEM. *, $p<0.01$ vs untransformed or PMA-transformed U937 cell membranes, respectively; °, $p<0.05$ vs untransformed or PMA-transformed U937 cell membranes in the presence of IL-1β or TNF-α; §, $p<0.01$ vs untransformed or PMA-transformed U937 cell membranes in the presence of IL-1β or TNF-α.

TABLE 8 – Adenosine receptors in HMC-1 cell membranes

HMC-1cell membrane treatments	[^{3}H]-DPCPX A$_1$AR K$_D$ (nM) Bmax (fmol/mg protein)	[^{3}H]-ZM 241385 A$_{2A}$AR K$_D$ (nM) Bmax (fmol/mg protein)	[^{3}H]-MRE2029F20 A$_{2B}$AR K$_D$ (nM) Bmax (fmol/mg protein)	[^{3}H]-MRE3008F20 A$_3$AR K$_D$ (nM) Bmax (fmol/mg protein)
-	N.D.	1.92±0.18 75±8	2.60±0.22 120±11	1.67±0.13 315±28
24 h H$_2$O$_2$ (100 μM)	N.D.	1.85±0.16 72±7	2.72±0.25 116±10	1.55±0.16 331±26
6 h SIN-1 (100 μM)	N.D.	1.78±0.17 77±8	2.53±0.21 127±12	1.63±0.14 322±31

Data are expressed as mean ± SEM. n=3 experiments.

Figure 2 - Immunolocalization of A_{2A} adenosine receptor in peripheral lung sections from a COPD patient
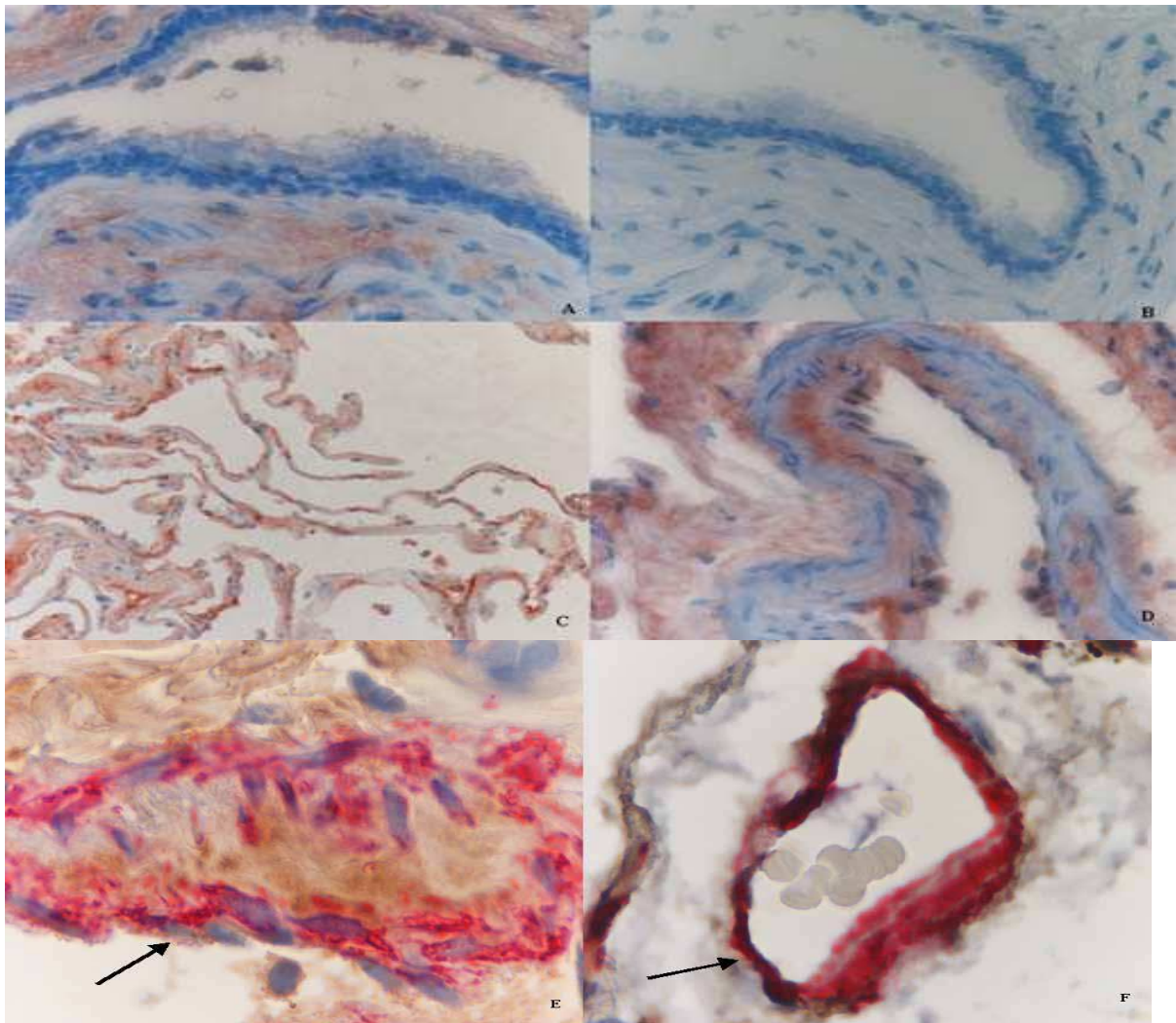
A_{2A}ARs immunostaining (red) in the bronchiole of COPD patient (A). Negative control section stained with the same concentration of non-specific isotype control antibody (B). Red immunostaining of cells in the alveolar septa (C) and a peripheral lung vessel (D). Magnification x400. Results are representative of those from 12 smokers with normal lung function and 6 mild to moderate stable COPD. Immunolocalization of A_{2A}AR in peripheral lung sections from a COPD patient. (E) bronchiolar wall double immunostained for smooth muscle specific actin (red), a marker of smooth muscle cells, and A_{2A} receptor (dark brown), x1000; (F) vessel double immunostained for smooth muscle specific actin (red) and A_{2A}AR (dark brown), x1000. Results are representative of those from 6 smokers with normal lung function and 6 mild to moderate stable COPD.

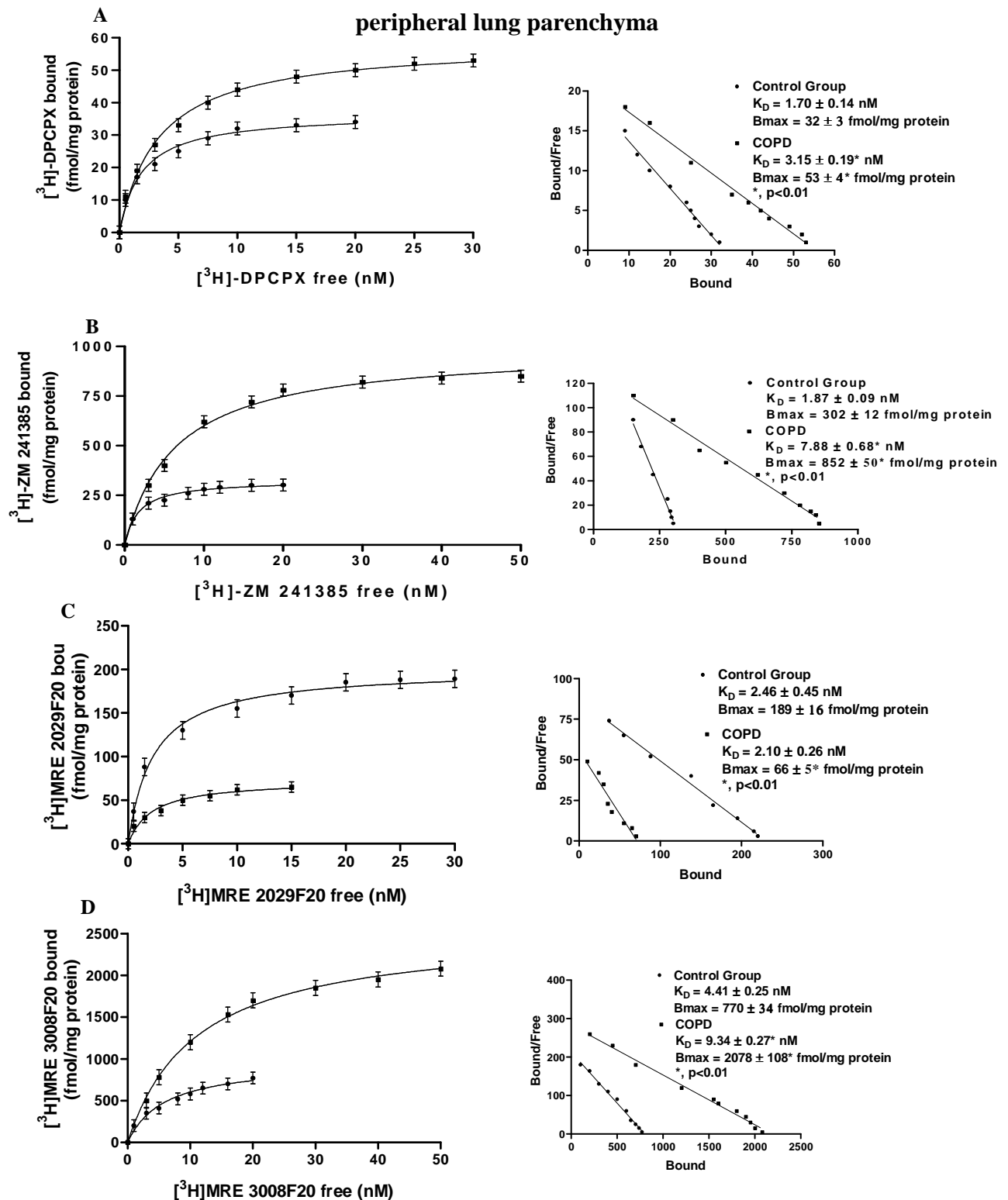**Figure 3 - Immunolocalization of A_1 adenosine receptor in peripheral lung sections from smoker healthy subject and COPD patient**
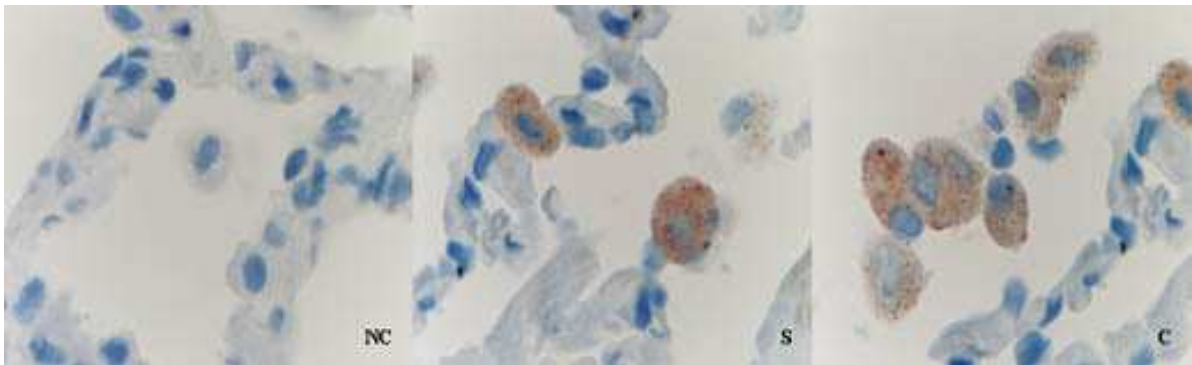
Alveolar septa in peripheral lung sections immunostained (red) for A_1ARs from a smoker with normal lung function (S) and a COPD patient (C) both at x1000. Alveolar septa in the negative control (NC) section stained with the same concentration of non-specific isotype control antibody, x1000. Results are representative of those from 12 smokers with normal lung function and 6 mild to moderate stable COPD.

Figure 4 - Immunolocalization of A_3 adenosine receptor in peripheral lung sections from a COPD patient
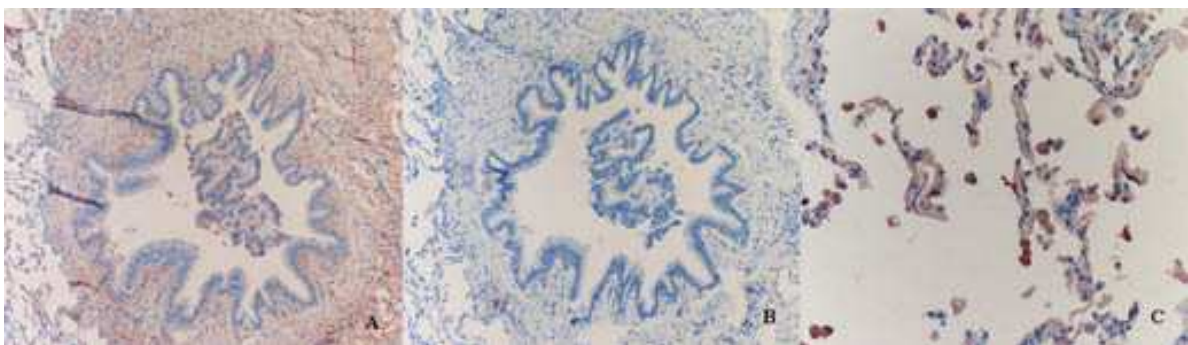
A bronchiole immunostained (red) for A_3AR, x200 (A); the same bronchiole in the negative control section stained with the same concentration of non-specific isotype control antibody, x200 (B); cells in the alveolar septa immunostained for A_3AR (red), x200 (C). Results are representative of those from 12 smokers with normal lung function and 6 mild to moderate stable COPD.

Figure 5 - Immunolocalization of A_{2B} adenosine receptor in peripheral lung sections from a COPD patient
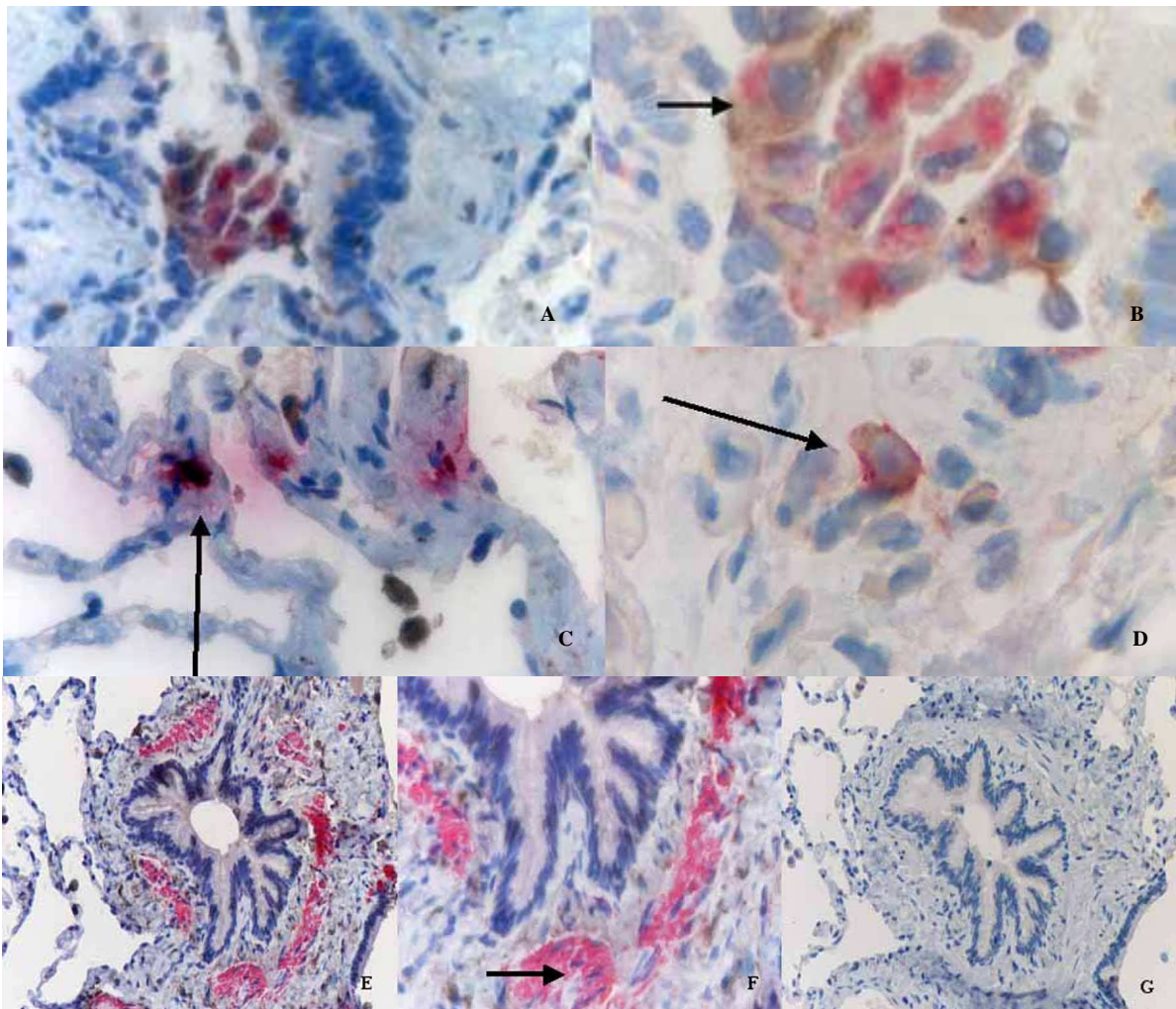

Cells inside the lumen of a bronchiole are double immunostained (black arrow) for CD68 (red), a marker of alveolar macrophages, and $A_{2B}AR$ (dark brown). Magnification x400 (A) and x1000 (B). Cells inside the lumen of a bronchiole double immunostained (black arrow) for tryptase (red), a marker of mast cells, and $A_{2B}AR$ (dark brown). Magnification x400 (C) and x1000 (D). A bronchiole immunostained for smooth muscle specific actin (red), a marker of smooth muscle cells, and $A_{2B}AR$ (dark brown), x200 (E) and x400 (F) showing the absence of co-localization of $A_{2B}AR$ in smooth muscle cells. (G) the same bronchiole in the negative control section stained with the same concentration of non-specific isotype control antibody, x200. Results are representative of those from 6 smokers with normal lung function and 6 mild to moderate stable COPD.

**Figure 6 - Density and affinity of A_1, A_{2A}, A_{2B} and A_3 adenosine receptors in peripheral lung parenchyma**

A

Control Group
$K_D = 1.70 \pm 0.14$ nM
Bmax = 32 ± 3 fmol/mg protein
COPD
$K_D = 3.15 \pm 0.19^*$ nM
Bmax = $53 \pm 4^*$ fmol/mg protein
*, p<0.01

B

Control Group
$K_D = 1.87 \pm 0.09$ nM
Bmax = 302 ± 12 fmol/mg protein
COPD
$K_D = 7.88 \pm 0.68^*$ nM
Bmax = $852 \pm 50^*$ fmol/mg protein
*, p<0.01

C

Control Group
$K_D = 2.46 \pm 0.45$ nM
Bmax = 189 ± 16 fmol/mg protein
COPD
$K_D = 2.10 \pm 0.26$ nM
Bmax = $66 \pm 5^*$ fmol/mg protein
*, p<0.01

D

Control Group
$K_D = 4.41 \pm 0.25$ nM
Bmax = 770 ± 34 fmol/mg protein
COPD
$K_D = 9.34 \pm 0.27^*$ nM
Bmax = $2078 \pm 108^*$ fmol/mg protein
*, p<0.01

Saturation curves of [³H]DPCPX binding to human A_1ARs (A) and of [³H]ZM 241385 binding to human A_{2A}ARs (B), of [³H]MRE 2029F20 binding to human A_{2B}ARs (C) and of [³H]MRE 3008F20 binding to human A_3ARs (D) on lung parenchyma membranes from COPD patients and control group. Scatchard plots of the same data are shown in the right. Results are reported as the mean ± SEM from 8 smokers with normal lung function and 8 mild to moderate stable COPD (*, p<0.01 versus control smokers).

54

Figure 7 - Expression of A_1, A_{2A}, A_{2B} and A_3 adenosine receptors mRNA in peripheral lung parenchyma
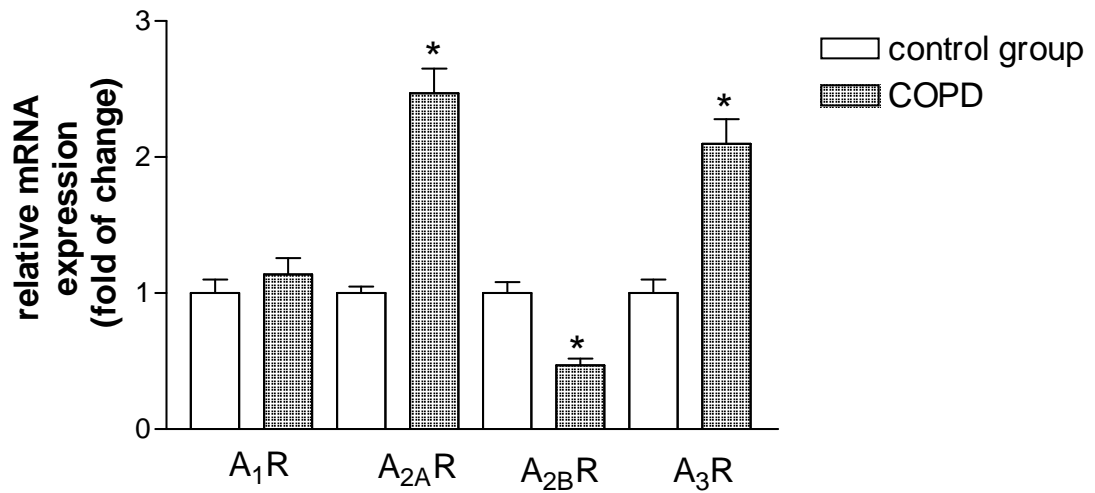

The relative adenosine receptor/GAPDH mRNA ratio for each adenosine receptor is expressed as fold of change in COPD patients compared to the control group of smokers with normal lung function. $A_{2A}R$ and A_3R mRNAs are significantly increased in COPD compared with control group (*, $p<0.01$). $A_{2B}R$ mRNA is significantly decreased in COPD compared with controls (*, $p<0.01$). A_1R mRNA is not significantly changed between the 2 groups. Results are representative of 8 smokers with normal lung function and 8 mild to moderate stable COPD.

Figure 8 - A$_{2B}$ adenosine receptor expression in human alveolar macrophages of control smokers and COPD patients
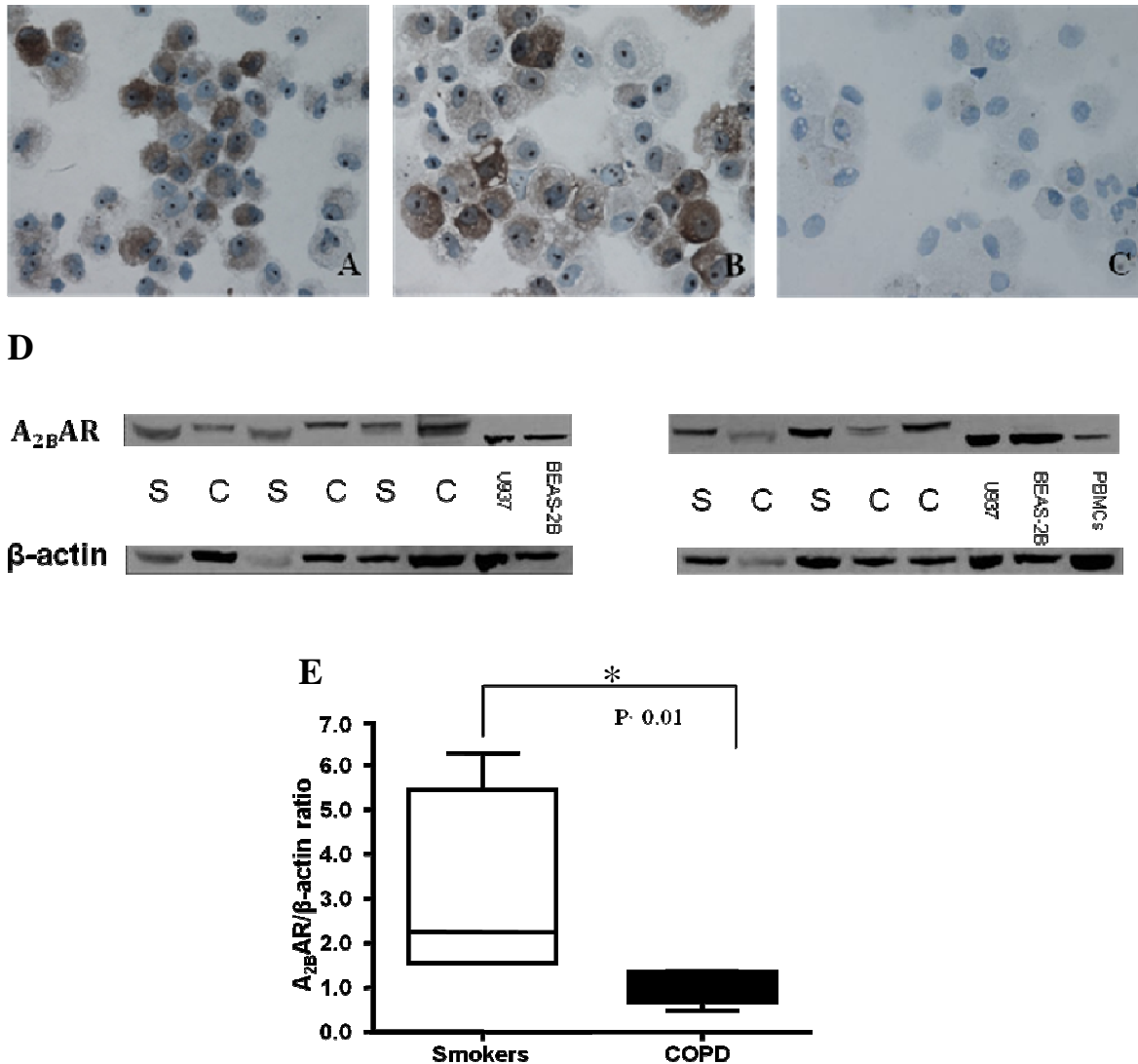
Representative immunocytochemical analysis of A$_{2B}$AR expression in bronchoalveolar lavage macrophages from a control smoker with normal lung function (A) and a smoker with COPD (B). (C) Negative control (non-specific Ig). Results are representative of those seen in 13 individual patients (6 healthy smokers/7 smokers with COPD). Western blotting analysis of A$_{2B}$AR expression in bronchoalveolar macrophages obtained from COPD (D) patients and control smokers (S) with normal lung function. Whole cell extracts from BEAS-2B, U937 and peripheral blood mononuclear cells (PBMCs) are used as positive controls (D). (E) Densitometric analysis of A$_{2B}$AR expression as a ratio of β-actin as a loading control. The median and interquartile ranges for each treatment are presented as a box and whiskers plot (n = 3-6).

**Figure 9 - Correlation between binding parameters of
adenosine receptors and clinical features**
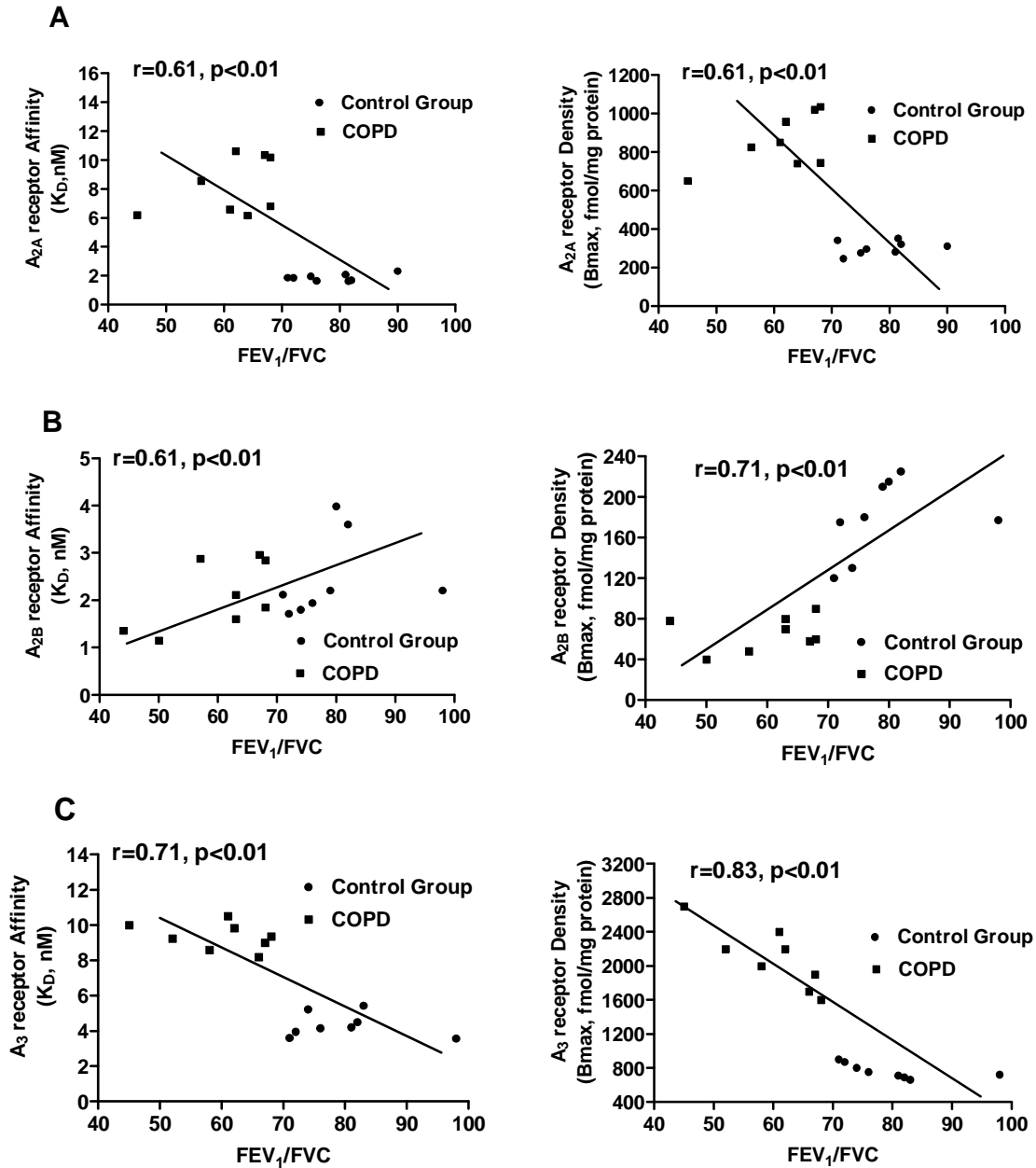
Correlation between the affinity and density of A_{2A}, A_3, and A_{2B}ARs and forced expiratory volume in one second (FEV_1)/forced vital capacity (FVC) ratio. Results are representative of 8 smokers with normal lung function (black circles) and 8 mild to moderate stable COPD (black squares).

**Figure 10 - Effect of inflammatory stimuli on adenosine receptor expression in A549 cells**
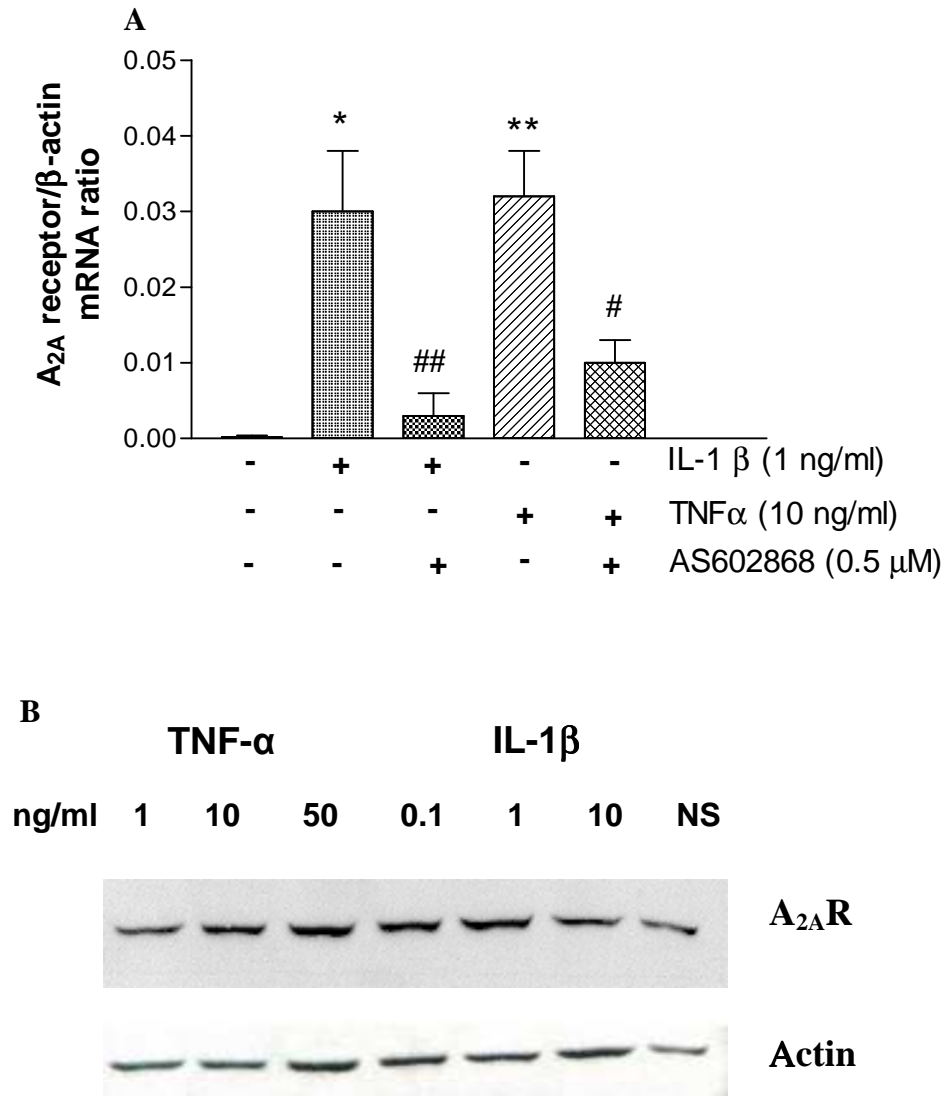
IL-1β (1 ng/ml) and TNF-α (10 ng/ml) increase $A_{2A}AR$ mRNA expression (A) in A549 cells. The effect of IL-1β and TNF-α is blocked by pre-treatment with NF-κB inhibitor AS602868 (0.5 μM). $A_{2A}AR$ mRNA expression is expressed relative to that of β-actin. *, $p<0.05$ and **, $p<0.01$ versus unstimulated cells and [#,] $p<0.05$ versus TNF-α stimulated cells and [##,] $p<0.01$ versus IL-1β stimulated cells. Similar effects of IL-1β and TNF-α on $A_{2A}AR$ expression were observed by Western blot analysis (B). Results are representative of 3 independent experiments.

**Figure 11 - Presence of adenosine receptors in untransformed or**

PMA-transformed U937 membranes
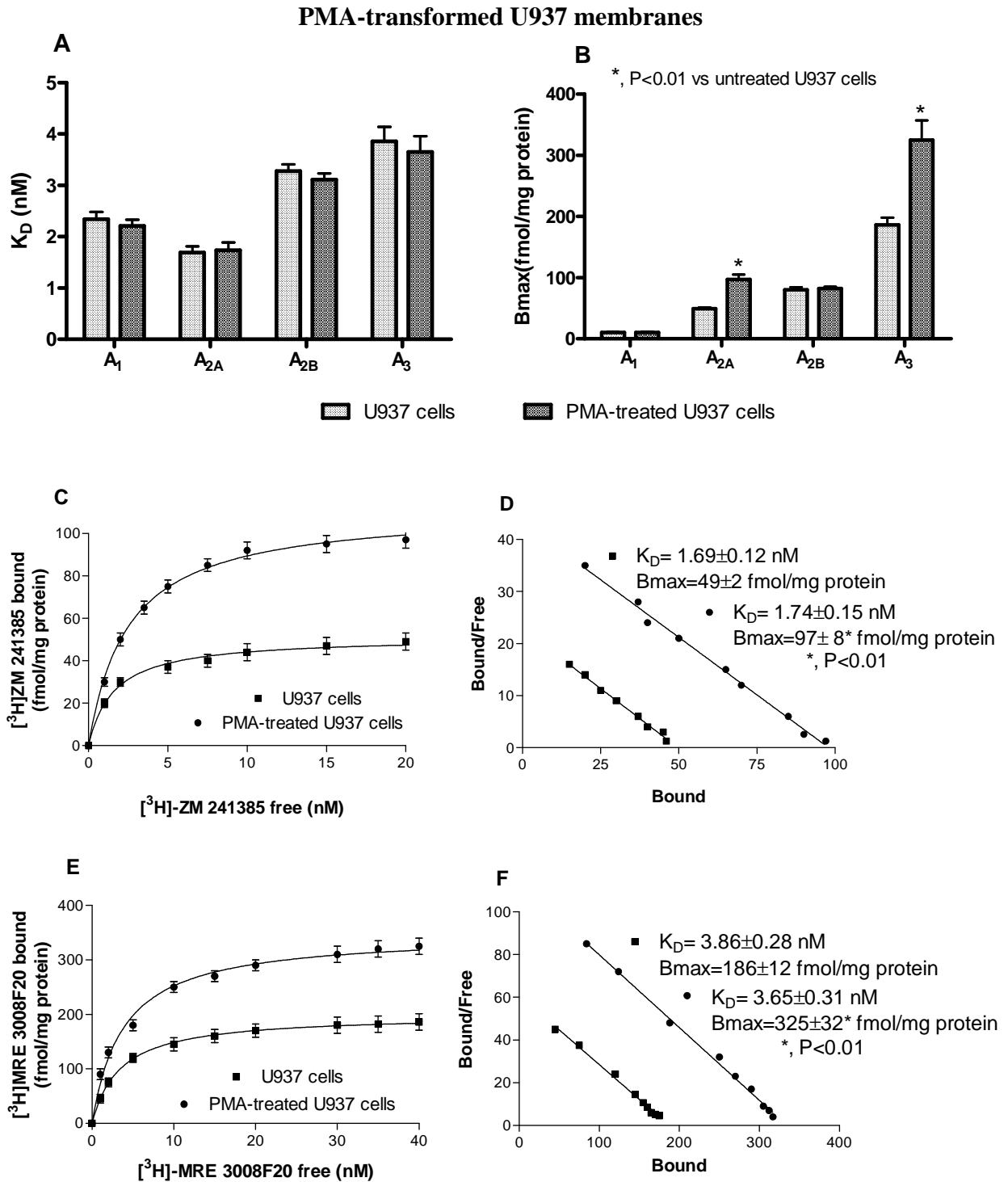
A_1, A_{2A}, A_{2B} and A_3 ARs affinity (K_D, nM; A) and density (Bmax, fmol/mg protein; B) in untrasformed or PMA-trasformed U937 membranes. Saturation curves of $A_{2A}AR$ (C) and A_3AR (E) in untransformed or PMA-transformed U937 membranes. Scatchard plot of the same data are represented (D and F). Binding parameters such as affinity (K_D, nM) and density (Bmax, fmol/mg protein) are also reported. The data are expressed as mean ± SEM; *, $p < 0.01$ versus untreated U937 membranes.

59

Figure 12 – Effect of H_2O_2, SIN-1 and cytokines on A_{2B} adenosine receptors in untransformed or PMA-transformed U937 membranes
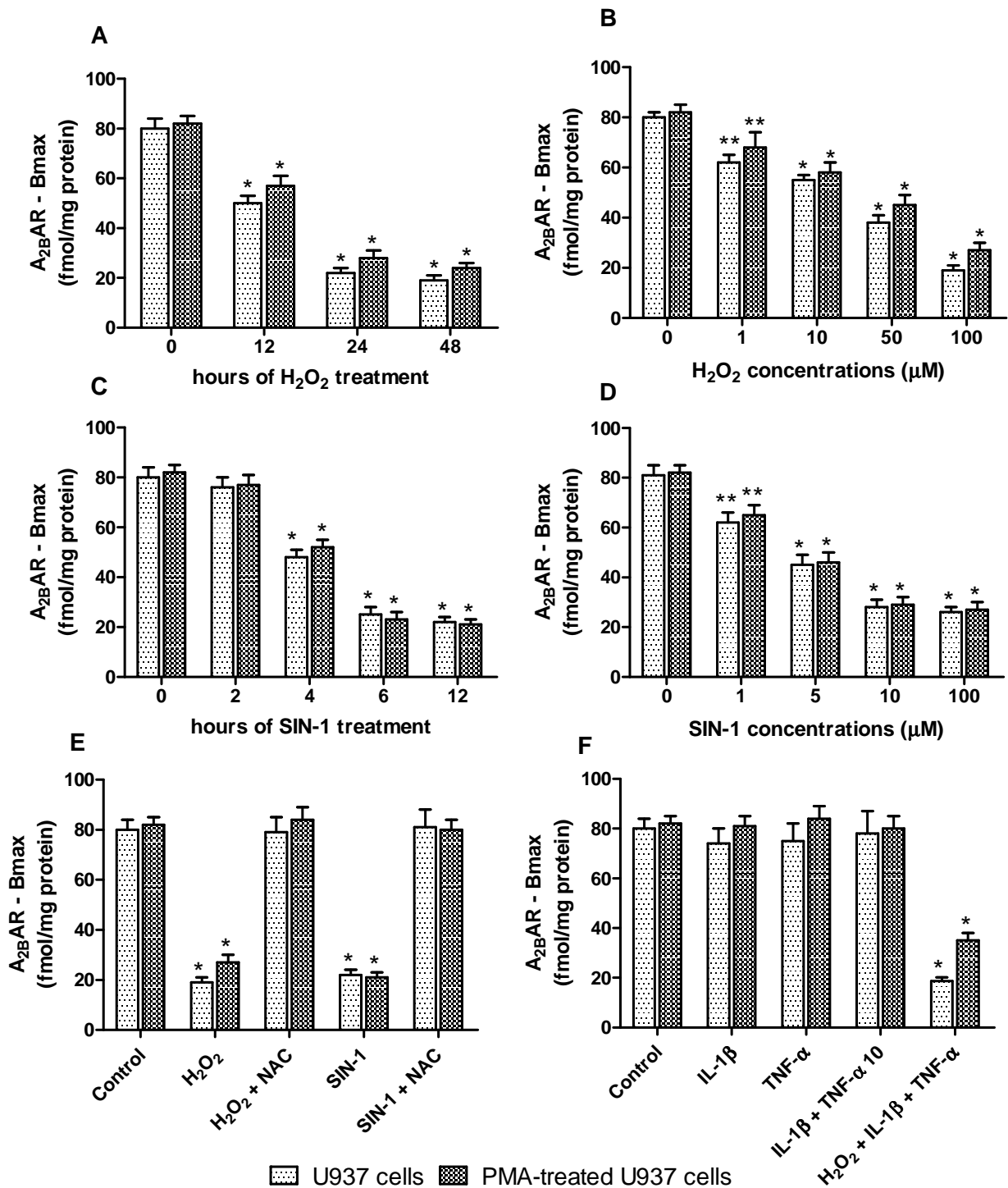

$A_{2B}AR$ density (Bmax, fmol/mg protein) at various incubation times (12, 24, 48 h) (A) and at different doses (1, 10, 50, 100 μM) (B) of H_2O_2. $A_{2B}AR$ density was also evaluated after 2, 4, 6, 12 h (C) and by using 1, 5, 10, 100 μM (D) of SIN-1. Effect of H_2O_2 (100 μM) and SIN-1 (100 μM) in the absence or in the presence of NAC (100 μM) (E). Effect of IL-1β (1 ng/ml), TNF-α (10 ng/ml), IL-1β + TNF-α, H_2O_2 (100 μM) + IL-1β + TNF-α on $A_{2B}AR$ density (F). The data are expressed as mean ± SEM; **, p<0.05; *, p<0.01 vs untreated U937 membranes.

60

Figure 13 - Effects of H_2O_2 and SIN-1 of A_{2B} adenosine receptors binding parameters on U937 cells
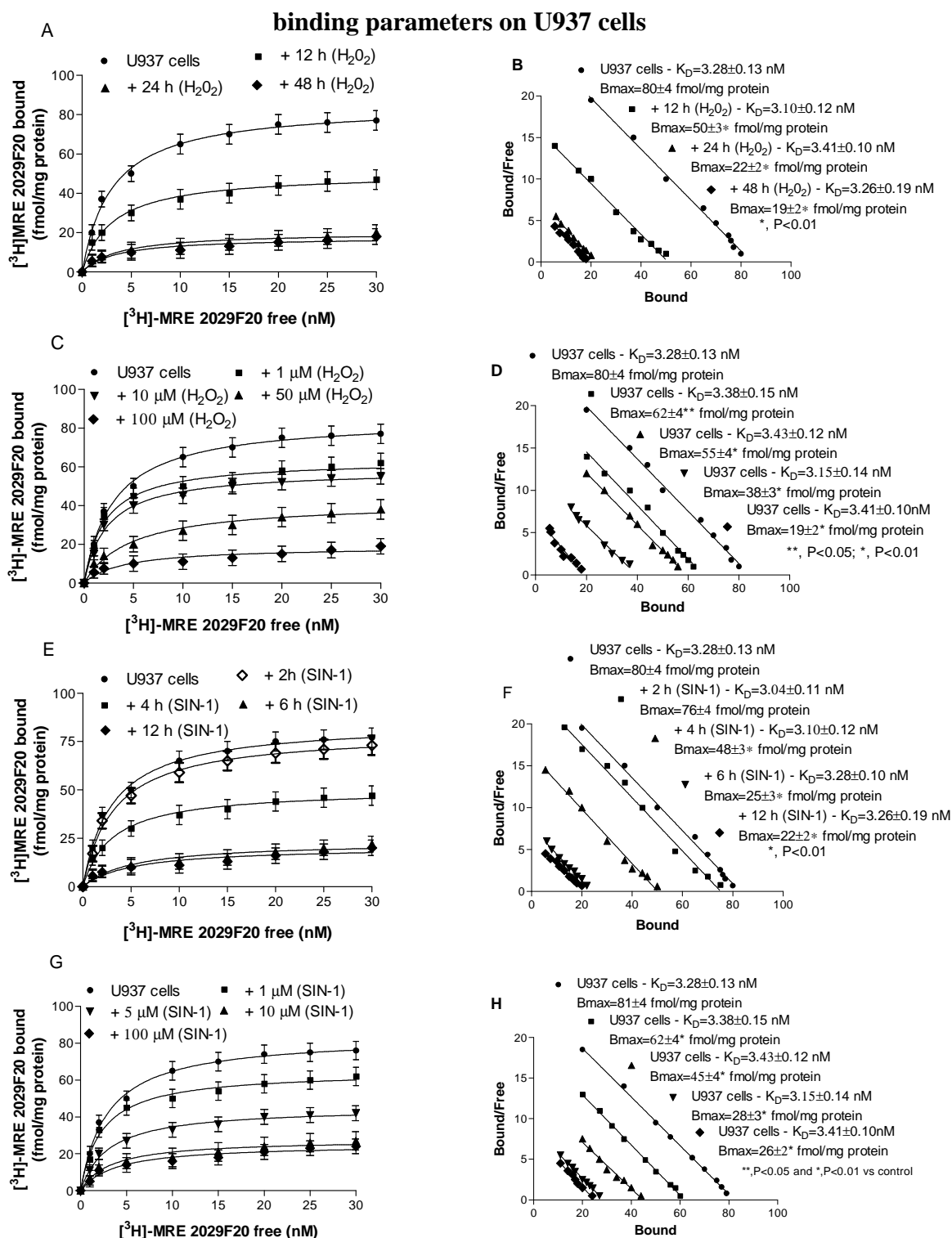

[³H] MRE 2029F20 saturation curves of A_{2B}ARs in the absence and in the presence of H_2O_2 (A and C) and SIN-1 (E and G) at different times and concentrations. Scatchard plot of the same data are shown after H_2O_2 (B and D) and SIN-1 (F and H) treatments. Binding parameters such as affinity (K_D, nM) and density (Bmax, fmol/mg protein) are also reported. The data are expressed as mean ± SEM; **, $p<0.05$; *, $p<0.01$ vs U937 membranes.

Figure 14 - Time course effect of H_2O_2 and SIN-1 on A_{2B} adenosine receptors in U937 cells
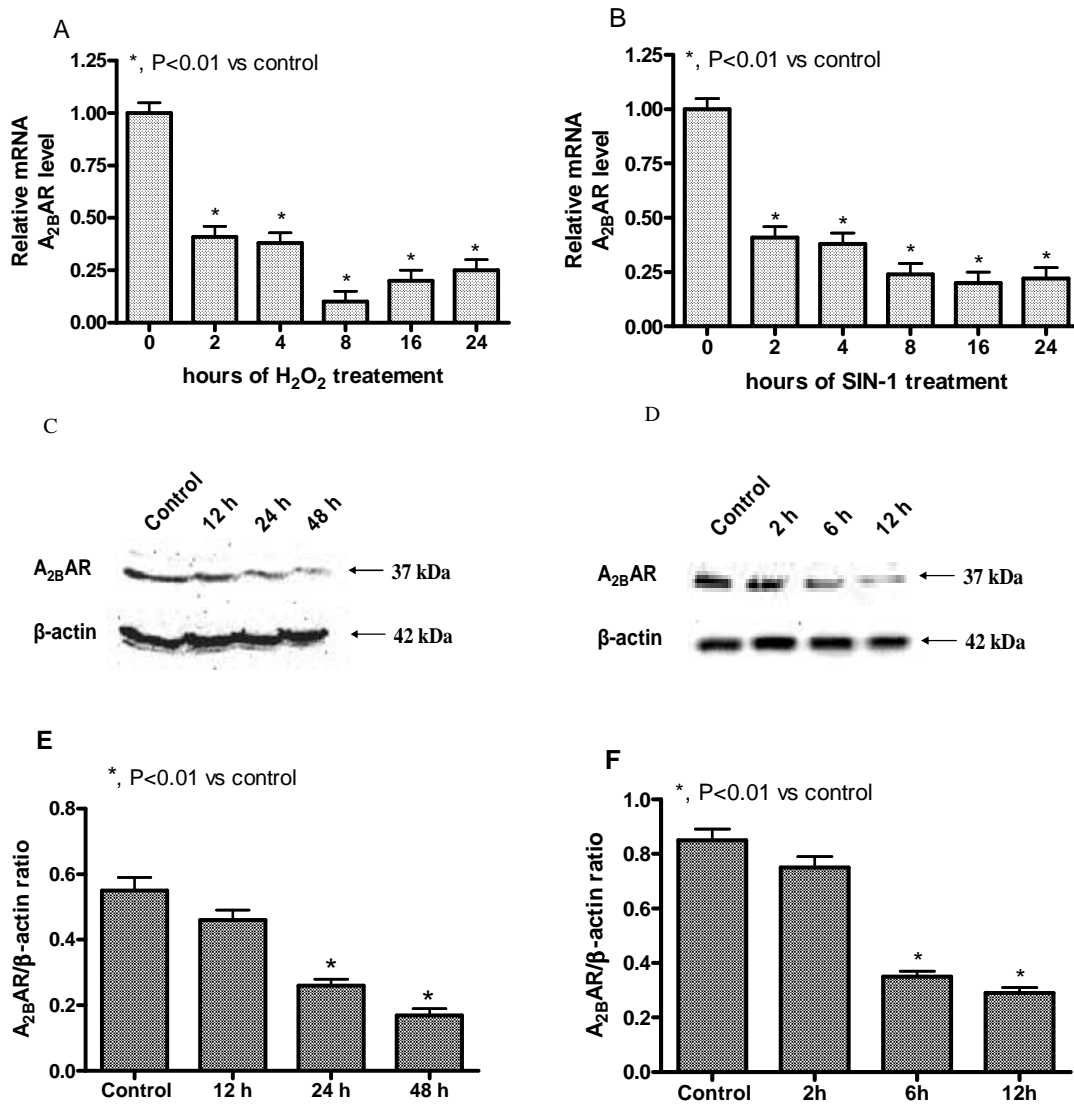

A_{2B}ARs mRNA was quantified, relative to β-actin mRNA, by Real-Time RT-PCR (A and B). Western blotting analysis of A_{2B}AR protein expression following treatment of U937 cells with H_2O_2 or SIN-1 (100 μM) by using typical anti-adenosine receptor polyclonal antibodies of protein extracts (C and D) and the relative densitometric analysis (E and F). *, p <0.01 vs control.

Figure 15 - Effect of A_{2B} adenosine receptor-silencing on relative A_{2B} adenosine receptor mRNA and protein expression in U937 cells
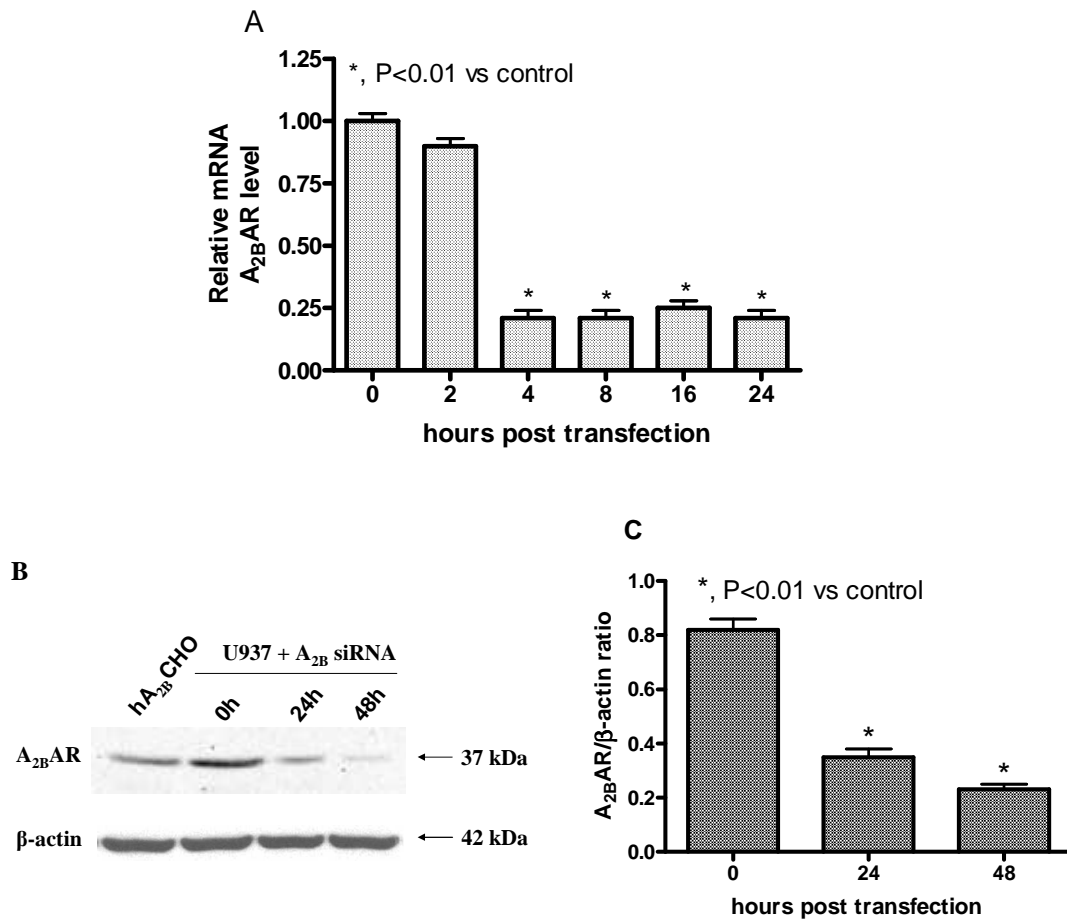
The effect of $A_{2B}AR$ siRNA on relative $A_{2B}AR$ mRNA as determined by RT-PCR (A) and protein expression as measured by western blotting (B). Chinese hamster ovary (CHO) cells expressing human $A_{2B}AR$ are used as a positive control ($hA_{2B}CHO$). The relative densitometric analysis for protein expression is quantified in (C) against β-actin as a loading control. Data are expressed as mean ± SEM of 3-6 independent experiments. *, p<0.01 with respect to control siRNA transfected cells.

Figure 16 - Effect of NECA on cAMP and proliferation assays in U937 cells
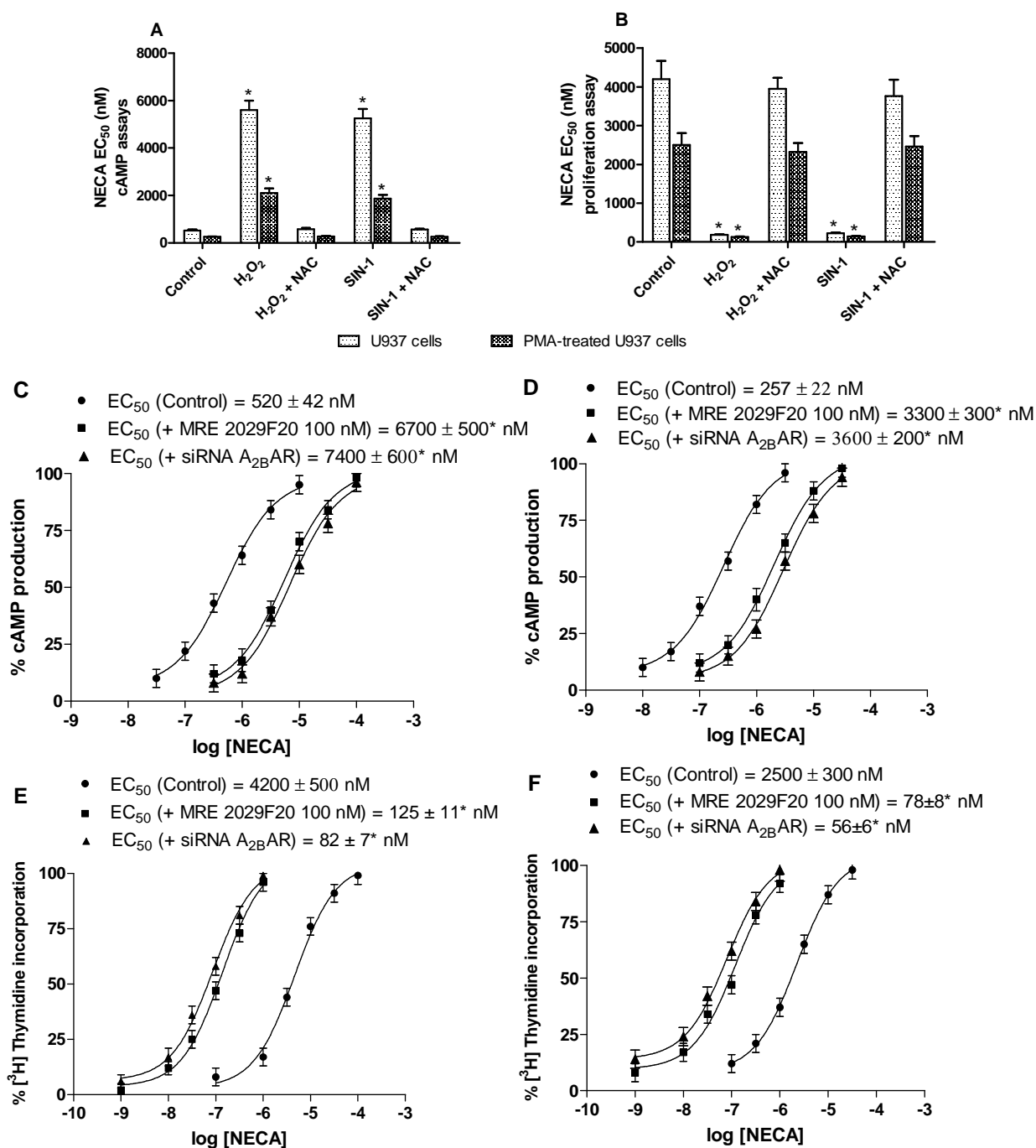
Effect of the adenosine receptor agonist NECA on cAMP (A) and cell proliferation (B) assays in untransformed and PMA-transformed U937 cells. Histograms represent the potency of NECA (EC_{50}) following exposure of cells to H_2O_2 (100 μM) and SIN-1 (100 μM) in the presence and absence of NAC (100 μM). Concentration-response curves of NECA (1 nM-100 μM) on inducing cAMP (C and D) and cell proliferation (E and F) in the absence and in the presence of MRE 2029F20 (1 μM) and after $A_{2B}AR$ expression was reduced by siRNA transfection of untransformed (C and E) and PMA-transformed U937 cells are shown (D and F). Results are presented as means±SEM of 3-6 independent experiments. *, p<0.01 compared with control.

Discussion

In this study, we report the localization, mRNA expression, affinity and density of A_1, A_{2A}, A_{2B} and A_3ARs in peripheral lung parenchyma from age-matched smokers with normal lung function (control group) and COPD patients. We have examined the peripheral lung because this is the major site of airflow obstruction in COPD patients and histopathological studies have demonstrated that most of the airway inflammation in COPD is localized in the small airways and lung parenchyma [136].

Radioligand binding and RT-QPCR experiments have demonstrated a significant decrease of the affinity, associated with an increased density of the A_{2A} and A_3ARs protein and mRNA in COPD patients compared with the control group.

In vitro studies have demonstrated that the long-term exposure of target cells to adenosine cause desensitization of adenosine receptors [9]. We hypothesize that high concentrations of adenosine in the peripheral lung of COPD patients might mediate desensitization of the A_{2A} and A_3ARs. Consequently the up-regulation of the A_{2A} and A_3ARs may represent a compensatory response mechanism and may contribute to the anti-inflammatory effects mediated by the stimulation of these receptors. This is in keeping with the increased expression in vitro of $A_{2A}AR$ after exposure of human lung type 2 alveolar-like cells A549 to the pro-inflammatory cytokines IL-1β and TNF-α, through the activation of the key pro-inflammatory NF-κB pathway. Radioligand binding experiments show the presence of A_1, A_{2A} and A_3ARs on A549 membranes. The pro-inflammatory cytokines IL-1β and TNF-α are able to increase the $A_{2A}ARs$ density but not that of A_1 and A_3ARs. On the contrary $A_{2B}ARs$ are not detectable on A549 membranes.

In the lower airways of patients with COPD compared to smokers with normal lung function both IL-1β and TNF-α expression are increased [137] and the NF-κB pathway is activated [128]. Consistent with this hypothesis, stimulation of the A_{2A} and A_3ARs in vitro has anti-inflammatory effects [60, 125]. Interestingly, we have also find a direct correlation between K_D and Bmax and FEV_1/FVC ratio and of A_{2A}, and A_3ARs indicating that may be involved in the pathogenesis of airflow obstruction in COPD. However, as with all association studies it is necessary to confirm the data in other groups of COPD and until selective agonists or antagonists are used clinically in patients with COPD we are unlikely to be able to resolve whether specific subsets of adenosine receptors have distinct roles in the pathogenesis or progression of COPD.

There is also a significant decrease of the affinity, associated with an increased density of the A_1ARs in COPD patients compared with the control group. However, both the radioligand binding and immunohistochemical studies demonstrate a low A_1ARs density in the peripheral lung parenchyma suggesting a secondary role for this receptor in the pathogenesis of COPD in contrast to the protective role of A_1ARs in the pulmonary inflammation and injury seen in ADA-deficient mice [45].

We have demonstrated that $A_{2B}ARs$ are expressed only in mast cells and macrophages and that there is reduced expression of their protein (Bmax) and mRNA in peripheral lung parenchyma from COPD patients compared with the control group. This data suggests that there may be a compensatory feedback mechanism regulating $A_{2B}ARs$ expression. Such reduction could be explained as the consequence of an increased adenosine concentration in peripheral lung with secondary down regulation of the $A_{2B}ARs$. The role of mast cells in the pathogenesis of COPD is controversial [136] but, in vitro, $A_{2B}ARs$ stimulation has shown to enhance the release of pro-inflammatory mediators from human lung mast cells [48, 138]. On the contrary, the number of alveolar macrophages is highly increased in the peripheral lung of COPD patients compared with control smokers and they seem to represent the key inflammatory cells in the pathogenesis of COPD [137]. Furthermore, there is a significant inverse correlation between binding parameters of the $A_{2B}ARs$ and FEV_1/FVC ratio suggesting a potential role of this receptor in the pathogenesis of airflow obstruction in COPD. A significant decrease of $A_{2B}ARs$ in BAL from patients with COPD compared to an age-matched group of control smokers with normal lung function was reported. Using the U937 cell line as a model of a monocyte/macrophage-like cells the oxidative (H_2O_2) and nitrosative (SIN-1) stress cause a selective decrease (~70%) in $A_{2B}AR$ mRNA and protein expression without affecting receptor affinity. This reduction in $A_{2B}AR$ expression by H_2O_2 and SIN-1 was blocked by the anti-oxidant NAC. In contrast, no effect of oxidative stress nor nitrosative stress on $A_{2B}AR$ expression was observed in the mast cell line HMC-1. The expression of $A_{2B}AR$ was not affected by pro-inflammatory cytokines. The attenuation of $A_{2B}AR$ expression or activity by H_2O_2 or SIN-1, by a specific antagonist or by using $A_{2B}AR$ specific siRNA affected both cell activation and proliferation. U937 proliferation is increased under these conditions and this may contribute to the increased proliferation of alveolar macrophages of smokers as previously demonstrated [139]. These data together with the prolonged survival of these cells in the lungs of smokers may contribute to the increased accumulation of alveolar macrophages present in the COPD lung [136, 140]. Undifferentiated U937 cells express all four adenosine receptor subtypes (A_1,

A_{2A}, A_{2B} and A_3ARs) with different affinity and density values. Differentiation of U937 cells towards a more mature macrophage-like phenotype induces an increase of A_{2A} and A_3ARs without affecting the expression of A_1 and A_{2B}ARs. The induction of A_{2A} and A_3AR expression may account for the altered sensitivity of these cells to NECA stimulation.

Increased levels of many pro-inflammatory cytokines, including IL-1β and TNF-α, have been reported in COPD and are known to regulate in vitro the expression of ARs in many cell types [141, 142]. It has been demonstrated that both IL-1β and TNF-α were able to induce A_{2A}AR mRNA and protein expression in epithelial cells through an NF-κB mediated process [143]. In untransformed U937 cells, IL-1β and TNF-α were both able to significantly increase A_{2A} and A_3ARs density to a similar extent and the co-stimulation resulted in a further enhancement of A_{2A} and A_3ARs expression. Similar results were obtained in PMA-transformed U937 cells even though the basal expression of these receptors is enhanced during the PMA-induced differentiation process. The addition of H_2O_2 to the pro-inflammatory stimulus, which may reflect a plausible condition present in the COPD lung, did not affect A_{2A} or A_3AR expression although it induced a significant reduction in A_{2B}AR expression. The in vitro effects of some pro-inflammatory cytokines and oxidative/nitrosative stress on the expression of ARs may explain the altered receptor expression in peripheral lung parenchyma from COPD patients compared with smokers with normal lung function as previously reported. In A549 cells the mechanism by which IL-1β and TNF-α enhanced A_{2A}AR mRNA expression relied upon differential use of alternative promoters or of distinct NF-κB binding sites in the A_{2A}AR promoter to regulate mRNA expression [143]. The mechanisms by which PMA and inflammatory mediators control A_{2A}AR expression in these U937 cells is unknown but clearly indicates distinct pathways compared to those operating for the A_{2B}AR. H_2O_2 and SIN-1 both induced a significant time- and concentration-dependent decrease in A_{2B}AR mRNA and protein expression which was reversed by NAC. The effect of oxidative/nitrosative stress on mRNA transcription is similar to that seen with HDAC2 expression in these cells [144]. It would be interesting to investigate whether similar mechanisms of transcriptional control occur for both A_{2B}ARs and HDAC2 protein and mRNA. HDAC2 protein loss is mediated through post-translational modification and subsequent degradation in the proteosome [145]. In contrast, HDAC2 mRNA degradation may be linked to changes in the activity of the hypoxia-related transcription factor HIF-1α or possibly to effects on mRNA stability

induced by oxidative stress [146]. The functional role of the $A_{2B}AR$ expressed in U937 cells in regulating their proliferation and cAMP production was well established. The potency of NECA, a pan-adenosine receptor agonist, on cAMP stimulation and cell proliferation was modulated after the treatment with oxidative/nitrosative stress to the same extent obtained when incubating these cells with the $A_{2B}AR$ antagonist MRE 2029F20 and in cells pre-treated with $A_{2B}AR$ siRNA to reduce $A_{2B}AR$ expression. NECA-induced effects on cAMP accumulation were abolished in cells in which $A_{2B}AR$ was knocked-down using a selective anti-human $A_{2B}AR$ siRNA compared with scramble-transfected cells. The reduced content of cAMP of alveolar macrophages can be considered an index of increased cell activation, because in vitro the treatment of alveolar macrophages with both β_2-receptor agonists or selective inhibitors of the phosphodiesterase (PDE)4 enzyme isoform increases the content of cAMP inside these cells and decreases their release of pro-inflammatory mediators representing effective treatment of COPD patients [147, 148]. Differential effects of $A_{2B}AR$ signalling were reported in several cellular and animal models suggesting a dual role of this receptor in airway inflammation [149]. In particular $A_{2B}AR$ activation mediated the increase of typical pro-inflammatory cytokines demonstrating that $A_{2B}AR$ antagonism can attenuate lung inflammation [49, 150]. In conclusion, these novel data highlight that $A_{2B}ARs$ are significantly reduced in BAL macrophages from COPD patients compared to control healthy smokers. We also demonstrated in U937 cells that $A_{2B}AR$ mRNA and protein expression is selectively decreased by oxidative/nitrosative stress, but not by inflammatory mediators. This is associated with increased proliferation and decreased cAMP content, a marker of cell activation. These data support the potential for modulating $A_{2B}AR$ function in alveolar macrophages as a novel pharmacological treatment for COPD.

ADENOSINE RECEPTORS IN MALIGNANT PLEURAL MESOTHELIOMA PATIENTS

Malignant pleural mesothelioma

Malignant pleural mesothelioma (MPM) is an aggressive, treatment-resistant tumor, and there is no approved targeted therapy for this disease [151]. The pathogenesis of MPM has remained obscure due to the long latency time until development of disease, up to 20 years [152]. Asbestos is linked to MPM pathogenesis, and the mechanisms of asbestos carcinogenesis are still under investigation [153]. There are also other factors relevant for the development of MPM, including other mineral fibers, genetic predisposition and presence of SV40 (a DNA tumor virus) [154]. In Western Europe, the incidence of MPM appears to be leveling, probably due to the actions taken to restrict asbestos exposures [155]. Worldwide, however, the incidence of MPM is expected to continue to increase for some time [155]. Most mesothelioma have abnormal karyotypes, aneuploidy and structural rearrangements. Chromosomal losses are more common than gains [156]. One of the most common deletions is at the 9p21 locus encoding two critical inhibitors of cyclin dependent kinases, and the p53 regulator [157]. The loss of these proteins results in loss of cell cycle control and neoplastic transformation. Inhibitor of apoptosis proteins and also numerous defects in the apoptotic machinery are suggested to have an important role in the apoptosis-resistance of MPM. Elevated levels of pro-survival B-cell lymphoma Bcl-xL is found in most MPM cell lines and tumor tissues investigated [158, 159], and down-regulation of Bcl-xL expression increases apoptosis per se [160]. There is less known about the role of the pro-apoptotic Bcl-2-family proteins in MPM resistance to apoptosis. It has been suggested that the pro-apoptotic Bcl-2–associated x protein Bax is either dysfunctional or antagonized downstream of its interaction with the outer mitochondrial membrane in MPM cells [161]. The epidermal grow factor receptor has been held as an attractive therapeutic target in MPM, however, it is not clear to what extent the epidermal grow factor receptor expression contributes to the resistance phenotype [162]. A more investigated target is akt/PKB signalling, which is frequently up-regulated in MPM, and can be targeted for inhibition to increase apoptosis [163, 164].

Patients suffering from MPM can present with any number of general symptoms; dull chest pain, dyspnea, cough, and/or weight loss and diagnosis can be difficult, especially in non-endemic regions [165, 166]. Although routine chest radiography will often reveal pleural effusion and occasional pleural masses evident of disease, histologic diagnosis is required to verify suspected MPM (differentiating MPM from lung adenocarcinoma, among other

entities can be difficult) and to identify the tumor's histology which affects prognosis and, in some cases, treatment decisions [167, 168]. Upon MPM diagnosis, aggressive therapy including surgery and chemotherapy has become the standard among eligible patients [169]. The median survival after diagnosis is less than 12 months, and during the progression of the disease the patient suffers increased dyspnea and pain that can become chronic [170, 171]. The best overall objective response rate (28%) was achieved by combining cisplatin and doxorubicin [172]. To delay symptom progression, chemotherapy should be started as soon after diagnosis as the performance status of the patient allows. Radical surgical approaches in treatment of this disease can include pleurectomy and decortication, and extrapleural pneumonectomy, and these are the most widely used treatments for MPM [170].

The single most important risk factor for MPM, asbestos exposure, is known (primarily as a result of epidemiologic studies employing patient self-reports of occupational and environmental history) to occur in 70-80% or more of MPM patients [173]. Although asbestos use has been declining in the United States and Europe for decades, the 20-50 year latency of MPM is responsible for the continued worldwide increasing disease incidence [155]. In contrast to the long latency period following asbestos exposure, MPM is a rapidly fatal cancer with a median survival time of less than one year upon diagnosis [168]. Further influencing survival is disease histology; patients with biphasic and sarcomatoid tumors have reduced survival compared to patients with epithelioid tumors [174]. Importantly, since asbestos exposure is often occupationally related, and men are more often employed in these positions, disease occurs three to five times more often in men than women [175].

The burden of both exposure and disease is heavier among men. Further, men are significantly more likely to have reduced survival compared to women with MPM [176]. Hence, while asbestos exposure burden could influence disease outcome, the relationship between asbestos exposure patterns and prognosis has been very poorly studied and is incompletely understood.

Asbestos is a group of crystalline-hydrated silicate minerals that occur in a naturally fibrous form. Derived from the Greek word for inextinguishable, asbestos was used centuries ago as a textile for clothing, and in oil lamp wicks [177]. There are two main groups of asbestos fibers; serpentine asbestos, also known as chrysolite, is comprised of shorter, curved fibers; and amphiboles, which are long and straight and have several forms such as crocidolite, amosite, anthophylite, tremolite, and actinolite [178]. Although those who have studied mesothelioma have formed a general consensus that amphibole fibers are more pathogenic

than serpentine fibers, evidence indicates that all types of asbestos fibers are carcinogenic [179]. Inhalation of asbestos fibers leads to deposition at alveolar duct bifurcations and eventual migration to the pleural membranes [180]. Unfortunately, the process of fiber translocation is not well understood, but redistribution through airspaces, tissue spaces, or travel via lymphatics are among popular hypotheses [181].

Importantly, animal models of mesothelioma have been very helpful in advancing the understanding of the pathogenic mechanisms of asbestos, revealing that heterozygosity at particular genes such as NF2 and the CDKN2 locus can accelerate the induction of disease in the context of asbestos exposure [182].

Adenosine receptors and MPM

Adenosine is present at high concentrations in cancer tissues and in the interstitial fluid of several tumors, at concentrations sufficient to interact with ARs, but no data are present on the involvement of ARs in MPM. Several evidence of a correlation between A_3ARs and cancer are presents in literature [183]. Nb2 rat lymphoma [64], A375 human melanoma [184], PGT-beta mouse pineal gland tumor cells [185], human glioblastoma [186, 187], and human prostatic cells [65]. This thesis describes an up-regulation of A_3ARs in human MPM in comparison with healthy mesothelial pleura (HMP). Similar results were also obtained in healthy mesothelial cells (HMC) treated with crocidolite asbestos and in malignant mesothelioma cells (MMC) respect to untreated HMC. A_3ARs mediated a reduction of Akt/PKB phosphorylation and NF-kB activation in tumor cells. Furthermore, A_3AR stimulation decreased proliferation and increased apoptosis in MMC and in HMC exposed to asbestos and TNF-α, but not in untreated HMC, suggesting that A_3AR could represent a novel target for therapeutic intervention in MPM.

Materials and methods

Subjects

The patients enrolled in this research were recruited from the Department of Anesthesiology and Radiological Sciences, Section of General and Thoracic Surgery, University of Ferrara, Ferrara, Italy. The study was approved by the local Ethic Committee of the University of Ferrara and informed consent was obtained from each participant in accordance with the principles outlined in the Declaration of Helsinki.

Surgical Technique

The mesothelial tissue was obtained with surgical biopsy performed without use of electrosurgery devices. The pathological pleural specimens were obtained from patients with previous diagnosis of MM who underwent open surgery (13 extend extrapleural pneumonectomies, 4 explorative thoracotomies). Healthy pleural specimens were taken from patients who underwent video-assisted-thoracoscopy (VATS) for spontaneous pneumothorax (11 cases treated with apicectomy and pleurodesis) and for hyperhidrosis (5 cases treated with bilateral sympathectomy) without clinical evidence of oncological disease.

Human Pleura and Cell Lines

Human pleura tissues derived from examined patients were washed twice with PBS and fragmented into small pieces. The fragments were homogenized in 50 mM Tris HCl buffer, pH 7.4 with a Polytron (Kinematica Inc, NY), filtered through two layers of gauze and centrifuged for 10 min, 1000 g at 4°C. The supernatant was centrifuged again for 30 min, 40000 g at 4°C. To study adenosine receptor expression through binding assays, the membrane pellet was resuspended in the following buffers: a) 50 mM Tris HCl, pH 7.4 for A_1ARs; b) 50 mM Tris HCl, pH 7.4 containing 10 mM $MgCl_2$ for $A_{2A}ARs$; c) 50 mM Tris HCl, pH 7.4 containing 10 mM $MgCl_2$ and 1 mM EDTA for A_{2B} and A_3ARs. Membrane suspensions were incubated with 2 IU/ml adenosine deaminase for 30 min at 37°C and used for radioligand binding assays [188]. Primary cell lines derived from human pleura specimens were obtained by enzymatic digestion incubating the tissues overnight at 37°C in RMPI 1640 medium containing 1.5 mg/ml of type II collagenase (Worthington

Biochemical Corporation). After digestion cells were recovered by centrifugation and plated in T75 culture flask in RPMI 1640 medium supplemented with 10% fetal bovine serum, 100 U/ml penicillin, 100 µg/ml streptomycin and grown at 37°C in 5% CO_2 atmosphere [189]. Cells were passed when reaching confluence and used at the 8th passages for in vitro experiments. For membrane preparation the culture medium was removed and the cells were washed with PBS and scraped off T75 flasks in ice-cold hypotonic buffer (5 mM Tris HCl, 2 mM EDTA, pH 7.4). The cell suspension was homogenized with Polytron and centrifuged for 30 min at 40000 x g. The membrane pellet was resuspended in 50 mM Tris HCl buffer pH 7.4 for A_1ARs, 50 mM Tris HCl, 10 mM $MgCl_2$ for $A_{2A}ARs$ and 50 mM Tris HCl, 10 mM $MgCl_2$ 1 mM EDTA for A_{2B} and A_3 ARs and incubated with 2 UI/ml of adenosine deaminase for 30 min at 37°C and used for radioligand binding assays.

Asbestos Preparation

Crocidolite asbestos fibers were obtained from the Union Internationale Contre le Cancer (average length, 3.2±1.0 µm; average diameter, 0.22±0.01 µm). Fibers were baked at 150°C for 18 h, suspended in Hanks' balanced salt solution at 2 mg/ml, triturated 10 times through a 22-gauge needle, and autoclaved. Crocidolite fibers from Union Internationale Contre le Cancer also were characterized previously and shown to be carcinogenic, to cause the release of reactive oxygen species, and to cause DNA damage [190].

Healthy mesothelial cells (HMC) and malignant mesothelioma cells (MMC). Treatment Conditions

At the onset of each experiment, cells were placed in fresh medium and cultivated with or without the addition (in various combinations) of: a) 2-chloro-N^6-(3-iodobenzyl)adenosine-5′-*N*-methylcarboxamide (Cl-IB-MECA, 1 nM-1 µM); b) 5N-(4-methoxyphenylcarbamoyl) amino-8-propyl-2-(2-furyl) pyrazolo [4,3-e]-1,2,4-triazolo [1,5-c]pyrimidine (MRE 3008F20, 1 µM); c) TNF-α (10 ng/ml); d) crocidolite asbestos (5 µg/cm^2).

Real-Time RT-PCR

Total cytoplasmic RNA was extracted from MPM, healthy mesothelial pleura (HMP), HMC and MMC by the acid guanidinium thiocyanate phenol method. Quantitative real-

time RT-PCR assay [45] of A_1, A_{2A}, A_{2B} and A_3ARs mRNAs was carried out using gene-specific fluorescently labelled TaqMan MGB probe (minor groove binder) in a ABI Prism 7700 Sequence Detection System (Applied Biosystems, CA). For the real-time RT-PCR of A_1, A_{2A}, A_{2B} and A_3ARs the assays-on-demandTM Gene expression Products NM 000674, NM 000675, NM 000676 and NM 000677 were used respectively. For the real-time RT-PCR of the reference gene the endogenous control human β-actin kits was used, and the probe was fluorescent-labeled with VICTM (Applied Biosystems, CA).

Western blotting

Human pleura fractions, HMC and MMC were washed with ice-cold PBS containing 1 mM sodium orthovanadate, 104 mM 4-(2-aminoethyl)-benzenesulfonyl fluoride, 0.08 mM aprotinin, 2 mM leupeptin, 4 mM bestatin, 1.5 mM pepstatin A, 1.4 mM E-64. Then cells or tissues were lysed in Triton lysis buffer and the protein concentration was determined using BCA protein assay kit (Pierce). Aliquots of total protein sample (50 µg) were analyzed using antibodies specific for human ARs (1 µg/ml dilution, Alpha Diagnostics Inc, TX) [45]. Filters were washed and incubated for 1 h at room temperature with peroxidase-conjugated secondary antibodies (1:2000 dilution). Specific reactions were revealed with Enhanced Chemiluminescence Western blotting detection reagent (GE Healthcare, UK).

Immunocytochemistry

HMC and MMC grown on coverslips incubated in polylysine-treated chambers were fixed with 4% formalin in PBS, pH 7.4 for 15 min at room temperature. After two 5-min washes with ice cold PBS, potential sites for nonspecific antibody binding were blocked by 30 min incubation with 1% BSA in PBST pH 7.4. The cells were then incubated with specific antibody with 1:50 dilution of the polyclonal primary antibody overnight at 4°C. Subsequently, they were incubated with secondary antibody (1:80) conjugated to fluorescein isothiocyanate (FITC)-conjugated goat anti-rabbit IgG for 1 h at room temperature and nuclear stain with 4′,6-diamidino-2- henylindole (DAPI, Sigma-Aldrich, MO) 1 µg/ml for 20 min. After washing with PBS, pH 7.4, the cells were mounted for microscopy with DABCO (1,4-Diazabicyclo (2.2.2) octane, Sigma-Aldrich, MO) and visualized by a microscopy Nikon Eclipse 50i. The antibody (Alpha Diagnostics Inc, TX) concentrations were: 1:50 polyclonal rabbit anti-rat A_1AR antibody; 1:50 polyclonal rabbit

anti-canine $A_{2A}AR$ antibody; 1:50 polyclonal rabbit anti-human $A_{2B}AR$ antibody; 1:50 polyclonal rabbit anti-human A_3AR antibody [191].

Saturation Binding Experiments to ARs

MPM and HMP membranes (100 µg protein/assay) with [3H]-1,3-dipropyl-8-cyclopentyl-xanthine ([3H]-DPCPX, 0.01-20 nM) as radioligand (specific activity, 120 Ci/mmol, Perkin Elmer Life and Analytical Sciences, MA) were incubated for 90 min at 25°C to study A_1ARs [122]. Non specific binding was determined in the presence of DPCPX 1 µM. Saturation binding experiments to $A_{2A}ARs$ in human pleura membranes (100 µg protein/assay) were carried out by using [3H]- 4-(2-[7-amino-2-(2-furyl) [1,2,4]-triazolo [2,3-a][1,3,5] triazin-5-ylamino] ethyl) phenol ([3H]-ZM 241385, 0.01-20 nM) (specific activity, 27 Ci/mmol, Biotrend, Germany) as radioligand and were incubated for 60 min at 4°C [123]. Non specific binding was determined in the presence of ZM 241385 1 µM. Saturation binding experiments to $A_{2B}ARs$ were performed incubating membranes (80 µg protein/assay)   and   [3H]-N-benzo[1,3]dioxol-5-yl-2-[5-(2,6-dioxo-1,3-dipropyl-2,3,6,7-tetrahydro-1H–purin-8-yl)-1-methyl-1H-pyrazol-3-yl-oxy] acetamide ([3H]-MRE 2029F20, 0.01-30 nM) as radioligand (specific activity, 123 Ci/mmol, GE Healthcare, UK) for 60 min at 4°C [37]. Non specific binding was determined by using MRE 2029F20 1 µM. Saturation binding experiments to A_3ARs were conducted in membranes (80 µg protein/assay) and [3H]-5N-(4-methoxyphenylcarbamoyl) amino-8-propyl-2-(2-furyl) pyrazolo [4,3-e]-1,2,4-triazolo [1,5-c]pyrimidine ([3H]-MRE 3008F20, 0.01-30 nM) as radioligand (specific activity, 67 Ci/mmol, GE Healthcare, UK) at 4°C for 150 min [122]. Non specific binding was determined in the presence of MRE 3008F20 1 µM. At the end of the incubation time, bound and free radioactivity were separated by filtering the assay mixture through Whatman GF/B glass fiber filters in Brandel cell harvester (Brandel Instruments, MD). Filter bound radioactivity was counted in Perkin Elmer Tri Carb 2810 TR liquid scintillation counter (Perkin Elmer Life and Analytical Sciences, MA). Similar experimental conditions were also carried out in HMC and MMC with the aim of verifying the affinity and density of ARs.

Competition Binding Experiments to ARs

In competition experiments, 2 nM [^{3}H]-MRE 3008F20 was incubated in duplicate with at least 10-12 different concentrations of Cl-IB-MECA and MRE 3008F20 from 0.01 nM to 1 µM [122]. In binding assays, membrane homogenate (100 µg/100 µl) were obtained from HMC untreated or pre-treated for 24 h with crocidolite asbestos and MMC. Incubation time was 150 min at 4°C to allow equilibrium to be reached. Non specific binding was determined in the presence of MRE 3008F20 1 µM. Bound and free radioactivity were separated by filtering the assay mixture through Whatman GF/B glass fibre filters in Brandel cell harvester (Brandel Instruments, MD). Filter bound radioactivity was counted in Perkin Elmer Tri Carb 2810 TR liquid scintillation counter (Perkin Elmer Life and Analytical Sciences, MA).

cAMP Levels in HMC and MMC

HMC and MMC (10^6 cells/sample) were suspended in Krebs Ringer phosphate buffer, containing 1.0 IU/ml adenosine deaminase and preincubated for 10 min in a shaking bath at 37°C. To evaluate the adenylyl cyclase activity and cAMP production the cells were incubated with forskolin (10 µM) and/or 4-(3-butoxy-4-methoxybenzyl)-2-imidazolidinone (Ro 20-1724) (0.5 mM) as phosphodiesterase inhibitor [122]. The effect of Cl-IB-MECA at different concentrations (1 nM-1 µM) and the effect of selective A_3 adenosine antagonist (MRE3008F20, 1 µM) were investigated. The final aqueous solution was tested through a competition protein binding assay by using [^{3}H]-cyclic AMP (specific activity, 21 Ci/mmol, GE Healthcare, UK), trizma base 0.1 M, aminophylline 8.0 mM, mercaptoethanol 6.0 mM.

Akt Assays in HMC and in MMC

Akt phosphorylation was evaluated by using a commercial FACE AKT kit (Active Motif, CA) following the manufacturer's instructions. HMC and MMC were seeded in 96-well plates and treated with Cl-IB-MECA and crocidolite asbestos for 24 h. Cells were fixed by replacing the medium with 100 µl of 4% formaldehyde in PBS. Then, cells were incubated with primary Akt antibody overnight at 4°C. After washing the cells, HRP-conjugated secondary antibody was added and incubated one hour at room temperature, the adsorbance was read on spectrophotomer at 450 nm with a reference wavelength of 655 nm [192].

NF-kB Activation in HMC and in MMC

Nuclear extracts from the examined cells were obtained by using a nuclear extract kit (Active Motif, CA) following the manufacturer's instructions. The NF-kB activation was evaluated by detecting phosphorylated p65 protein in nuclear extracts by using the TransAM NF-kB kit (Active Motif, CA). Phosphorylated NF-kB P65 subunit specifically bind to the immobilized oligonucleotides containing the NF-kB consensus site (5'-GGGACTTTCC-3'). The primary antibody used to detect NF-kB recognized an epitope on P65 subunit that is accessible only when activated and bound to its DNA target. A horseradish peroxidase (HRP)-conjugated secondary antibody provided a sensitive colorimetric readout that was quantified by spectrophotometry at 450 nm [45].

Cell Proliferation Assay in HMC and MMC

HMC cells were treated with Cl-IB-MECA (1 nM-1 µM) in the presence and in the absence of crocidolite asbestos (5 µg/cm^2) and/or TNF-α (10 ng/ml). Moreover, MMC were treated with Cl-IB-MECA (1 nM-1 µM) in the absence or in the presence of MRE 3008F20 (1 µM). The cells were seeded in fresh medium with 1 µCi/ml [^{3}H]-Thymidine for 24 h in Dulbecco's modified Eagle's medium containing 10% fetal calf serum, penicillin (100 units/ml), streptomycin (100 µg/ml). After 24 h of labeling, cells were trypsinized, dispensed in four wells of a 96-well plate, and filtered through Whatman GF/C glass fiber filters using a Micro-Mate 196 cell harvester (Perkin Elmer Life and Analytical Sciences, MA). The filter-bound radioactivity was counted on Top Count Microplate Scintillation Counter with Micro Scint 20 [193].

Apoptosis Assay in HMC and in MMC

Apoptosis assay was performed evaluating active caspase-3 levels after the treatment of the cells with Cl-IB-MECA (1 nM-1 µM) for 24 h in the presence and in the absence of crocidolite asbestos (5 µg/cm^2) and/or TNF-α (10 ng/ml). Moreover, the effect of Cl-IB-MECA was also investigated in the presence of MRE 3008F20 (1 µM). After 24 h, the cells were treated with biotin-ZVKD-fmk inhibitor (10 µM) for one hour at room temperature. After discarding the culture media, cells were rinsed with PBS and the extraction buffer

containing protease inhibitors was added to prepare cell extracts. After two hours of incubation at room temperature 100 µl of samples were transferred into a microplate pre-coated with a monoclonal antibody specific for caspase-3. After washing, 100 µl of streptavidin caspase-3 conjugated to horseradish peroxidases that binds to the biotin of the inhibitor were added. Following the wash, the substrate solution was added to the wells for 30 min and stop solution was used to block the reaction. The optical density was determined using a microplate reader set to 450 nm.

LDH Cytotoxicity Assay in HMC and in MMC

Cytotoxicity was assessed with an LDH detection kit (Biovision, Mountain View, CA), which measures LDH activity released from the cytosol of damaged cells. HMC cells were treated with Cl-IB-MECA (1 nM-1 µM) for 24 h in the presence and in the absence of crocidolite asbestos (5 µg/cm^2) and/or TNF-α (10 ng/ml). Moreover, MMC were treated for 24 h with Cl-IB-MECA (1 nM-1 µM) in the absence or in the presence of MRE 3008F20 (1 µM). After 24 h, 100 µl of supernatant per well was harvested and transferred into a new 96-well, flat-bottom plate. LDH substrate (100 µl) was added to each well and incubated for 30 min at room temperature protected from light. The absorbance of the samples was measured at 490 mm on spectrophotomer [190].

Statistical Analysis

Protein concentrations were determined by Bio-Rad assay with bovine albumin as reference standard (Bio-Rad Laboratories, CA). Dissociation equilibrium constants for saturation binding, affinity or K_D values, as well as the maximum densities of specific binding sites, Bmax were calculated for a system of one or two-binding site populations by non-linear curve fitting using the program Ligand (Kell Biosoft, MO). Functional experiments were calculated by non linear regression analysis using the equation for a sigmoid concentration-response curve (GraphPAD Prism, CA). Analysis of data was performed by one-way analysis of variance. Differences between the groups were analyzed with Dunnett's test and were considered significant at a value of $p < 0.01$. All experimental data are reported as mean±SEM of independent experiments as indicated in Results section.

Results

The diagnosis and stage of MPM was based from surgical pleural biopsy according to the international tumor, node and metastasis (TNM) classification system proposed by the International Mesothelioma Interest Group (IMIG) (31). Clinical information including histological diagnosis was obtained from pathology reports. All patients were free from pre-operative chemotherapy and radiotherapy. Thirty-three subjects who underwent surgical resection were included in the study. Seventeen subjects (13 men and 4 women) were affected by MPM including epithelial mesothelioma and biphasic subtype. IMIG stage was II in 8 patients, III in 5 patients and IV in 4 patients. Mean age of the MPM patients was 61.7 ± 10.8 years ($\pm$ SD). Healthy pleura specimens were obtained from sixteen patients (10 men and 6 women) who underwent thoracic surgery for reasons other than MPM or pleural disease (11 for spontaneous pneumothorax, 5 for primary hyperhidrosis). Mean age of the patients with healthy pleura was 42.3 ± 10.2 years ($\pm$ SD). Some of the pleura specimens derived from 9 patients affected by MPM and 8 patients with no pleural disease) were immediately frozen at -80°C until use in the experimental assays and the other samples (8 from MPM patients and 8 with no pleural disease) were used to obtain primary cell cultures as MMC and HMC, respectively.

A_3ARs overexpression in MPM patients

The relative levels of mRNAs of ARs expressed as ratio between MPM and HMP are represented in Figure 1A. No differences were found in mRNA expression of A_1, A_{2A} and $A_{2B}ARs$ from MPM and healthy pleura. In contrast, A_3AR mRNA expression in MPM was significantly increased in comparison with HMP (Figure 17A). Western blotting and densitometric analysis in pleura specimens indicates a significant 61% increase in A_3AR expression in MPM compared to HMP (A_3AR/β-actin ratio: $1.42 \pm 0.09^*$ vs 0.88 ± 0.06; *, $p < 0.01$). No differences were found in A_1, A_{2A} and $A_{2B}ARs$ protein expression in HMP and MPM (Figure 17B and 17C). The overexpression of A_3ARs in MPM was confirmed by saturation binding experiments (Table 9, Figure 18). All ARs are expressed in human pleura and no differences were found in binding parameters (K_D and Bmax) of A_1, A_{2A} and $A_{2B}ARs$ in MPM membranes compared with those obtained in HMP. Interestingly, A_3ARs density was significantly increased in MPM membranes compared with HMP membranes (Figure 18B) while affinity values were closely similar (Figure 18A). Figure 18C and D

shows saturation curves and relative Scatchard plot of [^{3}H]MRE 3008F20 in MPM and HMP membranes. The linearity of the Scatchard plot indicates the presence of one high affinity binding site with Bmax values of 113± 14 fmol/mg protein and 282±24* fmol/mg protein for HMP and MPM membranes, respectively (Figure 18C and D; *, p<0.01).

A$_3$AR expression and function are increased in MMC

Immunocytochemical analysis of HMC and MMC demonstrated a similar level of expression for A$_1$, A$_{2A}$ and A$_{2B}$ARs in normal and tumoral mesothelial cells. From this analysis, only A$_3$ARs appear to be over-expressed in MMC compared with HMC (Figure 19). Western blotting and densitometric analysis further confirmed the similar expression of A$_1$, A$_{2A}$ and A$_{2B}$ARs in HMC and MMC and an high level of expression of A$_3$AR in the mesothelioma cell line (Figure 20A and B). To evaluate the affinity and density of ARs in control and MM cells, saturation binding experiments were carried out in HMC and MMC (Table 9). No differences were found in affinity values for ARs and in receptor density of A$_1$, A$_{2A}$ and A$_{2B}$ARs. The saturation curves and the relative Scatchard plot highlight a marked difference in A$_3$AR expression between HMC and MMC (Figure 20C and D). In figure 20E are reported the histograms of receptor density, expressed as Bmax, of ARs in membranes from HMC and MMC. Interestingly, in MMC membranes A$_3$ARs were significantly increased by 3.5 fold as compared to HMC. The quantification of AR mRNA levels in HMC and MMC confirmed the increase of the A$_3$AR at a transcriptional level by 3.2 fold in the MMC compared with HMC while mRNA levels for A$_1$, A$_{2A}$ and A$_{2B}$ARs are similar in the cell examined (Figure 20F). To evaluate the affinity of the well known A$_3$ adenosine agonist and antagonist used in functional experiments, competition binding experiments were performed in HMC and MMC (Table 9). As expected, Cl-IB-MECA showed a biphasic competition binding curve versus A$_3$ARs, as suggested by a significantly better fit to a two site binding model and by an Hill coefficient less than unity (0.52). In HMC membranes, Cl-IB-MECA showed a K$_H$ value of 0.95±0.10 nM and a K$_L$ value of 82±9 nM. Similar results were obtained in MMC membranes. The Ki values of the A$_3$AR antagonist MRE 3008F20 in HMC and MMC show an a high affinity in the nanomolar range. The functional effect of A$_3$ARs in HMC and MMC was determined by examining the effect of Cl-IB-MECA and MRE 3008F20 on cAMP production. In HMC, the A$_3$AR agonist Cl-IB-MECA inhibited forskolin-stimulated cAMP levels in a concentration-dependent manner, with an EC$_{50}$ in the nanomolar range (Table 10). In MMC, Cl-IB-

MECA demonstrated a marked increase in potency ($EC_{50}=12\pm1^*$ vs 34 ± 3 nM; *, p<0.01) most likely due to the overexpression of A_3AR (Figure 21A). Forskolin 10 µM was able to stimulate cAMP levels in both HMC and MMC by 10 fold of increase respect to basal condition suggesting a similar activity of adenylyl cyclase. Cl-IB-MECA inhibited forskolin-stimulated cAMP levels with a major significant effect (p<0.01) in MMC than in HMC (Figure 21B). The selective A_3AR antagonist MRE 3008F20 showed a potency value in the nanomolar range with an IC_{50} of 10 ± 1 nM in HMC and of 3.45 ± 0.28 nM in MMC. MRE 3008F20 1 µM fully antagonized the effect of Cl-IB-MECA (100 nM) suggesting the involvement of A_3ARs (Figure 21B).

Crocidolite asbestos exposure up-regulates A_3ARs in HMC

The effect of crocidolite asbestos exposure in HMC on A_3AR was evaluated by means of binding experiments and cAMP assays (Table 10). Saturation binding experiments to A_3AR showed an affinity value in the nanomolar range ($K_D= 2.25\pm0.21$ nM) and a receptor density, Bmax of 260 ± 24 fmol/mg protein suggesting a statistically significant increase of A_3ARs after 24 h of asbestos treatment. The affinity and density of A_3ARs in HMC treated with asbestos were closely associated to those obtained in MMC (Table 9).

Competition binding experiments revealed an affinity value for Cl-IB-MECA and MRE 3008F20 similar to those found in untreated HMC or MMC. Interestingly, in cAMP assays the potency of Cl-IB-MECA and MRE 3008F20 was higher than untreated HMC and analogous to those obtained in MMC (Table 10).

Cl-IB-MECA de-regulates Akt/NF-kB pathway

In HMC, Cl-IB-MECA at 10 and 100 nM concentration did not modify phospho Akt levels in comparison with control condition. The presence of asbestos (5 µg/cm^2) significantly increased (p<0.01) phospho Akt levels by 1.4 fold, an effect inhibited by Cl-IB-MECA at 10 and 100 nM concentration by 42 and 74%, respectively (Figure 21C). In MMC, Cl-IB-MECA at the same concentrations decreased the basal levels of phospho Akt by 25 and 38%, respectively (Figure 21D). MRE 3008F20 (1 µM) in HMC and in MMC was able to block the effect of Cl-IB-MECA suggesting the involvement of A_3ARs.

In HMC, treatment with TNF-α (10 ng/ml) significantly increased NF-kB p65 subunit activation. This effect was inhibited by the A_3AR agonist Cl-IB-MECA at the concentration

of 10 nM and 100 nM with a reduction of 45% and 68%, respectively (Figure 22A, p<0.01). Interestingly, also asbestos treatment (5 µg/cm^2) was able to markedly increase NF-kB activation after 24 hours in HMC. The presence of Cl-IB-MECA 10 nM or 100 nM significantly abolished the asbestos-induced p65 activation (Figure 22B). Furthermore, the evaluation of p65 subunit activation in MMC revealed a significantly higher basal level than HMC. In MMC, Cl-IB-MECA was able to reduce the basal level of NF-kB activation by 35% at 10 nM and by 58% at 100 nM concentration (Figure 22C). In these experiments, the involvement of A$_3$ARs in the Cl-IB-MECA-induced reduction of NF-kB p65 activation was demonstrated by using MRE 3008F20 1 µM that abolished the effect of Cl-IB-MECA 10 nM or 100 nM.

Dual effect of Cl-IB-MECA on cell proliferation and death

Cl-IB-MECA did not affect cell proliferation in HMC whilst mediated a reduction in MMC (Figure 22D and 22E). As expected asbestos exposure (5 µg/cm^2) caused a significant reduction of cell proliferation and this effect was not modified by Cl-IB-MECA 10 and 100 nM. The co-presence of asbestos and TNF-α (10 ng/ml) was able to increase cell proliferation reaching a level higher than control. In these experimental conditions Cl-IB-MECA was able to reduce cell proliferation abolishing the pro-survival effect of TNF-α on HMC exposed to asbestos. In both cell lines examined, MRE 3008F20 counteracted the effect of the A$_3$ARs agonist, Cl-IB-MECA.

In HMC, Cl-IB-MECA 10 nM and 100 nM did not modify the caspase-3 activation in comparison with the control condition in the absence or in the presence of asbestos (5 µg/cm^2). Asbestos treatment showed a marked increase in the active caspase-3 levels by 2.4 fold and the presence of TNF-α (10 ng/ml) was able to significantly reduce asbestos-induced caspase-3 activation. The co-presence of Cl-IB-MECA (10 nM and 100 nM) with asbestos and TNF-α significantly increased caspase-3 activation (Figure 23A). In MMC, Cl-IB-MECA at 10 nM was ineffective whilst at 100 nM was able to increase active caspase-3 levels by 29% (Figure 23B). MRE 3008F20 at 1 µM concentration counteracted the effect of A$_3$AR agonist Cl-IB-MECA in both cells examined.

In HMC, Cl-IB-MECA 10 nM and 100 nM was not cytotoxic as demonstrated by the similar levels of LDH release in the culture media or in the presence of asbestos. In addition, asbestos treatment (5 µg/cm^2) showed a marked cytotoxicity in HMC increasing the release of LDH by 2.1 fold. Interestingly, TNF-α (10 ng/ml) significantly reduced

asbestos-induced cytotoxicity, an effect abolished by the treatment with Cl-IB-MECA 10 and 100 nM (Figure 23C). In MMC, Cl-IB-MECA was able to increase LDH release suggesting a cytotoxicity effect mediated by A_3AR stimulation in these tumor cells (Figure 23D). MRE 3008F20 reduced the effect of A_3AR agonist Cl-IB-MECA in both cells examined.

**TABLE 9 – Affinity and density of adenosine receptors in HMP and MPM specimens in comparison with HMC and MMC**

membranes	[³H]-DPCPX A$_1$AR K$_D$ (nM) Bmax (fmol/mg protein)	[³H]-ZM 241385 A$_{2A}$AR K$_D$ (nM) Bmax (fmol/mg protein)	[³H]-MRE2029F20 A$_{2B}$AR K$_D$ (nM) Bmax (fmol/mg protein)	[³H]-MRE3008F20 A$_3$AR K$_D$ (nM) Bmax (fmol/mg protein)
HMP	2.48 ± 0.31 36 ± 4	3.02 ± 0.30 106 ± 10	1.97 ± 0.16 106 ± 9	2.17 ± 0.23 113 ± 14
MPM	2.19 ± 0.23 43 ± 5	2.86 ± 0.27 118 ± 14	1.95 ± 0.20 111 ± 12	2.21 ± 0.21 282 ± 24*
HMC	1.35 ± 0.12 32 ± 3	2.07 ± 0.18 95 ± 8	1.78 ± 0.15 102 ± 10	1.83 ± 0.16 93 ± 8
MMC	1.28 ± 0.11 38 ± 3	2.45 ± 0.16 104 ± 9	1.65 ± 0.15 108 ± 11	2.12 ± 0.17 325 ± 28**

K$_D$ and Bmax were obtained from saturation binding experiments. The data are expressed as mean ± SEM. *, $p < 0.01$ vs HMP; **, $p < 0.01$ vs HMC

TABLE 10 - Affinity and potency of a selected A$_3$ adenosine receptor agonist, Cl-IB-MECA and antagonist, MRE 300f20 in HMC and MMC

Compounds	HMC		MMC		HMC treated with asbestos	
	binding A$_3$ AR Affinity nM	cAMP assay Potency nM	binding A$_3$AR Affinity nM	cAMP assay Potency nM	binding A$_3$AR Affinity nM	cAMP assay Potency nM)
Cl-IB-MECA	K$_H$=0.95±0.10 K$_L$=82±9	EC$_{50}$ = 34±3	K$_H$=0.83±0.09 K$_L$=75 ±8	EC$_{50}$ = 12±1*	K$_H$=0.89±0.09 K$_L$=80±9	EC$_{50}$ = 14±2*
MRE 3008F20	Ki=2.13±0.16	IC$_{50}$ = 10±1	Ki=2.18±0.17	IC$_{50}$= 3.45±0.28**	Ki=2.27±0.03	IC$_{50}$= 3.14±0.29**

Affnity values expressed as K$_H$, K$_L$ and Ki (nM) were obtained from competition binding experiments. Potency values expressed as EC$_{50}$ or IC$_{50}$ (nM) were performed as described in cAMP assays. The data are expressed as mean ± SEM (N=4 independent experiments). *, $p < 0.01$ vs HMC for Cl-IB-MECA; **, $p < 0.01$ vs HMC for MRE 3008F20

Figure 17 - mRNA and protein expression of A_3 adenosine receptors in MPM patients
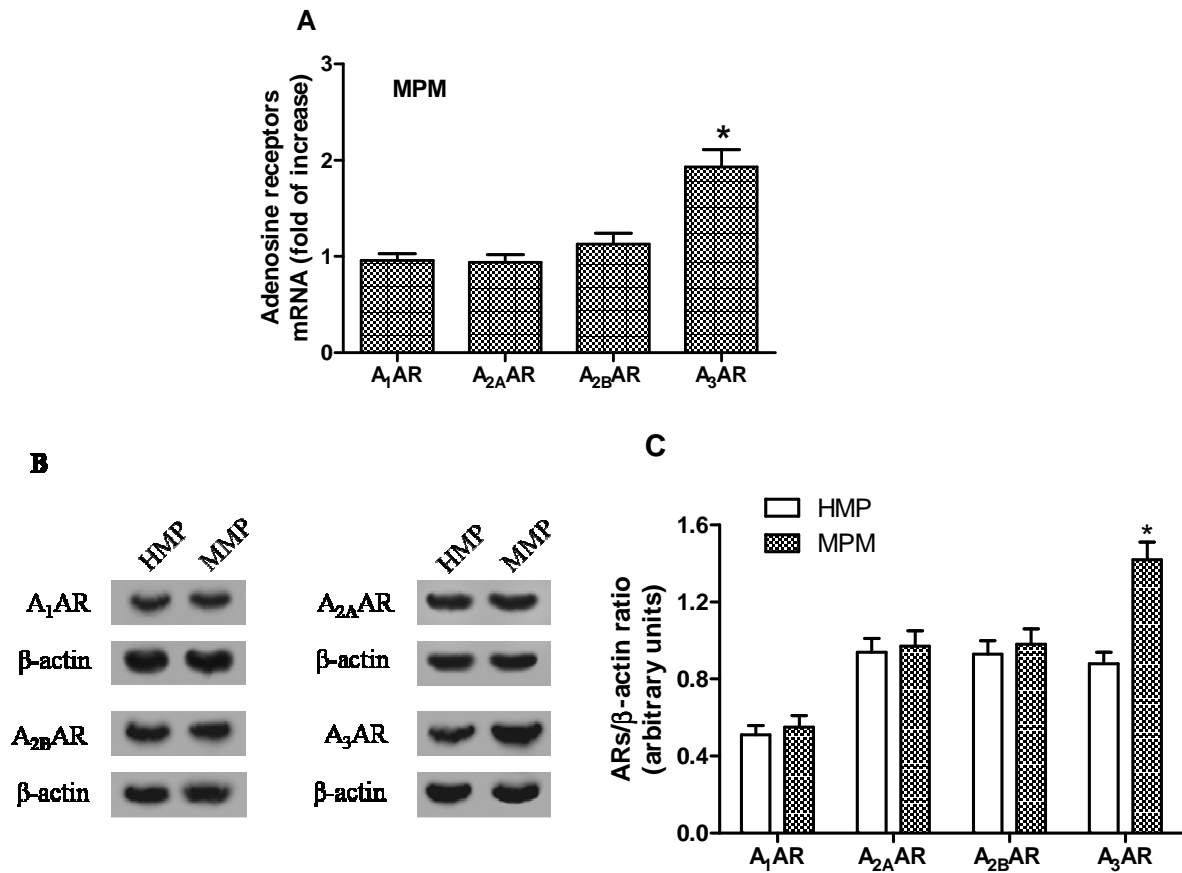

Relative mRNA expression in MPM versus HMP (A), western blotting and densitometric analysis of ARs (B, C). Data were normalized, HMP was set to 100%. The error bars give SE of three independent experiments. *, p<0.01 respect to HMP.

**Figure 18 - Binding parameters of A_1, A_{2A}, A_{2B} and A_3 adenosine receptors in MPM patients**
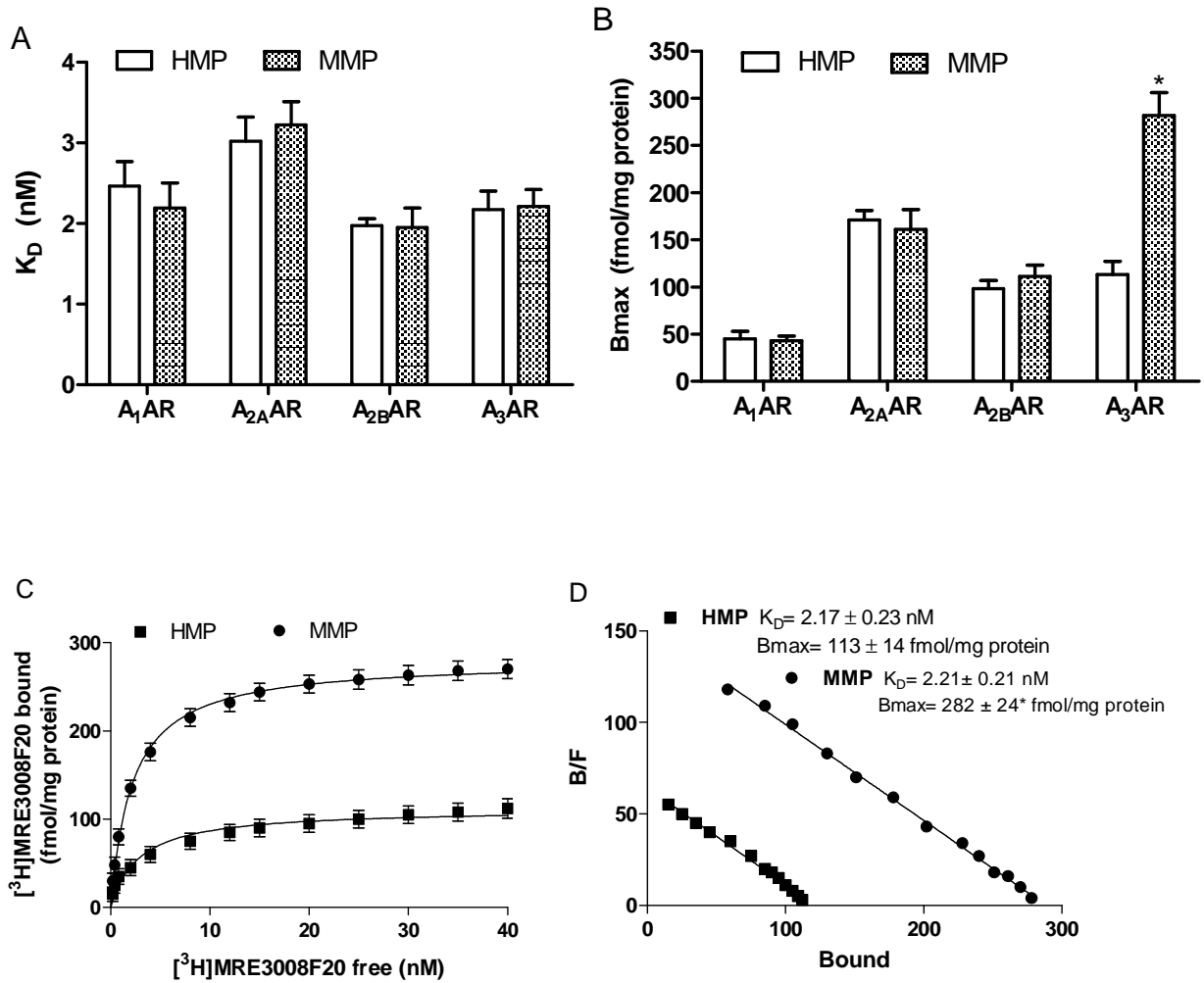
Affinity (A) and density (B) of the ARs in MMP and HMP. Saturation curves (C) and Scatchard plot (D) of [^{3}H]MRE 3008F20 to A_3ARs in MMP and HMP tissues. Values are the mean and vertical lines SE of the mean of 6 separate experiments performed in duplicate. *, p<0.01 respect to HMP.

**Figure 19 - Immunocytochemical analysis of adenosine receptors
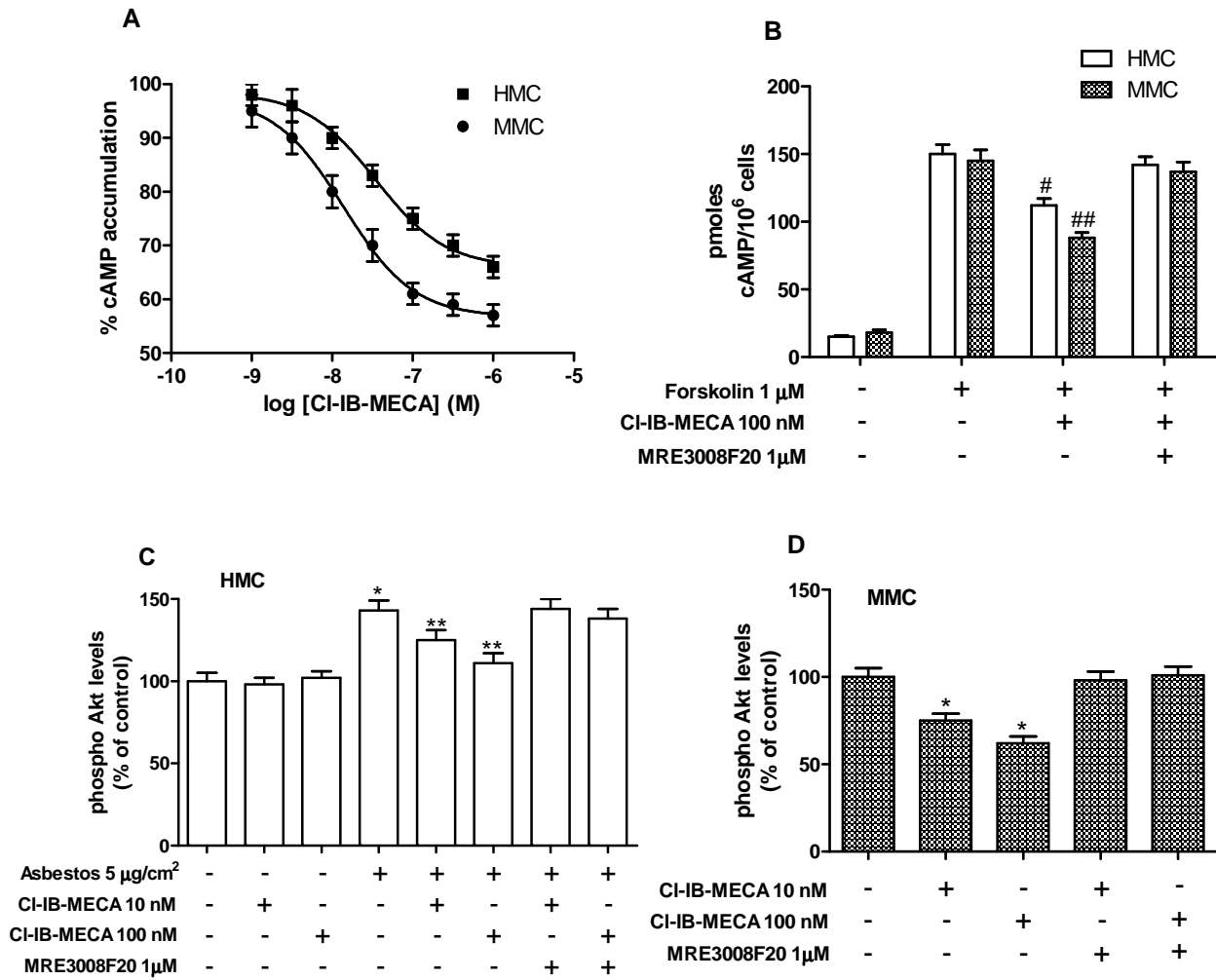in HMC and in MMC**
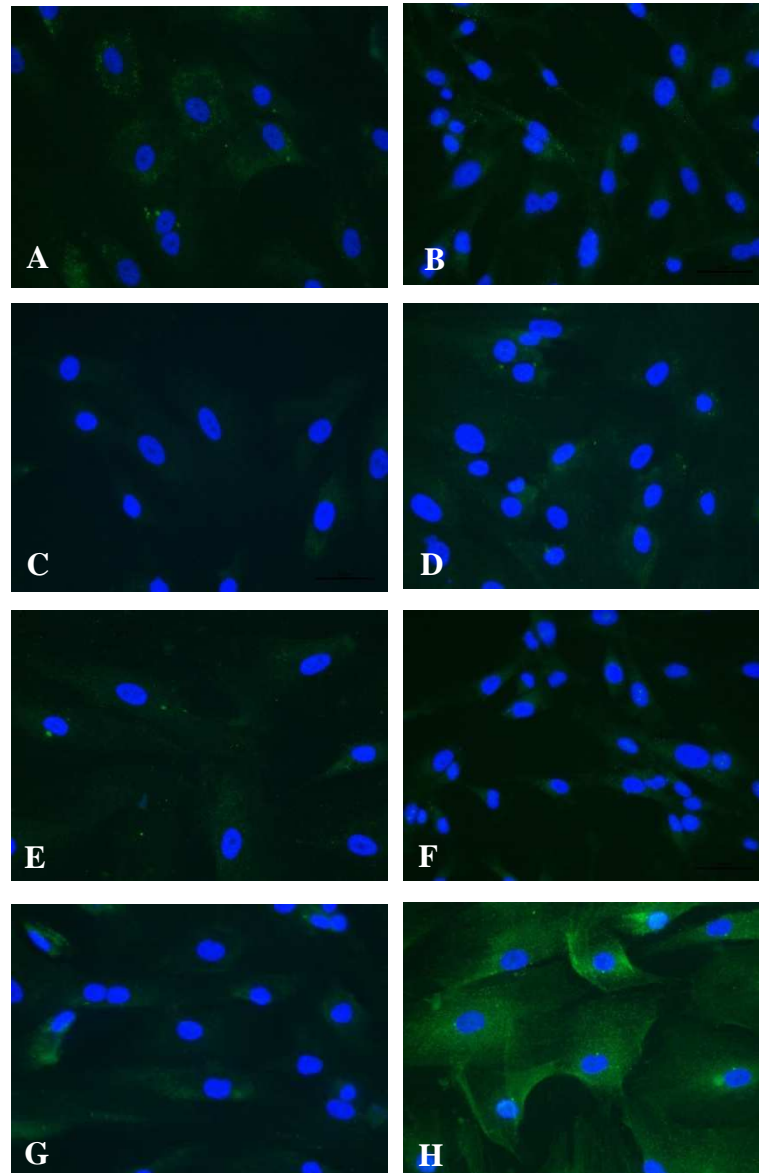
Immunocytochemical analysis of ARs in HMC (A,C,E,G) and MMC (B,D,F,H). DAPI was used for counterstaining of nuclei. Specific antibodies were used to label A_1 (A,B), A_{2A} (C,D), A_{2B} (E,F) and A_3 (G,H) ARs.

## Figure 20 – Western blotting and binding experiments of adenosine receptors in MMC and HMC
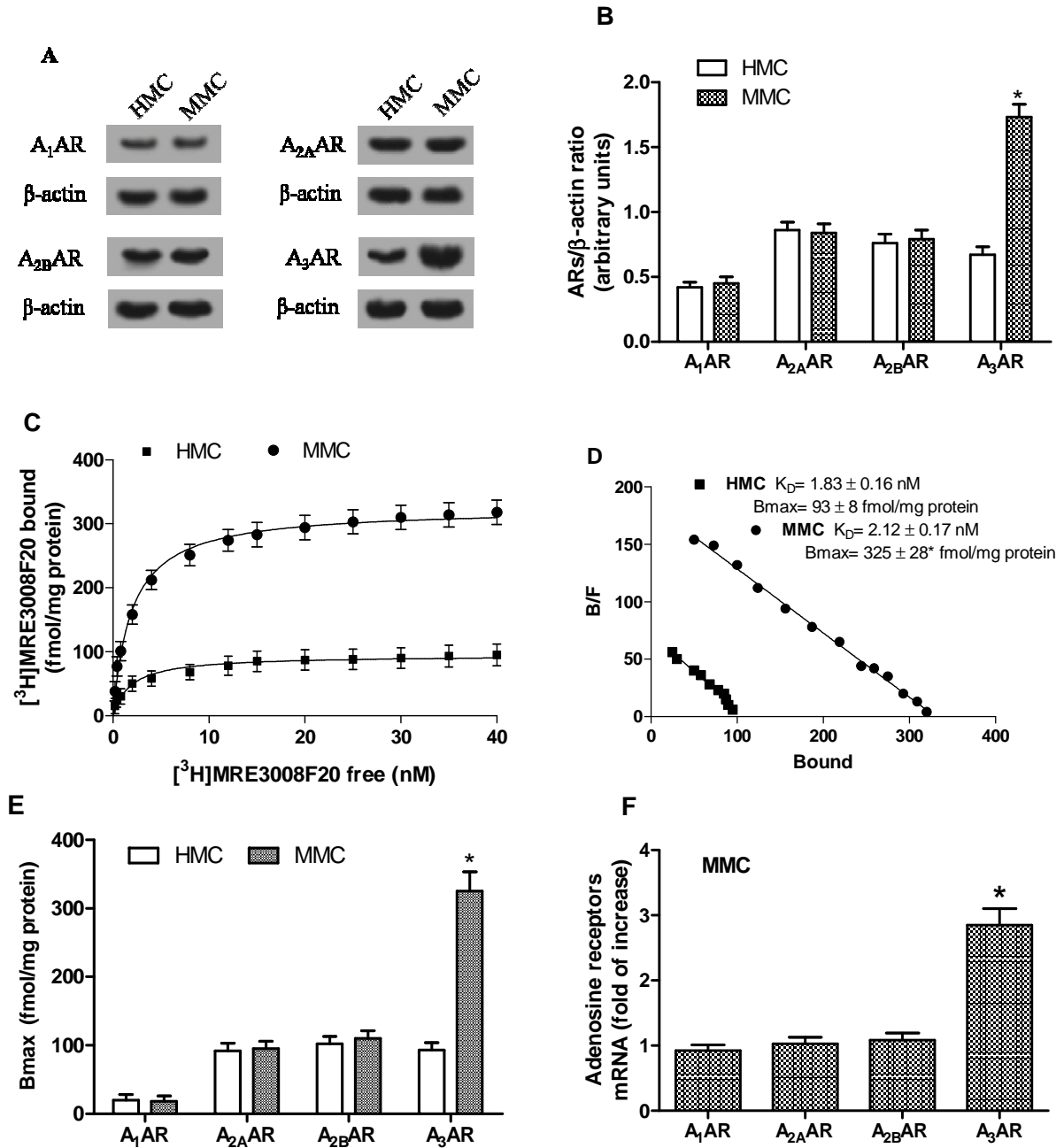
Western blotting and densitometric analysis of ARs in MMC versus HMC (A, B). Saturation curves (C) and Scatchard plot (D) of [³H]MRE 3008F20 to A_3ARs in HMC and MMC. Values are the mean and vertical lines SE of the mean of 8 separate experiments performed in duplicate. Density (E) of the ARs in HMC and MMC. Relative mRNA expression: data were normalized, HMC was set to 100% and the error bars give SE of three independent experiments (F). *, $p<0.01$ respect to HMC.

Figure 21 - Effect of Cl-IB-MECA, asbestos and MRE 3008F20

on A_3ARs in HMC and MMC

Effect of Cl-IB-MECA on cAMP accumulation in HMC and MMC (A). Effect of forskolin (1 µM) in the absence and in the presence of Cl-IB-MECA (100 nM) and A_3AR antagonism by MRE 3008F20 (1µM) (B). Effect of Cl-IB-MECA, asbestos and MRE 3008F20 on phospho-Akt levels in HMC (C) and MMC (D). Results are presented as the mean ± SE of 4 independent experiments. #, $p<0.01$ respect to forskolin 1 µM; ##, $p<0.01$ versus HMC treated with Cl-IB-MECA. *, $p<0.01$ respect to control condition; **, $p<0.01$ versus HMC treated with asbestos (5µg/cm^2).

Figure 22 - Effect of Cl-IB-MECA, MRE 3008F20, asbestos and TNF- α on cell proliferation
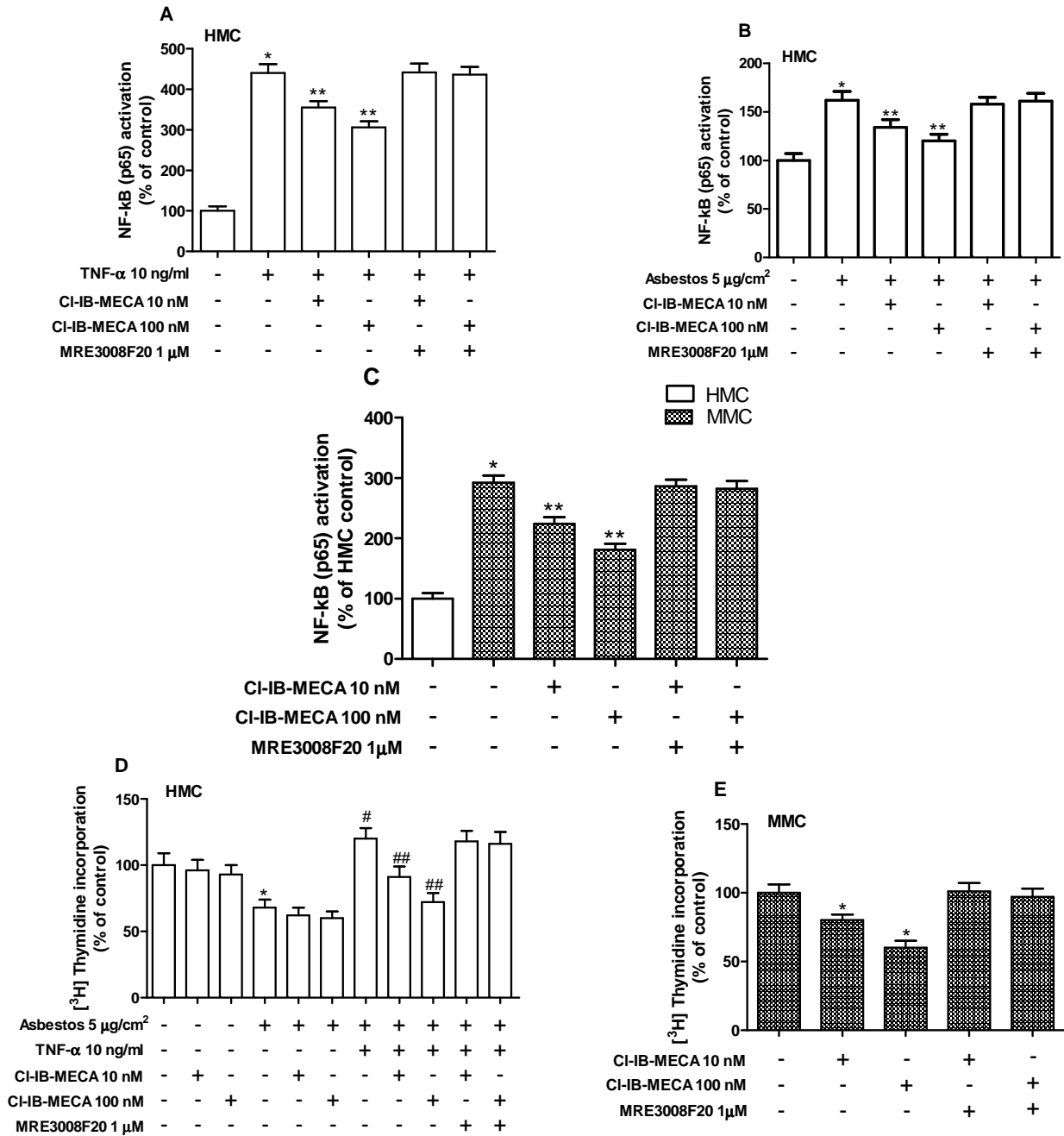
Effect of Cl-IB-MECA and MRE 3008F20 in HMC treated with TNF-α (A) or asbestos (B) and in MMC (C) on NF-kB p65 subunit activation. Effect of Cl-IB-MECA, asbestos, TNF-α and MRE 3008F20 on [³H]-Thymidine incorporation in HMC (D) and MMC (E). Results are presented as the mean ± SE of 4 independent experiments. *, p<0.01 respect to HMC control condition; **, p<0.01 versus HMC treated with TNF-α (A) or versus asbestos treated-HMC (B) or MMC control condition (C). #, p<0.01 versus HMC treated with asbestos (5µg/cm²) (D); ##, p<0.01 versus HMC treated with asbestos and TNF-α (D).

Figure 23 - Effect of Cl-IB-MECA, MRE 3008F20, asbestos and TNF- α on apoptosis
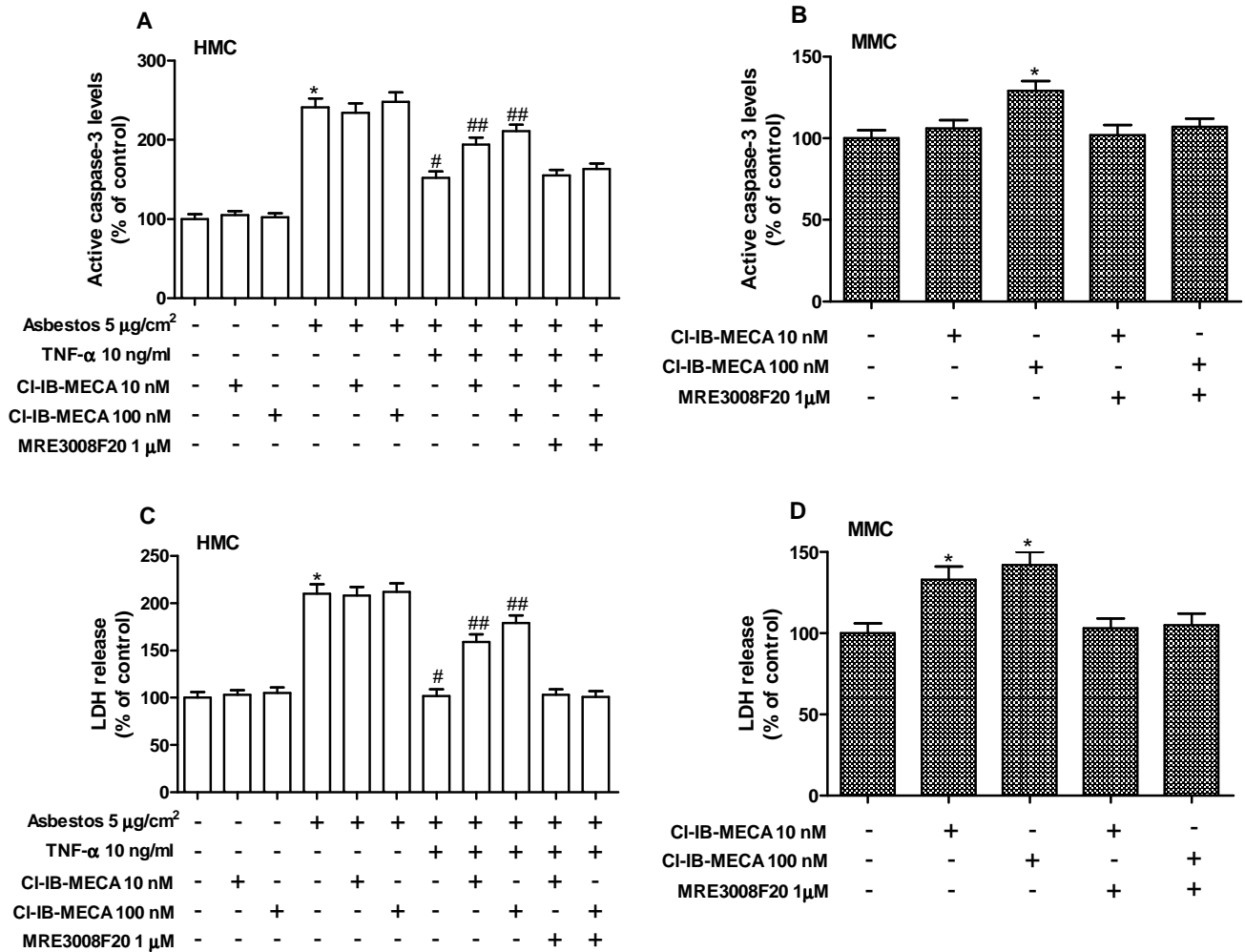
Effect of Cl-IB-MECA, asbestos, TNF-α and MRE 3008F20 on active caspase-3 levels in HMC (A) and MMC (B). Effect of Cl-IB-MECA, asbestos, TNF-α and MRE 3008F20 on LDH levels in HMC (C) and MMC (D). Results are presented as the mean ± SE of 4 independent experiments. *, p<0.01 respect to control condition; #, p<0.01 versus HMC treated with asbestos (5µg/cm^2); ##, p<0.01 versus HMC treated with asbestos and TNF-α.

Discussion

A large body of literature attributed to A_3ARs a pivotal role in the development of cancer highlighting the receptor as a potential target in the pharmacological treatment of tumors [59]. In particular, A_3AR overexpression has been demonstrated in various cancer tissues or cells such as colon carcinoma, melanoma, breast, small-cell lung and pancreatic carcinoma tissues [194]. A substantial amount of work has cleared that adenosine could be implicated in developing airway chronic inflammation [195]. In addition, ARs are present in many cell types involved in airway inflammation and airways are highly responsive to adenosine [113]. It has been also reported that elevated adenosine deaminase levels are present in some malignancies such as lymphoma and MPM [196]. No data are reported in the literature on the expression and/or the function of the ARs in human MPM.

The present study was undertaken to investigate the presence of ARs in human MPM and HMP. Interestingly, mRNA and protein expression of A_3ARs was statistically increased in MPM respect to HMP. In particular, the density of A_3ARs in MPM was increased by 2.5 fold in comparison with HMP. To evaluate the functionality of A_3ARs it has been studied a cellular in vitro model represented by normal HMC and tumoral MMC obtained from human healthy and MPM. No differences were found for A_1, A_{2A} and $A_{2B}ARs$ in HMC and MMC whilst A_3ARs were overexpressed in tumoral cells respect to the controls. Saturation binding experiments in MMC revealed a significantly increase in Bmax by 3.5 fold in comparison with HMC suggesting that the tumor could influence receptor characteristics. These data confirmed the A_3AR overexpression in cancer tissues or cells previously found in other tumors [59]. A comparison between A_3AR expression in tumor versus normal tissues supported the assumption that the receptor is up-regulated in different types of malignancies such as breast carcinoma, colon carcinoma and thyroid cancers [66, 194, 197]. In the present thesis, cAMP production assays revealed an increase of potency of Cl-IB-MECA and MRE 3008F20 in MMC in comparison with HMC suggesting that the overexpression of A_3ARs was correlated with an high functionality of these receptors.

Because asbestos is the main cause of human MPM, we evaluated the effect of crocidolite asbestos exposure on A_3ARs in HMC. Saturation binding assays showed that asbestos treatment induced an increase in A_3AR density suggesting an involvement of asbestos in the receptor overexpression. Competition binding experiments revealed that A_3AR affinity did not change in the presence of asbestos. The potency in cAMP production of Cl-IB-MECA and MRE 3008F20 was significantly increased after asbestos treatment obtaining

similar values to those found in MMC. It is well known that activation of A_3ARs inhibits adenylate cyclase activity, thereby leading to the decrease in the cAMP level. The latter modulates the level and activity of PKA that phosphorylates elements of the MAPK and Akt/PKB signalling pathways [198]. Both PKA and Akt/PKB regulate the NF-kB signalling pathway by phosphorylating the IKB kinase (IKK). As a consequence NF-kB induces the transcription of genes such as cyclin D1 and *c-Myc* that control cell cycle progression [199]. These data have suggested to investigate the effect of Cl-IB-MECA on cell growth regulatory proteins in HMC and MMC. Interestingly, the level of the cell survival protein Akt/PKB was reduced on asbestos-treated HMC and MMC by Cl-IB-MECA suggesting a key role of A_3ARs in the inhibition of Akt phosphorylation. The down regulation of Akt activation by A_3ARs has been also demonstrated in other tumor cells such as melanoma, colon, prostate and hepatocellular carcinomas [69, 200-202]. Because of the close association between Akt and NF-kB activation the role of A_3ARs on NF-kB signal transduction pathway was analized. It has been demonstrated that asbestos activates the NF-kB pathway, which leads to the transcription of multiple pro-survival genes that promote tumor development. In particular, the activation of NF-kB by TNF-α allows, to the mesothelial cells with asbestos-induced DNA damage, eventually to develop into cancer cells [203]. We found that in HMC, Cl-IB-MECA was able to inhibit NF-kB p65 subunit activation induced by TNF-α or crocidolite asbestos, suggesting the role of the A_3AR agonist in the inhibition of the survival pathway and thus potentially blocking the asbestos-induced tumor development. Interestingly in MMC, p65 subunit was constitutively more activated than in HMC and was down-regulated by Cl-IB-MECA, suggesting its capability to inhibit NF-kB survival pathway also in this tumor cells. NF-kB signal transduction pathways are involved in modulating a wide range of cellular processes including proliferation, surviving and apoptosis. The inhibitory effect of Cl-IB-MECA on cell proliferation was evident in HMC treated with asbestos and TNF-α and in MMC confirming the involvement of A_3AR activation in blocking tumor development or proliferation. At the present, the anti-proliferative effect of Cl-IB-MECA has been extensively investigated with opposite results depending on the tissues or cells examined. Recently, it has been demonstrated that Thio-Cl-IB-MECA mediates the inhibition of cell proliferation through cell cycle arrest in A549 human lung cancer cells [72]. A similar effect of A_3AR agonists was also reported in murine NB2-11C lymphoma cells, human A375 melanoma cells, human MCF-7 breast carcinoma cells [86, 200, 201].

Several papers have reported that asbestos exposure caused apoptosis in mesothelial and alveolar epithelial cells mainly through the generation of reactive oxygen species that lead to caspase-3 activation [204-206]. In our experimental conditions in HMC the presence of TNF-α inhibited asbestos-induced apoptosis and this effect was counteracted by Cl-IB-MECA. In MMC the A_3AR agonist was able to increase caspase-3 activation that is blocked by the presence of MRE 3008F20. It is well reported that A_3AR agonists mediate the induction of apoptosis in various tumor cells such as human HL-60 promyeolocytic leukemia cells and human NPA papillary thyroid carcinoma cells [207, 208]. Literature data report a possible mechanistic rationale for asbestos mediated HMC transformation. It was found that the TNF-α treatment significantly reduced crocidolite asbestos cytotoxicity mediating NF-kB activation which in turn inhibited asbestos-induced cytotoxicity and increased the number of HMC that survived asbestos exposure and thus the percentage of cells that could become transformed [190]. Our results indicate that Cl-IB-MECA is able to prevent the surviving effect of TNF-α on HMC exposed to asbestos suggesting a potential use of A_3AR agonists as blocking agents for the malignant transformation of asbestos-exposed HMC. Furthermore, while Cl-IB-MECA is not cytotoxic for control HMC, it has a significant citotoxic effect on MMC as demonstrated by the increase of LDH released in the culture medium. These results are consistent with those previously reported demonstrating that an A_3AR agonist, CF101, potentiates the cytotoxic effect of the chemotherapic agent 5-FU in HTC-116 colon carcinoma cells [209]. In conclusion, this is the first study reporting the up-regulation of A_3AR in pleura from MPM patients when compared with healthy pleura. A_3AR mRNA and protein expression was significantly increased in MMC and in asbestos-treated HMC respect to untreated HMC. Furthermore, the A_3AR agonist Cl-IB-MECA decreases proliferation and exerts cytotoxic and pro-apoptotic effect on HMC exposed to asbestos and TNF-α and on tumoral MMC, but not in control HMC. These effects appear to be related to the de-regulation of the Akt/NF-kB cell survival pathways contributing to the processes that lead to the malignant transformation of asbestos-exposed mesothelial cells. Taken together, these new findings suggest that A_3AR could represent a possible target for pharmacological intervention to prevent mesothelial tumor development after asbestos exposure and to treat full blown MPM.

GENERAL CONCLUSION

_____

Chronic obstructive pulmonary disease (COPD) and malignant pleural mesothelioma (MPM) are degenerative pathology in which environmental factors interact with multiple polymorphic genes to influence susceptibility to disease [210, 211]. In both, COPD and MPM, the inhalation of exogenous particles, smokes of cigarette for COPD and asbestos for MPM, may lead to the activation of many intracellular pathways including kinases, transcription factors and epigenetic events that modulate the inflammatory response and cell cycling/proliferation [74]. The transcription factor NF-kB, is activated by inflammatory mediators and by oxidative stress and may provide a molecular link between inflammation and cancer. COPD has been described as a pulmonary disease characterized by airflow limitation that is not fully reversible. The airflow limitation is usually progressive and associated with an abnormal inflammatory response of the lung to noxious particles or gases [88]. The inflammation of COPD is characterized by an accumulation of neutrophils, macrophages, B cells, lymphoid aggregates and CD4+ and CD8+ T cells particularly in the small airways [99] and the degree of inflammation increases with the disease severity as classified by the Global Initiative for Chronic Obstructive Lung Disease (GOLD) [88]. Neutrophils and activated macrophages release oxygen radicals, elastase, and cytokines that are essential to the pathogenesis of COPD, with effects on goblet cells and submucosal glands, and on the induction of emphysema and inflammation. Monocytes/macrophages are important effector cells in COPD due to the release of reactive oxygen species, extracellular matrix proteins, lipid mediators, cytokines, chemokines and matrix metalloproteinases and their numbers increase with increasing severity [99].

Adenosine is a signalling molecule, that is generated at sites of organ damage and tissue injury, and engage cell surface adenosine receptors (ARs) to regulate numerous pathological processes. ARs signalling can influence cellular physiology through a variety of mechanisms and access multiple intracellular signalling pathways including transcription factors, inflammatory mediators, and cell cycling/proliferation.

The first part of the present research, report the localization, mRNA expression, affinity and density of A_1, A_{2A}, A_{2B} and A_3ARs in peripheral lung parenchyma and bronchoalveolar lavage (BAL) macrophages from age-matched smokers with normal lung function (control group) and COPD patients. We have examined the peripheral lung because this is the major site of airflow obstruction in COPD patients and histopathological studies demonstrated that most of the airway inflammation in COPD is localized in the small airways and lung parenchyma [136].

These results suggest that A_1, A_{2A}, A_{2B} and A_3ARs are differentially expressed in peripheral lung parenchyma and the affinity and/or density of these receptors are altered in COPD patients compared with control smokers with normal lung function, with a significant correlation between the density and affinity of A_{2A}, A_{2B} and A_3ARs and the FEV_1/FVC ratio, an established index of airflow obstruction. Furthermore our data highlight that $A_{2B}ARs$ are significantly reduced in BAL macrophages from COPD patients compared to control healthy smokers. Also was demonstrated that in U937 cells, $A_{2B}AR$ mRNA and protein expression is selectively decreased by oxidative/nitrosative stress, but not by inflammatory mediators. This is associated with increased proliferation and decreased cAMP content, a marker of cell activation. As a consequence, $A_{2B}AR$ activation mediated the increase of typical pro-inflammatory cytokines demonstrating that $A_{2B}AR$ antagonism can attenuate lung inflammation [49, 150].

More than two centuries ago, it was recognized a close relationship between inflammation and tumorigenesis, because the tumors arise more easily where there are foci of inflammation. The inflammatory cells are present in tumors and the overexpression of cytokines and chemokines may lead to the onset of tumors. Several studies in literature and obtained in our laboratory have shown that adenosine exert important modulatory function in the growth of tumors, giving an essential role in this to the A_3ARs.

MPM is an insidious tumor historically associated historically with occupational exposure to asbestos [190, 203]. The average survival of patients with MPM is less than 1 year after initial diagnosis, and no successful treatment options exist. Although the mechanisms of development of MPM are obscure, the initiation of signalling events after interaction with asbestos fibers may govern transactivation of genes governing cell proliferation and transformation [151, 212].

The second part of the study was undertaken to investigate the presence of ARs in human MPM and healthy mesothelial pleura, reporting the up-regulation of A_3AR in pleura from MPM patients when compared with healthy pleura. A_3AR mRNA and protein expression was significantly increased in malignant mesothelial cells and in asbestos-treated healthy mesothelial cells respect to untreated cells. Furthermore, the A_3AR agonist Cl-IB-MECA decreases proliferation and exerts cytotoxic and pro-apoptotic effect on healthy mesothelial cells exposed to asbestos and TNF-α and on tumoral mesothelial cells, but not in control healthy mesothelial cells. These effects appear to be related to the de-regulation of the Akt/NF-kB cell survival pathways contributing to the processes that lead to the malignant transformation of asbestos-exposed mesothelial cells.

Overall these studies suggest the modulation of ARs as molecular targets of early inflammatory and carcinogenesis processes and may render the early diagnosis and treatment of COPD and MPM a reality. The data of the first part of the study, suggest a potential role of ARs in the pathogenesis of COPD, and support the potential for modulating $A_{2B}AR$ function with antagonists, in alveolar macrophages as a novel pharmacological treatment for this disease. While the new findings of the second part of the research, suggest that use of A_3AR agonist could represent a possible pharmacological intervention to prevent mesothelial tumor development after asbestos exposure and to treat full blown MPM.

By understanding the ARs signalling pathways involved in COPD and MPM the hope is to treat the disorders associated with inflammation and cancer.

REFERENCES

1.   Drury AN, Szent-Gyorgyi A: **The physiological activity of adenine compounds with especial reference to their action upon the mammalian heart**. *The Journal of physiology* 1929, **68**(3):213-237.

2.   Fredholm BB, Chern Y, Franco R, Sitkovsky M: **Aspects of the general biology of adenosine A2A signalling**. *Progress in neurobiology* 2007, **83**(5):263-276.

3.   Sebastiao AM, Ribeiro JA: **Adenosine receptors and the central nervous system**. *Handbook of experimental pharmacology* 2009(193):471-534.

4.   Reichelt ME, Ashton KJ, Tan XL, Mustafa SJ, Ledent C, Delbridge LM, Hofmann PA, Headrick JP, Morrison RR: **The adenosine A(2A) receptor - Myocardial protectant and coronary target in endotoxemia**. *International journal of cardiology* 2011.

5.   Hussey MJ, Clarke GD, Ledent C, Kitchen I, Hourani SM: **Deletion of the adenosine A(2A) receptor in mice enhances spinal cord neurochemical responses to an inflammatory nociceptive stimulus**. *Neuroscience letters* 2012, **506**(2):198-202.

6.   Gessi S, Varani K, Merighi S, Fogli E, Sacchetto V, Benini A, Leung E, Mac-Lennan S, Borea PA: **Adenosine and lymphocyte regulation**. *Purinergic signalling* 2007, **3**(1-2):109-116.

7.   Cronstein BN: **Adenosine, an endogenous anti-inflammatory agent**. *Journal of applied physiology* 1994, **76**(1):5-13.

8.   Merighi S, Mirandola P, Milani D, Varani K, Gessi S, Klotz KN, Leung E, Baraldi PG, Borea PA: **Adenosine receptors as mediators of both cell proliferation and cell death of cultured human melanoma cells**. *The Journal of investigative dermatology* 2002, **119**(4):923-933.

9.   Fredholm BB, AP IJ, Jacobson KA, Klotz KN, Linden J: **International Union of Pharmacology. XXV. Nomenclature and classification of adenosine receptors**. *Pharmacological reviews* 2001, **53**(4):527-552.

10.   Zimmermann H: **Extracellular metabolism of ATP and other nucleotides**. *Naunyn-Schmiedeberg's archives of pharmacology* 2000, **362**(4-5):299-309.

11.   Gu JG, Foga IO, Parkinson FE, Geiger JD: **Involvement of bidirectional adenosine transporters in the release of L-[3H]adenosine from rat brain synaptosomal preparations**. *Journal of neurochemistry* 1995, **64**(5):2105-2110.

12.   Parkinson FE, Sinclair CJ, Othman T, Haughey NJ, Geiger JD: **Differences between rat primary cortical neurons and astrocytes in purine release evoked by ischemic conditions**. *Neuropharmacology* 2002, **43**(5):836-846.

13.   Flower DR: **Modelling G-protein-coupled receptors for drug design**. *Biochimica et biophysica acta* 1999, **1422**(3):207-234.

14.   Dixon RA, Kobilka BK, Strader DJ, Benovic JL, Dohlman HG, Frielle T, Bolanowski MA, Bennett CD, Rands E, Diehl RE *et al*: **Cloning of the gene and cDNA for mammalian beta-adrenergic receptor and homology with rhodopsin**. *Nature* 1986, **321**(6065):75-79.

15.   Palczewski K, Kumasaka T, Hori T, Behnke CA, Motoshima H, Fox BA, Le Trong I, Teller DC, Okada T, Stenkamp RE *et al*: **Crystal structure of rhodopsin: A G protein-coupled receptor**. *Science* 2000, **289**(5480):739-745.

16.   Burnstock G: **Purinergic cotransmission**. *Experimental physiology* 2009, **94**(1):20-24.

17.   Bruns RF, Katims JJ, Annau Z, Snyder SH, Daly JW: **Adenosine receptor interactions and anxiolytics**. *Neuropharmacology* 1983, **22**(12B):1523-1529.

18. Gessi S, Merighi S, Fazzi D, Stefanelli A, Varani K, Borea PA: **Adenosine receptor targeting in health and disease**. *Expert opinion on investigational drugs* 2011, **20**(12):1591-1609.

19. Baraldi PG, Zaid AN, Lampronti I, Fruttarolo F, Pavani MG, Tabrizi MA, Shryock JC, Leung E, Romagnoli R: **Synthesis and biological effects of a new series of 2-amino-3-benzoylthiophenes as allosteric enhancers of A1-adenosine receptor**. *Bioorganic & medicinal chemistry letters* 2000, **10**(17):1953-1957.

20. Elzein E, Zablocki J: **A1 adenosine receptor agonists and their potential therapeutic applications**. *Expert opinion on investigational drugs* 2008, **17**(12):1901-1910.

21. Dunwiddie TV, Masino SA: **The role and regulation of adenosine in the central nervous system**. *Annual review of neuroscience* 2001, **24**:31-55.

22. Moore KA, Nicoll RA, Schmitz D: **Adenosine gates synaptic plasticity at hippocampal mossy fiber synapses**. *Proceedings of the National Academy of Sciences of the United States of America* 2003, **100**(24):14397-14402.

23. Moro S, Gao ZG, Jacobson KA, Spalluto G: **Progress in the pursuit of therapeutic adenosine receptor antagonists**. *Medicinal research reviews* 2006, **26**(2):131-159.

24. Ciruela F, Saura C, Canela EI, Mallol J, Lluis C, Franco R: **Ligand-induced phosphorylation, clustering, and desensitization of A1 adenosine receptors**. *Molecular pharmacology* 1997, **52**(5):788-797.

25. Lee YC, Chien CL, Sun CN, Huang CL, Huang NK, Chiang MC, Lai HL, Lin YS, Chou SY, Wang CK *et al*: **Characterization of the rat A2A adenosine receptor gene: a 4.8-kb promoter-proximal DNA fragment confers selective expression in the central nervous system**. *The European journal of neuroscience* 2003, **18**(7):1786-1796.

26. Ferre S, Quiroz C, Woods AS, Cunha R, Popoli P, Ciruela F, Lluis C, Franco R, Azdad K, Schiffmann SN: **An update on adenosine A2A-dopamine D2 receptor interactions: implications for the function of G protein-coupled receptors**. *Current pharmaceutical design* 2008, **14**(15):1468-1474.

27. Tomiyama M, Kimura T, Maeda T, Tanaka H, Kannari K, Baba M: **Upregulation of striatal adenosine A2A receptor mRNA in 6-hydroxydopamine-lesioned rats intermittently treated with L-DOPA**. *Synapse* 2004, **52**(3):218-222.

28. Marvanova M, Wong G: **Adenosine A2A receptor mRNA expression is increased in rat striatum and nucleus accumbens after memantine administration**. *Brain research Molecular brain research* 2004, **120**(2):193-196.

29. Corvol JC, Studler JM, Schonn JS, Girault JA, Herve D: **Galpha(olf) is necessary for coupling D1 and A2a receptors to adenylyl cyclase in the striatum**. *Journal of neurochemistry* 2001, **76**(5):1585-1588.

30. Khoa ND, Postow M, Danielsson J, Cronstein BN: **Tumor necrosis factor-alpha prevents desensitization of Galphas-coupled receptors by regulating GRK2 association with the plasma membrane**. *Molecular pharmacology* 2006, **69**(4):1311-1319.

31. Josselyn SA, Nguyen PV: **CREB, synapses and memory disorders: past progress and future challenges**. *Current drug targets CNS and neurological disorders* 2005, **4**(5):481-497.

32. Schulte G, Fredholm BB: **Signalling from adenosine receptors to mitogen-activated protein kinases**. *Cellular signalling* 2003, **15**(9):813-827.

33. Fresco P, Oliveira JM, Kunc F, Soares AS, Rocha-Pereira C, Goncalves J, Diniz C: **A2A adenosine-receptor-mediated facilitation of noradrenaline release in rat tail artery involves protein kinase C activation and betagamma subunits formed after alpha2-adrenoceptor activation**. *Neurochemistry international* 2007, **51**(1):47-56.

34.   Spicuzza L, Di Maria G, Polosa R: **Adenosine in the airways: implications and applications**. *European journal of pharmacology* 2006, **533**(1-3):77-88.

35.   Dixon AK, Gubitz AK, Sirinathsinghji DJ, Richardson PJ, Freeman TC: **Tissue distribution of adenosine receptor mRNAs in the rat**. *British journal of pharmacology* 1996, **118**(6):1461-1468.

36.   Fiebich BL, Biber K, Lieb K, van Calker D, Berger M, Bauer J, Gebicke-Haerter PJ: **Cyclooxygenase-2 expression in rat microglia is induced by adenosine A2a-receptors**. *Glia* 1996, **18**(2):152-160.

37.   Varani K, Gessi S, Merighi S, Vincenzi F, Cattabriga E, Benini A, Klotz KN, Baraldi PG, Tabrizi MA, Lennan SM *et al*: **Pharmacological characterization of novel adenosine ligands in recombinant and native human A2B receptors**. *Biochemical pharmacology* 2005, **70**(11):1601-1612.

38.   Zhou QY, Li C, Olah ME, Johnson RA, Stiles GL, Civelli O: **Molecular cloning and characterization of an adenosine receptor: the A3 adenosine receptor**. *Proceedings of the National Academy of Sciences of the United States of America* 1992, **89**(16):7432-7436.

39.   Atkinson MR, Townsend-Nicholson A, Nicholl JK, Sutherland GR, Schofield PR: **Cloning, characterisation and chromosomal assignment of the human adenosine A3 receptor (ADORA3) gene**. *Neuroscience research* 1997, **29**(1):73-79.

40.   Palmer TM, Stiles GL: **Identification of threonine residues controlling the agonist-dependent phosphorylation and desensitization of the rat A(3) adenosine receptor**. *Molecular pharmacology* 2000, **57**(3):539-545.

41.   Trincavelli ML, Tuscano D, Marroni M, Falleni A, Gremigni V, Ceruti S, Abbracchio MP, Jacobson KA, Cattabeni F, Martini C: **A3 adenosine receptors in**

human astrocytoma cells: agonist-mediated desensitization, internalization, and down-regulation. *Molecular pharmacology* 2002, **62**(6):1373-1384.

42. Varani K, Massara A, Vincenzi F, Tosi A, Padovan M, Trotta F, Borea PA: **Normalization of A2A and A3 adenosine receptor up-regulation in rheumatoid arthritis patients by treatment with anti-tumor necrosis factor alpha but not methotrexate**. *Arthritis and rheumatism* 2009, **60**(10):2880-2891.

43. Press NJ, Gessi S, Borea PA, Polosa R: **Therapeutic potential of adenosine receptor antagonists and agonists**. *Expert opinion on therapeutic patents* 2007, **17**(8):979-991.

44. Baraldi PG, Tabrizi MA, Gessi S, Borea PA: **Adenosine receptor antagonists: translating medicinal chemistry and pharmacology into clinical utility**. *Chemical reviews* 2008, **108**(1):238-263.

45. Sun CX, Young HW, Molina JG, Volmer JB, Schnermann J, Blackburn MR: **A protective role for the A1 adenosine receptor in adenosine-dependent pulmonary injury**. *The Journal of clinical investigation* 2005, **115**(1):35-43.

46. Mohsenin A, Mi T, Xia Y, Kellems RE, Chen JF, Blackburn MR: **Genetic removal of the A2A adenosine receptor enhances pulmonary inflammation, mucin production, and angiogenesis in adenosine deaminase-deficient mice**. *American journal of physiology Lung cellular and molecular physiology* 2007, **293**(3):L753-761.

47. Sitkovsky MV: **T regulatory cells: hypoxia-adenosinergic suppression and re-direction of the immune response**. *Trends in immunology* 2009, **30**(3):102-108.

48. Feoktistov I, Biaggioni I: **Adenosine A2b receptors evoke interleukin-8 secretion in human mast cells. An enprofylline-sensitive mechanism with implications for asthma**. *The Journal of clinical investigation* 1995, **96**(4):1979-1986.

49. Sun CX, Zhong H, Mohsenin A, Morschl E, Chunn JL, Molina JG, Belardinelli L, Zeng D, Blackburn MR: **Role of A2B adenosine receptor signalling in adenosine-dependent pulmonary inflammation and injury**. *The Journal of clinical investigation* 2006, **116**(8):2173-2182.

50. Schingnitz U, Hartmann K, Macmanus CF, Eckle T, Zug S, Colgan SP, Eltzschig HK: **Signalling through the A2B adenosine receptor dampens endotoxin-induced acute lung injury**. *Journal of immunology* 2010, **184**(9):5271-5279.

51. Feng MG, Navar LG: **Afferent arteriolar vasodilator effect of adenosine predominantly involves adenosine A2B receptor activation**. *American journal of physiology Renal physiology* 2010, **299**(2):F310-315.

52. Brown RA, Spina D, Page CP: **Adenosine receptors and asthma**. *British journal of pharmacology* 2008, **153 Suppl 1**:S446-456.

53. Morschl E, Molina JG, Volmer JB, Mohsenin A, Pero RS, Hong JS, Kheradmand F, Lee JJ, Blackburn MR: **A3 adenosine receptor signalling influences pulmonary inflammation and fibrosis**. *American journal of respiratory cell and molecular biology* 2008, **39**(6):697-705.

54. Young HW, Molina JG, Dimina D, Zhong H, Jacobson M, Chan LN, Chan TS, Lee JJ, Blackburn MR: **A3 adenosine receptor signalling contributes to airway inflammation and mucus production in adenosine deaminase-deficient mice**. *Journal of immunology* 2004, **173**(2):1380-1389.

55. Wagner R, Ngamsri KC, Stark S, Vollmer I, Reutershan J: **Adenosine receptor A3 is a critical mediator in LPS-induced pulmonary inflammation**. *American journal of physiology Lung cellular and molecular physiology* 2010, **299**(4):L502-512.

56. Gessi S, Merighi S, Sacchetto V, Simioni C, Borea PA: **Adenosine receptors and cancer**. *Biochimica et biophysica acta* 2011, **1808**(5):1400-1412.

_____

57. Merighi S, Benini A, Mirandola P, Gessi S, Varani K, Simioni C, Leung E, Maclennan S, Baraldi PG, Borea PA: **Caffeine inhibits adenosine-induced accumulation of hypoxia-inducible factor-1alpha, vascular endothelial growth factor, and interleukin-8 expression in hypoxic human colon cancer cells**. *Molecular pharmacology* 2007, **72**(2):395-406.

58. Harish A, Hohana G, Fishman P, Arnon O, Bar-Yehuda S: **A3 adenosine receptor agonist potentiates natural killer cell activity**. *International journal of oncology* 2003, **23**(4):1245-1249.

59. Fishman P, Bar-Yehuda S, Synowitz M, Powell JD, Klotz KN, Gessi S, Borea PA: **Adenosine receptors and cancer**. *Handbook of experimental pharmacology* 2009(193):399-441.

60. Varani K, Padovan M, Vincenzi F, Targa M, Trotta F, Govoni M, Borea PA: **A2A and A3 adenosine receptor expression in rheumatoid arthritis: upregulation, inverse correlation with disease activity score and suppression of inflammatory cytokine and metalloproteinase release**. *Arthritis research & therapy* 2011, **13**(6):R197.

61. Cohen S, Stemmer SM, Zozulya G, Ochaion A, Patoka R, Barer F, Bar-Yehuda S, Rath-Wolfson L, Jacobson KA, Fishman P: **CF102 an A3 adenosine receptor agonist mediates anti-tumor and anti-inflammatory effects in the liver**. *J Cell Physiol* 2011, **226**(9):2438-2447.

62. Gessi S, Merighi S, Varani K, Cattabriga E, Benini A, Mirandola P, Leung E, Mac Lennan S, Feo C, Baraldi S *et al*: **Adenosine receptors in colon carcinoma tissues and colon tumoral cell lines: focus on the A(3) adenosine subtype**. *J Cell Physiol* 2007, **211**(3):826-836.

63. Gao Z, Li BS, Day YJ, Linden J: **A3 adenosine receptor activation triggers phosphorylation of protein kinase B and protects rat basophilic leukemia 2H3 mast cells from apoptosis**. *Mol Pharmacol* 2001, **59**(1):76-82.

64. Fishman P, Bar-Yehuda S, Ohana G, Pathak S, Wasserman L, Barer F, Multani AS: **Adenosine acts as an inhibitor of lymphoma cell growth: a major role for the A3 adenosine receptor**. *European journal of cancer* 2000, **36**(11):1452-1458.

65. Jajoo S, Mukherjea D, Watabe K, Ramkumar V: **Adenosine A(3) receptor suppresses prostate cancer metastasis by inhibiting NADPH oxidase activity**. *Neoplasia* 2009, **11**(11):1132-1145.

66. Gessi S, Cattabriga E, Avitabile A, Gafa R, Lanza G, Cavazzini L, Bianchi N, Gambari R, Feo C, Liboni A *et al*: **Elevated expression of A3 adenosine receptors in human colorectal cancer is reflected in peripheral blood cells**. *Clinical cancer research : an official journal of the American Association for Cancer Research* 2004, **10**(17):5895-5901.

67. Morello S, Sorrentino R, Porta A, Forte G, Popolo A, Petrella A, Pinto A: **Cl-IB-MECA enhances TRAIL-induced apoptosis via the modulation of NF-kappaB signalling pathway in thyroid cancer cells**. *Journal of cellular physiology* 2009, **221**(2):378-386.

68. Bar-Yehuda S, Rath-Wolfson L, Del Valle L, Ochaion A, Cohen S, Patoka R, Zozulya G, Barer F, Atar E, Pina-Oviedo S *et al*: **Induction of an antiinflammatory effect and prevention of cartilage damage in rat knee osteoarthritis by CF101 treatment**. *Arthritis Rheum* 2009, **60**(10):3061-3071.

69. Bar-Yehuda S, Stemmer SM, Madi L, Castel D, Ochaion A, Cohen S, Barer F, Zabutti A, Perez-Liz G, Del Valle L *et al*: **The A3 adenosine receptor agonist CF102 induces apoptosis of hepatocellular carcinoma via de-regulation of the Wnt and NF-kappaB signal transduction pathways**. *International journal of oncology* 2008, **33**(2):287-295.

70. Fishman P, Bar-Yehuda S: **Pharmacology and therapeutic applications of A3 receptor subtype**. *Current topics in medicinal chemistry* 2003, **3**(4):463-469.

71. Panjehpour M, Karami-Tehrani F: **Adenosine modulates cell growth in the human breast cancer cells via adenosine receptors**. *Oncology research* 2007, **16**(12):575-585.

72. Kim SJ, Min HY, Chung HJ, Park EJ, Hong JY, Kang YJ, Shin DH, Jeong LS, Lee SK: **Inhibition of cell proliferation through cell cycle arrest and apoptosis by thio-Cl-IB-MECA, a novel A3 adenosine receptor agonist, in human lung cancer cells**. *Cancer letters* 2008, **264**(2):309-315.

73. van Troostenburg AR, Clark EV, Carey WD, Warrington SJ, Kerns WD, Cohn I, Silverman MH, Bar-Yehuda S, Fong KL, Fishman P: **Tolerability, pharmacokinetics and concentration-dependent hemodynamic effects of oral CF101, an A3 adenosine receptor agonist, in healthy young men**. *International journal of clinical pharmacology and therapeutics* 2004, **42**(10):534-542.

74. Chung KF, Adcock IM: **Multifaceted mechanisms in COPD: inflammation, immunity, and tissue repair and destruction**. *The European respiratory journal : official journal of the European Society for Clinical Respiratory Physiology* 2008, **31**(6):1334-1356.

75. Mannino DM: **COPD: epidemiology, prevalence, morbidity and mortality, and disease heterogeneity**. *Chest* 2002, **121**(5 Suppl):121S-126S.

76. Zaher C, Halbert R, Dubois R, George D, Nonikov D: **Smoking-related diseases: the importance of COPD**. *The international journal of tuberculosis and lung disease : the official journal of the International Union against Tuberculosis and Lung Disease* 2004, **8**(12):1423-1428.

77. Zhou Y, Murthy JN, Zeng D, Belardinelli L, Blackburn MR: **Alterations in adenosine metabolism and signalling in patients with chronic obstructive pulmonary disease and idiopathic pulmonary fibrosis**. *PloS one* 2010, **5**(2):e9224.

78. Ponnoth DS, Nadeem A, Tilley S, Mustafa SJ: **Involvement of A1 adenosine receptors in altered vascular responses and inflammation in an allergic mouse model of asthma**. *American journal of physiology Heart and circulatory physiology* 2010, **299**(1):H81-87.

79. Sugiura H, Ichinose M: **Nitrative stress in inflammatory lung diseases**. *Nitric oxide : biology and chemistry / official journal of the Nitric Oxide Society* 2011, **25**(2):138-144.

80. Kotz D, Wesseling G, Aveyard P, van Schayck OC: **Smoking cessation and development of respiratory health in smokers screened with normal spirometry**. *Respiratory medicine* 2011, **105**(2):243-249.

81. Gonzalez NC, Wood JG: **Alveolar hypoxia-induced systemic inflammation: what low PO(2) does and does not do**. *Advances in experimental medicine and biology* 2010, **662**:27-32.

82. O'Reilly KM, McLaughlin AM, Beckett WS, Sime PJ: **Asbestos-related lung disease**. *American family physician* 2007, **75**(5):683-688.

83. Heintz NH, Janssen-Heininger YM, Mossman BT: **Asbestos, lung cancers, and mesotheliomas: from molecular approaches to targeting tumor survival pathways**. *American journal of respiratory cell and molecular biology* 2010, **42**(2):133-139.

84. Kim H, Kang JW, Lee S, Choi WJ, Jeong LS, Yang Y, Hong JT, Yoon do Y: **A3 adenosine receptor antagonist, truncated Thio-Cl-IB-MECA, induces apoptosis in T24 human bladder cancer cells**. *Anticancer research* 2010, **30**(7):2823-2830.

85. Gessi S, Merighi S, Varani K, Leung E, Mac Lennan S, Borea PA: **The A3 adenosine receptor: an enigmatic player in cell biology**. *Pharmacology & therapeutics* 2008, **117**(1):123-140.

86.   Merighi S, Benini A, Mirandola P, Gessi S, Varani K, Leung E, Maclennan S, Borea PA: **A3 adenosine receptor activation inhibits cell proliferation via phosphatidylinositol 3-kinase/Akt/PKB-dependent inhibition of the extracellular signal-regulated kinase 1/2 phosphorylation in A375 human melanoma cells**. *The Journal of biological chemistry* 2005, **280**(20):19516-19526.

87.   Manning BD, Cantley LC: **AKT/PKB/PKB signalling: navigating downstream**. *Cell* 2007, **129**(7):1261-1274.

88.   Petsonk EL, Hnizdo E, Attfield M: **Definition of COPD GOLD stage I**. *Thorax* 2007, **62**(12):1107-1108; author reply 1108-1109.

89.   Shaker SB, von Wachenfeldt KA, Larsson S, Mile I, Persdotter S, Dahlback M, Broberg P, Stoel B, Bach KS, Hestad M *et al*: **Identification of patients with chronic obstructive pulmonary disease (COPD) by measurement of plasma biomarkers**. *The clinical respiratory journal* 2008, **2**(1):17-25.

90.   Berry CE, Wise RA: **Mortality in COPD: causes, risk factors, and prevention**. *Copd* 2010, **7**(5):375-382.

91.   Rabe KF, Hurd S, Anzueto A, Barnes PJ, Buist SA, Calverley P, Fukuchi Y, Jenkins C, Rodriguez-Roisin R, van Weel C *et al*: **Global strategy for the diagnosis, management, and prevention of chronic obstructive pulmonary disease: GOLD executive summary**. *American journal of respiratory and critical care medicine* 2007, **176**(6):532-555.

92.   Ezzati M, Lopez AD: **Estimates of global mortality attributable to smoking in 2000**. *Lancet* 2003, **362**(9387):847-852.

93.   Rutgers SR, Postma DS, ten Hacken NH, Kauffman HF, van Der Mark TW, Koeter GH, Timens W: **Ongoing airway inflammation in patients with COPD who Do not currently smoke**. *Chest* 2000, **117**(5 Suppl 1):262S.

94.   Mayer AS, Newman LS: **Genetic and environmental modulation of chronic obstructive pulmonary disease**. *Respiration physiology* 2001, **128**(1):3-11.

95.   Matheson MC, Benke G, Raven J, Sim MR, Kromhout H, Vermeulen R, Johns DP, Walters EH, Abramson MJ: **Biological dust exposure in the workplace is a risk factor for chronic obstructive pulmonary disease**. *Thorax* 2005, **60**(8):645-651.

96.   Silva GE, Sherrill DL, Guerra S, Barbee RA: **Asthma as a risk factor for COPD in a longitudinal study**. *Chest* 2004, **126**(1):59-65.

97.   Stoller JK, Aboussouan LS: **Alpha1-antitrypsin deficiency**. *Lancet* 2005, **365**(9478):2225-2236.

98.   Barnes PJ, Shapiro SD, Pauwels RA: **Chronic obstructive pulmonary disease: molecular and cellular mechanisms**. *The European respiratory journal : official journal of the European Society for Clinical Respiratory Physiology* 2003, **22**(4):672-688.

99.   Baraldo S, Lokar Oliani K, Turato G, Zuin R, Saetta M: **The Role of Lymphocytes in the Pathogenesis of Asthma and COPD**. *Current medicinal chemistry* 2007, **14**(21):2250-2256.

100.   Collins A, Walden A, Parker R: **GOLD COPD classification and prognostic pessimism regarding ICU admission**. *Thorax* 2011.

101.   Babusyte A, Stravinskaite K, Jeroch J, Lotvall J, Sakalauskas R, Sitkauskiene B: **Patterns of airway inflammation and MMP-12 expression in smokers and ex-smokers with COPD**. *Respiratory research* 2007, **8**:81.

102.   Baraldo S, Bazzan E, Zanin ME, Turato G, Garbisa S, Maestrelli P, Papi A, Miniati M, Fabbri LM, Zuin R *et al*: **Matrix metalloproteinase-2 protein in lung periphery is related to COPD progression**. *Chest* 2007, **132**(6):1733-1740.

103.   Barnes PJ: **Alveolar macrophages as orchestrators of COPD**. *Copd* 2004, **1**(1):59-70.

104. MacNee W: **Oxidative stress and lung inflammation in airways disease**. *European journal of pharmacology* 2001, **429**(1-3):195-207.

105. MacNee W: **Oxidants/antioxidants and chronic obstructive pulmonary disease: pathogenesis to therapy**. *Novartis Foundation symposium* 2001, **234**:169-185; discussion 185-168.

106. Cosio MG, Saetta M, Agusti A: **Immunologic aspects of chronic obstructive pulmonary disease**. *The New England journal of medicine* 2009, **360**(23):2445-2454.

107. Higashimoto Y, Yamagata Y, Taya S, Iwata T, Okada M, Ishiguchi T, Sato H, Itoh H: **Systemic inflammation in chronic obstructive pulmonary disease and asthma: Similarities and differences**. *Respirology* 2008, **13**(1):128-133.

108. Yao H, Yang SR, Kode A, Rajendrasozhan S, Caito S, Adenuga D, Henry R, Edirisinghe I, Rahman I: **Redox regulation of lung inflammation: role of NADPH oxidase and NF-kappaB signalling**. *Biochemical Society transactions* 2007, **35**(Pt 5):1151-1155.

109. Drost EM, Skwarski KM, Sauleda J, Soler N, Roca J, Agusti A, MacNee W: **Oxidative stress and airway inflammation in severe exacerbations of COPD**. *Thorax* 2005, **60**(4):293-300.

110. Repine JE, Bast A, Lankhorst I: **Oxidative stress in chronic obstructive pulmonary disease. Oxidative Stress Study Group**. *American journal of respiratory and critical care medicine* 1997, **156**(2 Pt 1):341-357.

111. Okamoto K, Tanaka H, Ogawa H, Makino Y, Eguchi H, Hayashi S, Yoshikawa N, Poellinger L, Umesono K, Makino I: **Redox-dependent regulation of nuclear import of the glucocorticoid receptor**. *The Journal of biological chemistry* 1999, **274**(15):10363-10371.

112. Barnes PJ, Adcock IM: **Glucocorticoid resistance in inflammatory diseases**. *Lancet* 2009, **373**(9678):1905-1917.

113. Polosa R: **Adenosine-receptor subtypes: their relevance to adenosine-mediated responses in asthma and chronic obstructive pulmonary disease**. *The European respiratory journal : official journal of the European Society for Clinical Respiratory Physiology* 2002, **20**(2):488-496.

114. Esther CR, Jr., Lazaar AL, Bordonali E, Qaqish B, Boucher RC: **Elevated airway purines in COPD**. *Chest* 2011, **140**(4):954-960.

115. Bauerle JD, Grenz A, Kim JH, Lee HT, Eltzschig HK: **Adenosine generation and signalling during acute kidney injury**. *Journal of the American Society of Nephrology : JASN* 2011, **22**(1):14-20.

116. Fan M, Jamal Mustafa S: **Role of adenosine in airway inflammation in an allergic mouse model of asthma**. *International immunopharmacology* 2006, **6**(1):36-45.

117. Fredholm BB: **Adenosine receptors as targets for drug development**. *Drug news & perspectives* 2003, **16**(5):283-289.

118. Varani K, Vincenzi F, Tosi A, Targa M, Masieri FF, Ongaro A, De Mattei M, Massari L, Borea PA: **Expression and functional role of adenosine receptors in regulating inflammatory responses in human synoviocytes**. *British journal of pharmacology* 2010, **160**(1):101-115.

119. van den Berge M, Hylkema MN, Versluis M, Postma DS: **Role of adenosine receptors in the treatment of asthma and chronic obstructive pulmonary disease: recent developments**. *Drugs in R&D* 2007, **8**(1):13-23.

120. Lee HS, Chung HJ, Lee HW, Jeong LS, Lee SK: **Suppression of inflammation response by a novel A adenosine receptor agonist thio-Cl-IB-MECA through**

inhibition of Akt/PKB and NF-kappaB signalling. *Immunobiology* 2011, **216**(9):997-1003.

121. Hasko G, Szabo C, Nemeth ZH, Kvetan V, Pastores SM, Vizi ES: **Adenosine receptor agonists differentially regulate IL-10, TNF-alpha, and nitric oxide production in RAW 264.7 macrophages and in endotoxemic mice**. *Journal of immunology* 1996, **157**(10):4634-4640.

122. Varani K, Merighi S, Gessi S, Klotz KN, Leung E, Baraldi PG, Cacciari B, Romagnoli R, Spalluto G, Borea PA: **[(3)H]MRE 3008F20: a novel antagonist radioligand for the pharmacological and biochemical characterization of human A(3) adenosine receptors**. *Molecular pharmacology* 2000, **57**(5):968-975.

123. Varani K, Laghi-Pasini F, Camurri A, Capecchi PL, Maccherini M, Diciolla F, Ceccatelli L, Lazzerini PE, Ulouglu C, Cattabeni F *et al*: **Changes of peripheral A2A adenosine receptors in chronic heart failure and cardiac transplantation**. *The FASEB journal : official publication of the Federation of American Societies for Experimental Biology* 2003, **17**(2):280-282.

124. Gessi S, Varani K, Merighi S, Cattabriga E, Pancaldi C, Szabadkai Y, Rizzuto R, Klotz KN, Leung E, Mac Lennan S *et al*: **Expression, pharmacological profile, and functional coupling of A2B receptors in a recombinant system and in peripheral blood cells using a novel selective antagonist radioligand, [3H]MRE 2029-F20**. *Molecular pharmacology* 2005, **67**(6):2137-2147.

125. Gessi S, Varani K, Merighi S, Cattabriga E, Iannotta V, Leung E, Baraldi PG, Borea PA: **A(3) adenosine receptors in human neutrophils and promyelocytic HL60 cells: a pharmacological and biochemical study**. *Molecular pharmacology* 2002, **61**(2):415-424.

126. Papi A, Romagnoli M, Baraldo S, Braccioni F, Guzzinati I, Saetta M, Ciaccia A, Fabbri LM: **Partial reversibility of airflow limitation and increased exhaled NO and sputum eosinophilia in chronic obstructive pulmonary disease**. *American journal of respiratory and critical care medicine* 2000, **162**(5):1773-1777.

127. Quanjer PH, Tammeling GJ, Cotes JE, Pedersen OF, Peslin R, Yernault JC: **Lung volumes and forced ventilatory flows. Report Working Party Standardization of Lung Function Tests, European Community for Steel and Coal. Official Statement of the European Respiratory Society**. *The European respiratory journal Supplement* 1993, **16**:5-40.

128. Caramori G, Romagnoli M, Casolari P, Bellettato C, Casoni G, Boschetto P, Chung KF, Barnes PJ, Adcock IM, Ciaccia A *et al*: **Nuclear localisation of p65 in sputum macrophages but not in sputum neutrophils during COPD exacerbations**. *Thorax* 2003, **58**(4):348-351.

129. Ito K, Ito M, Elliott WM, Cosio B, Caramori G, Kon OM, Barczyk A, Hayashi S, Adcock IM, Hogg JC *et al*: **Decreased histone deacetylase activity in chronic obstructive pulmonary disease**. *The New England journal of medicine* 2005, **352**(19):1967-1976.

130. Higuchi R, Fockler C, Dollinger G, Watson R: **Kinetic PCR analysis: real-time monitoring of DNA amplification reactions**. *Bio/technology* 1993, **11**(9):1026-1030.

131. Ito K, Barnes PJ, Adcock IM: **Glucocorticoid receptor recruitment of histone deacetylase 2 inhibits interleukin-1beta-induced histone H4 acetylation on lysines 8 and 12**. *Molecular and cellular biology* 2000, **20**(18):6891-6903.

132. Butterfield JH, Weiler D, Dewald G, Gleich GJ: **Establishment of an immature mast cell line from a patient with mast cell leukemia**. *Leukemia research* 1988, **12**(4):345-355.

133. Martinet W, Schrijvers DM, Kockx MM: **Nucleofection as an efficient nonviral transfection method for human monocytic cells**. *Biotechnology letters* 2003, **25**(13):1025-1029.

134.   Bradford MM: **A rapid and sensitive method for the quantitation of microgram quantities of protein utilizing the principle of protein-dye binding**. *Analytical biochemistry* 1976, **72**:248-254.

135.   Munson PJ, Rodbard D: **Ligand: a versatile computerized approach for characterization of ligand-binding systems**. *Analytical biochemistry* 1980, **107**(1):220-239.

136.   Hogg JC, Chu F, Utokaparch S, Woods R, Elliott WM, Buzatu L, Cherniack RM, Rogers RM, Sciurba FC, Coxson HO *et al*: **The nature of small-airway obstruction in chronic obstructive pulmonary disease**. *The New England journal of medicine* 2004, **350**(26):2645-2653.

137.   Barnes PJ: **Mediators of chronic obstructive pulmonary disease**. *Pharmacological reviews* 2004, **56**(4):515-548.

138.   Feoktistov I, Polosa R, Holgate ST, Biaggioni I: **Adenosine A2B receptors: a novel therapeutic target in asthma?** *Trends in pharmacological sciences* 1998, **19**(4):148-153.

139.   Tomita K, Caramori G, Lim S, Ito K, Hanazawa T, Oates T, Chiselita I, Jazrawi E, Chung KF, Barnes PJ *et al*: **Increased p21(CIP1/WAF1) and B cell lymphoma leukemia-x(L) expression and reduced apoptosis in alveolar macrophages from smokers**. *American journal of respiratory and critical care medicine* 2002, **166**(5):724-731.

140.   Caramori G, Pandit A, Papi A: **Is there a difference between chronic airway inflammation in chronic severe asthma and chronic obstructive pulmonary disease?** *Current opinion in allergy and clinical immunology* 2005, **5**(1):77-83.

141.   Khoa ND, Montesinos MC, Reiss AB, Delano D, Awadallah N, Cronstein BN: **Inflammatory cytokines regulate function and expression of adenosine A(2A) receptors in human monocytic THP-1 cells**. *Journal of immunology* 2001, **167**(7):4026-4032.

142. Zhou Y, Schneider DJ, Blackburn MR: **Adenosine signalling and the regulation of chronic lung disease**. *Pharmacology & therapeutics* 2009, **123**(1):105-116.

143. Morello S, Ito K, Yamamura S, Lee KY, Jazrawi E, Desouza P, Barnes P, Cicala C, Adcock IM: **IL-1 beta and TNF-alpha regulation of the adenosine receptor (A2A) expression: differential requirement for NF-kappa B binding to the proximal promoter**. *Journal of immunology* 2006, **177**(10):7173-7183.

144. Ito K, Jazrawi E, Cosio B, Barnes PJ, Adcock IM: **p65-activated histone acetyltransferase activity is repressed by glucocorticoids: mifepristone fails to recruit HDAC2 to the p65-HAT complex**. *The Journal of biological chemistry* 2001, **276**(32):30208-30215.

145. Adenuga D, Yao H, March TH, Seagrave J, Rahman I: **Histone deacetylase 2 is phosphorylated, ubiquitinated, and degraded by cigarette smoke**. *American journal of respiratory cell and molecular biology* 2009, **40**(4):464-473.

146. Ito K, Hanazawa T, Tomita K, Barnes PJ, Adcock IM: **Oxidative stress reduces histone deacetylase 2 activity and enhances IL-8 gene expression: role of tyrosine nitration**. *Biochemical and biophysical research communications* 2004, **315**(1):240-245.

147. Chung KF: **Cytokines as targets in chronic obstructive pulmonary disease**. *Current drug targets* 2006, **7**(6):675-681.

148. Rabe KF, Bateman ED, O'Donnell D, Witte S, Bredenbroker D, Bethke TD: **Roflumilast--an oral anti-inflammatory treatment for chronic obstructive pulmonary disease: a randomised controlled trial**. *Lancet* 2005, **366**(9485):563-571.

149. Zhou Y, Mohsenin A, Morschl E, Young HW, Molina JG, Ma W, Sun CX, Martinez-Valdez H, Blackburn MR: **Enhanced airway inflammation and remodeling in adenosine deaminase-deficient mice lacking the A2B adenosine receptor**. *Journal of immunology* 2009, **182**(12):8037-8046.

150. Ham J, Rees DA: **The adenosine a2b receptor: its role in inflammation**. *Endocrine, metabolic & immune disorders drug targets* 2008, **8**(4):244-254.

151. Lee AY, Raz DJ, He B, Jablons DM: **Update on the molecular biology of malignant mesothelioma**. *Cancer* 2007, **109**(8):1454-1461.

152. Robinson BW, Musk AW, Lake RA: **Malignant mesothelioma**. *Lancet* 2005, **366**(9483):397-408.

153. Carbone M, Bedrossian CW: **The pathogenesis of mesothelioma**. *Seminars in diagnostic pathology* 2006, **23**(1):56-60.

154. Qi F, Carbone M, Yang H, Gaudino G: **Simian virus 40 transformation, malignant mesothelioma and brain tumors**. *Expert review of respiratory medicine* 2011, **5**(5):683-697.

155. Bianchi C, Bianchi T: **Malignant mesothelioma: global incidence and relationship with asbestos**. *Industrial health* 2007, **45**(3):379-387.

156. Musti M, Kettunen E, Dragonieri S, Lindholm P, Cavone D, Serio G, Knuutila S: **Cytogenetic and molecular genetic changes in malignant mesothelioma**. *Cancer genetics and cytogenetics* 2006, **170**(1):9-15.

157. Whitson BA, Kratzke RA: **Molecular pathways in malignant pleural mesothelioma**. *Cancer letters* 2006, **239**(2):183-189.

158. Soini Y, Kinnula V, Kaarteenaho-Wiik R, Kurttila E, Linnainmaa K, Paakko P: **Apoptosis and expression of apoptosis regulating proteins bcl-2, mcl-1, bcl-X, and bax in malignant mesothelioma**. *Clinical cancer research : an official journal of the American Association for Cancer Research* 1999, **5**(11):3508-3515.

159. O'Kane SL, Pound RJ, Campbell A, Chaudhuri N, Lind MJ, Cawkwell L: **Expression of bcl-2 family members in malignant pleural mesothelioma**. *Acta oncologica* 2006, **45**(4):449-453.

160. Cao XX, Mohuiddin I, Ece F, McConkey DJ, Smythe WR: **Histone deacetylase inhibitor downregulation of bcl-xl gene expression leads to apoptotic cell death in mesothelioma**. *American journal of respiratory cell and molecular biology* 2001, **25**(5):562-568.

161. Fennell DA, Rudd RM: **Defective core-apoptosis signalling in diffuse malignant pleural mesothelioma: opportunities for effective drug development**. *The lancet oncology* 2004, **5**(6):354-362.

162. Okuda K, Sasaki H, Kawano O, Yukiue H, Yokoyama T, Yano M, Fujii Y: **Epidermal growth factor receptor gene mutation, amplification and protein expression in malignant pleural mesothelioma**. *Journal of cancer research and clinical oncology* 2008, **134**(10):1105-1111.

163. Altomare DA, You H, Xiao GH, Ramos-Nino ME, Skele KL, De Rienzo A, Jhanwar SC, Mossman BT, Kane AB, Testa JR: **Human and mouse mesotheliomas exhibit elevated AKT/PKB/PKB activity, which can be targeted pharmacologically to inhibit tumor cell growth**. *Oncogene* 2005, **24**(40):6080-6089.

164. Rascoe PA, Cao X, Daniel JC, Miller SD, Smythe WR: **Receptor tyrosine kinase and phosphoinositide-3 kinase signalling in malignant mesothelioma**. *The Journal of thoracic and cardiovascular surgery* 2005, **130**(2):393-400.

165. Antman K, Hassan R, Eisner M, Ries LA, Edwards BK: **Update on malignant mesothelioma**. *Oncology* 2005, **19**(10):1301-1309; discussion 1309-1310, 1313-1306.

166. Scagliotti GV, Novello S: **State of the art in mesothelioma**. *Annals of oncology : official journal of the European Society for Medical Oncology / ESMO* 2005, **16 Suppl 2**:ii240-245.

167. Boutin C, Schlesser M, Frenay C, Astoul P: **Malignant pleural mesothelioma**. *The European respiratory journal : official journal of the European Society for Clinical Respiratory Physiology* 1998, **12**(4):972-981.

168. Robinson BW, Lake RA: **Advances in malignant mesothelioma**. *The New England journal of medicine* 2005, **353**(15):1591-1603.

169. Sugarbaker DJ, Heher EC, Lee TH, Couper G, Mentzer S, Corson JM, Collins JJ, Jr., Shemin R, Pugatch R, Weissman L *et al*: **Extrapleural pneumonectomy, chemotherapy, and radiotherapy in the treatment of diffuse malignant pleural mesothelioma**. *The Journal of thoracic and cardiovascular surgery* 1991, **102**(1):10-14; discussion 14-15.

170. Baas P: **Optimising survival in malignant mesothelioma**. *Lung cancer* 2007, **57 Suppl 2**:S24-29.

171. Kaufman AJ, Pass HI: **Current concepts in malignant pleural mesothelioma**. *Expert review of anticancer therapy* 2008, **8**(2):293-303.

172. Berghmans T, Paesmans M, Lalami Y, Louviaux I, Luce S, Mascaux C, Meert AP, Sculier JP: **Activity of chemotherapy and immunotherapy on malignant mesothelioma: a systematic review of the literature with meta-analysis**. *Lung cancer* 2002, **38**(2):111-121.

173. Tammilehto L, Maasilta P, Kostiainen S, Appelqvist P, Holsti LR, Mattson K: **Diagnosis and prognostic factors in malignant pleural mesothelioma: a retrospective analysis of sixty-five patients**. *Respiration; international review of thoracic diseases* 1992, **59**(3):129-135.

174. Flores RM, Pass HI, Seshan VE, Dycoco J, Zakowski M, Carbone M, Bains MS, Rusch VW: **Extrapleural pneumonectomy versus pleurectomy/decortication in the surgical management of malignant pleural mesothelioma: results in 663 patients**. *The Journal of thoracic and cardiovascular surgery* 2008, **135**(3):620-626, 626 e621-623.

175. McDonald AD, McDonald JC: **Malignant mesothelioma in North America**. *Cancer* 1980, **46**(7):1650-1656.

176. Spirtas R, Connelly RR, Tucker MA: **Survival patterns for malignant mesothelioma: the SEER experience**. *International journal of cancer Journal international du cancer* 1988, **41**(4):525-530.

177. Cugell DW, Kamp DW: **Asbestos and the pleura: a review**. *Chest* 2004, **125**(3):1103-1117.

178. Sporn TA: **Mineralogy of asbestos**. *Recent results in cancer research Fortschritte der Krebsforschung Progres dans les recherches sur le cancer* 2011, **189**:1-11.

179. Godleski JJ: **Role of asbestos in etiology of malignant pleural mesothelioma**. *Thoracic surgery clinics* 2004, **14**(4):479-487.

180. Kamp DW: **Asbestos-induced lung diseases: an update**. *Translational research : the journal of laboratory and clinical medicine* 2009, **153**(4):143-152.

181. Nishimura SL, Broaddus VC: **Asbestos-induced pleural disease**. *Clinics in chest medicine* 1998, **19**(2):311-329.

182. Kane AB: **Animal models of malignant mesothelioma**. *Inhalation toxicology* 2006, **18**(12):1001-1004.

183. Gessi S, Varani K, Merighi S, Morelli A, Ferrari D, Leung E, Baraldi PG, Spalluto G, Borea PA: **Pharmacological and biochemical characterization of A(3) adenosine receptors in Jurkat T cells**. *Br J Pharmacol* 2001, **134**(1):116-126.

184. Merighi S, Varani K, Gessi S, Cattabriga E, Iannotta V, Ulouglu C, Leung E, Borea PA: **Pharmacological and biochemical characterization of adenosine receptors in the human malignant melanoma A375 cell line**. *British journal of pharmacology* 2001, **134**(6):1215-1226.

185. Suh BC, Kim TD, Lee JU, Seong JK, Kim KT: **Pharmacological characterization of adenosine receptors in PGT-beta mouse pineal gland tumour cells**. *Br J Pharmacol* 2001, **134**(1):132-142.

186. Gessi S, Sacchetto V, Fogli E, Merighi S, Varani K, Baraldi PG, Tabrizi MA, Leung E, Maclennan S, Borea PA: **Modulation of metalloproteinase-9 in U87MG glioblastoma cells by A3 adenosine receptors**. *Biochem Pharmacol* 2010, **79**(10):1483-1495.

187. Merighi S, Benini A, Mirandola P, Gessi S, Varani K, Leung E, Maclennan S, Borea PA: **Adenosine modulates vascular endothelial growth factor expression via hypoxia-inducible factor-1 in human glioblastoma cells**. *Biochemical pharmacology* 2006, **72**(1):19-31.

188. Varani K, Caramori G, Vincenzi F, Adcock I, Casolari P, Leung E, Maclennan S, Gessi S, Morello S, Barnes PJ *et al*: **Alteration of adenosine receptors in patients with chronic obstructive pulmonary disease**. *American journal of respiratory and critical care medicine* 2006, **173**(4):398-406.

189. Cacciotti P, Libener R, Betta P, Martini F, Porta C, Procopio A, Strizzi L, Penengo L, Tognon M, Mutti L *et al*: **SV40 replication in human mesothelial cells induces HGF/Met receptor activation: a model for viral-related carcinogenesis of human malignant mesothelioma**. *Proceedings of the National Academy of Sciences of the United States of America* 2001, **98**(21):12032-12037.

190. Yang H, Bocchetta M, Kroczynska B, Elmishad AG, Chen Y, Liu Z, Bubici C, Mossman BT, Pass HI, Testa JR *et al*: **TNF-alpha inhibits asbestos-induced cytotoxicity via a NF-kappaB-dependent pathway, a possible mechanism for asbestos-induced oncogenesis**. *Proceedings of the National Academy of Sciences of the United States of America* 2006, **103**(27):10397-10402.

191. Panzarini E, Tenuzzo B, Palazzo F, Chionna A, Dini L: **Apoptosis induction and mitochondria alteration in human HeLa tumour cells by photoproducts of**

Rose Bengal acetate. *Journal of photochemistry and photobiology B, Biology* 2006, **83**(1):39-47.

192. Zampetaki A, Zeng L, Margariti A, Xiao Q, Li H, Zhang Z, Pepe AE, Wang G, Habi O, deFalco E *et al*: **Histone deacetylase 3 is critical in endothelial survival and atherosclerosis development in response to disturbed flow**. *Circulation* 2010, **121**(1):132-142.

193. Varani K, Caramori G, Vincenzi F, Tosi A, Barczyk A, Contoli M, Casolari P, Triggiani M, Hansel T, Leung E *et al*: **Oxidative/nitrosative stress selectively altered A(2B) adenosine receptors in chronic obstructive pulmonary disease**. *The FASEB journal : official publication of the Federation of American Societies for Experimental Biology* 2010, **24**(4):1192-1204.

194. Madi L, Ochaion A, Rath-Wolfson L, Bar-Yehuda S, Erlanger A, Ohana G, Harish A, Merimski O, Barer F, Fishman P: **The A3 adenosine receptor is highly expressed in tumor versus normal cells: potential target for tumor growth inhibition**. *Clinical cancer research : an official journal of the American Association for Cancer Research* 2004, **10**(13):4472-4479.

195. Caruso M, Varani K, Tringali G, Polosa R: **Adenosine and adenosine receptors: their contribution to airway inflammation and therapeutic potential in asthma**. *Current medicinal chemistry* 2009, **16**(29):3875-3885.

196. Yildirim H, Metintas M, Ak G, Erginel S, Alatas F, Kurt E, Metintas S, Ucgun I: **Increased pleural fluid adenosine deaminase levels in patients with malignant pleural effusions: a potential predictor of talc pleurodesis outcome**. *Lung* 2007, **185**(6):349-354.

197. Morello S, Petrella A, Festa M, Popolo A, Monaco M, Vuttariello E, Chiappetta G, Parente L, Pinto A: **Cl-IB-MECA inhibits human thyroid cancer cell proliferation independently of A3 adenosine receptor activation**. *Cancer biology & therapy* 2008, **7**(2):278-284.

198. Seino S, Shibasaki T: **PKA-dependent and PKA-independent pathways for cAMP-regulated exocytosis**. *Physiological reviews* 2005, **85**(4):1303-1342.

199. Karin M, Ben-Neriah Y: **Phosphorylation meets ubiquitination: the control of NF-[kappa]B activity**. *Annual review of immunology* 2000, **18**:621-663.

200. Fishman P, Bar-Yehuda S, Madi L, Cohn I: **A3 adenosine receptor as a target for cancer therapy**. *Anti-cancer drugs* 2002, **13**(5):437-443.

201. Fishman P, Bar-Yehuda S, Ardon E, Rath-Wolfson L, Barrer F, Ochaion A, Madi L: **Targeting the A3 adenosine receptor for cancer therapy: inhibition of prostate carcinoma cell growth by A3AR agonist**. *Anticancer research* 2003, **23**(3A):2077-2083.

202. Ohana G, Bar-Yehuda S, Arich A, Madi L, Dreznick Z, Rath-Wolfson L, Silberman D, Slosman G, Fishman P: **Inhibition of primary colon carcinoma growth and liver metastasis by the A3 adenosine receptor agonist CF101**. *British journal of cancer* 2003, **89**(8):1552-1558.

203. Bolognesi C, Martini F, Tognon M, Filiberti R, Neri M, Perrone E, Landini E, Canessa PA, Ivaldi GP, Betta P *et al*: **A molecular epidemiology case control study on pleural malignant mesothelioma**. *Cancer epidemiology, biomarkers & prevention : a publication of the American Association for Cancer Research, cosponsored by the American Society of Preventive Oncology* 2005, **14**(7):1741-1746.

204. Kamp DW, Panduri V, Weitzman SA, Chandel N: **Asbestos-induced alveolar epithelial cell apoptosis: role of mitochondrial dysfunction caused by iron-derived free radicals**. *Molecular and cellular biochemistry* 2002, **234-235**(1-2):153-160.

205. Panduri V, Surapureddi S, Soberanes S, Weitzman SA, Chandel N, Kamp DW: **P53 mediates amosite asbestos-induced alveolar epithelial cell mitochondria-**

regulated apoptosis. *American journal of respiratory cell and molecular biology* 2006, **34**(4):443-452.

206. Baldys A, Pande P, Mosleh T, Park SH, Aust AE: **Apoptosis induced by crocidolite asbestos in human lung epithelial cells involves inactivation of Akt/PKB and MAPK pathways**. *Apoptosis : an international journal on programmed cell death* 2007, **12**(2):433-447.

207. Lee EJ, Min HY, Chung HJ, Park EJ, Shin DH, Jeong LS, Lee SK: **A novel adenosine analog, thio-Cl-IB-MECA, induces G0/G1 cell cycle arrest and apoptosis in human promyelocytic leukemia HL-60 cells**. *Biochemical pharmacology* 2005, **70**(6):918-924.

208. Kim SG, Ravi G, Hoffmann C, Jung YJ, Kim M, Chen A, Jacobson KA: **p53-Independent induction of Fas and apoptosis in leukemic cells by an adenosine derivative, Cl-IB-MECA**. *Biochemical pharmacology* 2002, **63**(5):871-880.

209. Bar-Yehuda S, Madi L, Silberman D, Gery S, Shkapenuk M, Fishman P: **CF101, an agonist to the A3 adenosine receptor, enhances the chemotherapeutic effect of 5-fluorouracil in a colon carcinoma murine model**. *Neoplasia* 2005, **7**(1):85-90.

210. Craighead JE: **Epidemiology of mesothelioma and historical background**. *Recent results in cancer research Fortschritte der Krebsforschung Progres dans les recherches sur le cancer* 2011, **189**:13-25.

211. Caramori G, Adcock I: **Gene-environment interactions in the development of chronic obstructive pulmonary disease**. *Current opinion in allergy and clinical immunology* 2006, **6**(5):323-328.

212. Ramos-Nino ME, Blumen SR, Sabo-Attwood T, Pass H, Carbone M, Testa JR, Altomare DA, Mossman BT: **HGF mediates cell proliferation of human mesothelioma cells through a PI3K/MEK5/Fra-1 pathway**. *American journal of respiratory cell and molecular biology* 2008, **38**(2):209-217.

CURRICULUM VITAE

2006 Degree in Molecular Biology at the University of Padova.

2007 Stage at the centre IMAGE, at the University of Perpignan, France.

2008 Degree in Biomolecular and Cellular Sciences, magna cum laude, at the University of Ferrara.

2009-2011 PhD Student in "Pharmacology and Molecular Oncology", Department of Clinical and Experimental Medicine, Section of Pharmacology, University of Ferrara.

From 01/02/2012 Research Fellowship at the Department of Clinical and Experimental Medicine, Section of Pharmacology, University of Ferrara.

LIST OF PUBLICATIONS

Varani K, Padovan M, Vincenzi F, **Targa M**, Trotta F, Govoni M, Borea P.A. A2A and A3 adenosine receptor expression in rheumatoid arthritis: upregulation, inverse correlation with disease activity score and suppression of inflammatory cytokine and metalloproteinase release. Arthritis Res Ther. 2011 Dec 6; in press.

Varani K, Vincenzi F, **Targa M**, Corciulo C, Fini M, Setti S, Cadossi R, Borea P.A. Effect of pulsed electromagnetic field exposure on adenosine receptors in rat brain. Bioelectromagnetics. 2011 Oct 19; in press.

Varani K, Maniero S, Vincenzi F, **Targa M**, Stefanelli A, Maniscalco P, Martini F, Tognon M, Borea P.A. A_3 receptors are overexpressed in pleura from patients with mesothelioma and reduce cell growth via Akt/PKB/nuclear factor-κB pathway. Am J Respir Crit Care Med. 2011;183(4):522-30.

Varani K, Vincenzi F, Tosi A, **Targa M**, Masieri F.F, Ongaro A, De Mattei M, Massari L, Borea P.A. Expression and functional role of adenosine receptors in regulating inflammatory responses in human synoviocytes. Br J Pharmacol. 2010;160(1):101-15.

Varani K, De Mattei M, Vincenzi F, Tosi A, **Targa M**, Masieri F.F, Pellati A, Massari L, Borea P.A. P2X(1) and P2X(3) purinergic receptors differentially modulate the inflammatory response in human osteoarthritic synovial fibroblasts. Cell Physiol Biochem. 2010;25(2-3):325-36.

Radoi A, **Targa M**, Prieto-Simon B, Marty J.L. Enzyme-linked immunosorbent assay (ELISA) based on superparamagnetic nanoparticles for aflatoxin M1 detection. Talanta. 2008;77(1):138-43.

MEETINGS

Varani K, Vincenzi F, **Targa M**, Stefanelli A, Tognon M and Borea PA. A_3 adenosine receptors are overexpressed in pleura from patients with mesothelioma and reduce malignant mesothelioma cell growth. 35° Congresso Nazionale di Farmacologia, SIF, Bologna, 14-17 Settembre 2011.

Borghi V, Impagnatiello F, Borea PA, Vincenzi F, **Targa M**, Ongini E and Varani K. NCX 1236, a novel gabapentin endowed of nitric oxide-releasing properties, reverse the development of mechanical allodynia in streptozotocin-treated diabetic mice. 35° Congresso Nazionale di Farmacologia, SIF, Bologna, 14-17 Settembre 2011.

Varani K, Vincenzi F, **Targa M**, Corciulo C, Setti S, Borea PA, Cadossi R. Effect of Pulsed Electromagnetic Field Exposure on A_{2A} Adenosine Receptors in Rat Brain. Ebea 2011, Roma, 21-24 Febbraio 2011.

Varani K, Vincenzi F, **Targa M**, Masieri F, Ongaro A, De Mattei M, Massari L, Setti S, Borea PA, Cadossi R. Effects of Pulsed Electromagnetic Field Exposure on Adenosine Receptors in Human Fibroblast-like Synoviocytes. ORS 2011 Annual Meeting. Long Beach, California, 13-16 January 2011.

Varani K, Vincenzi F, **Targa M**, Masieri F, Ongaro A, De Mattei M, Massari L, Borea PA. Expression and functional role of adenosine receptors in regulating inflammatory responses in human synoviocytes. Purines 2010, Terragona, 30 May-2 June 2010.

Tosi A, Varani K, Romagnoli R, Vincenzi F, **Targa M**, Preti D, Baraldi PG, Borea PA. Pharmacological characterization of novel allosteric enhancers of the A_1 adenosine receptors. 34° Congresso Nazionale di Farmacologia, SIF, Rimini, 14-17 Ottobre 2009.

Vincenzi F, Varani K, **Targa M**, Tosi A, Gessi S, Merighi S, Borea PA. Thermodynamic analysis in drug-receptor binding: the A_3 adenosine receptor. 34° Congresso Nazionale di Farmacologia, SIF, Rimini, 14-17 Ottobre 2009.

ACKNOWLEDGEMENTS